TITLE: **Planck-LFI CPV: stability check before bias tuning**
(P_PVP_LFI_0102_01)

DOC. TYPE: **Test Report**

PROJECT REF.: **PL-LFI-PST-RP-066** **PAGE: I of IV, 11**

ISSUE/REV.: **1.0**

Prepared by	**The Planck-LFI calibration team**	**Date:** **Signature:**	July, 2009
Agreed by	**C. BUTLER** **LFI Program Manager**	**Date:** **Signature:**	July, 2009
Approved by	**N. MANDOLESI** **LFI Principal Investigator**	**Date:** **Signature:**	July, 2009

The Planck-LFI calibration team

- Paola Battaglia (SCOS/TQL operator)
- Marco Bersanelli (LFI instrument scientist, test leader)
- Francesco Cuttaia (CPV responsible, test leader)
- Richard Davis (30/44 GHz data analysis)
- Marco Frailis (Level 1 manager)
- Cristian Franceschet (SCOS/TQL operator)
- Enrico Franceschi (GSE manager)
- Samuele Galeotta (LIFE/PEGASO development)
- Anna Gregorio (Instrument Operation Manager)
- Rodrigo Leonardi (data analysis)
- Stuart Lowe (LIFE/PEGASO development)
- Reno Mandolesi (PI)
- Michele Maris (data analysis, LIFE/PEGASO development)
- Peter Meinhold (Test leader, data analysis)
- Luis Mendes (data analysis)
- Aniello Mennella (Calibration Scientist, test leader)
- Torsti Poutanen (data analysis)
- Maura Sandri (Test leader, data analysis)
- Daniele Tavagnacco (SCOS/TQL operator)
- Luca Terenzi (Tests leader, data analysis and LIFE/PEGASO development)
- Maurizio Tomasi (Test leader, data analysis and LIFE/PEGASO development)
- Fabrizio Villa (Test leader, data analysis)
- Andrea Zacchei (LFI DPC manager)
- Andrea Zonca (SCOS/TQL operator, LIFE/PEGASO development)

DISTRIBUTION LIST

M. BERSANELLI	UNIMI – Milano	marco.bersanelli@mi.infn.it	Yes
R.C. BUTLER	INAF/IASF – Bologna	butler@iasfbo.inaf.it	Yes
F. CUTTAIA	INAF/IASF – Bologna	cuttaia@iasfbo.inaf.it	Yes
A. GREGORIO	UniTs – Trieste	Anna.gregorio@ts.infn.it	Yes
D. MAINO	UNIMI – Milano	davide.maino@mi.infn.it	Yes
N. MANDOLESI	INAF/IASF – Bologna	mandolesi@iasfbo.inaf.it	Yes
A. MENNELLA	UNIMI – Milano	aniello.mennella@fisica.unimi.it	Yes
A. ZACCHEI	INAF/OATs – Trieste	zacchei@oats.inaf.it	Yes
G. GUYOT	IAS - Orsay	guy.guyot@ias.u-psud.fr	Yes
J.M. LAMARRE	IAS - Orsay	lamarre@ias.u-psud.fr	Yes
F. PAJOT	IAS - Orsay	francois.pajot@ias.u-psud.fr	Yes
J.L. PUGET	IAS - Orsay	puget@ias.u-psud.fr	Yes
L. VIBERT	IAS - Orsay	laurent.vibert@ias.u-psud.fr	Yes
D. DEXIER	ESA - ESAC	damien.texier@sciops.esa.int	Yes
S. FOLEY	ESA - ESOC	Steve.Foley@esa.int	Yes
R. LAUREIIS	ESA - PSO	rlaureij@rssd.esa.int	Yes
L. MENDES	ESA - PSO	lmendes@rssd.esa.int	Yes
J. TAUBER	ESA- PSO	jtauber@rssd.esa.int	Yes
C. WATSON	ESA - ESOC	Christopher.J.Watson@esa.int	Yes
LFI Core team coordinators		lfi_ctc@iasfbo.inaf.it	Yes
LFI radiometer core team		planck_cta02@fisica.unimi.it	Yes
LFI calibration team			
LFI System PCC	INAF/IASF – Bologna	lfispcc@iasfbo.inaf.it	Yes

CHANGE RECORD

Issue	Date	Sheet	Description of Change	Release
0.1	July 2009	All	First draft of document	0.1
0.2	July 2009	All	Second draft of document	0.2
0.3	July 2009	All	Third draft of document. Added comparison with CSL	0.3
1.0	July 2009	All	First issue of document	0.3

TABLE OF CONTENTS

1 ACRONYMS

AIV	Assembly, Integration, Verification
ASW	Application Software
BEM	Back End Module
BEU	Back End Unit
CCS	Central Check-out System
CDMU	Central Data Management Unit
CPV	Calibration Performance Verification
CSL	Centre Spatiale de Liège
DAE	Data Acquisition Electronics
DPU	Digital Processing Unit
EGSE	Electrical ground Support Equipment
FEM	Front End Module
I-EGSE	Instrument EGSE
IST	Integrated Satellite Test
OBC	On Board Clock
RAA	Radiometer Array Assembly
REBA	Radiometric Electronic Box Assembly
S/C	Spacecraft
SCOE	Spacecraft Control and Operation System
SCS	Sorption Cooler System
SPU	Signal Processing Unit
SUSW	Start- Up Software
SVM	Service Module
TBC	To Be Checked
TBW	To Be Written
TC	Telecommand
TM	Telemetry
UFT	Unit Functional Test

2 APPLICABLE AND REFERENCE DOCUMENTS

2.1 Applicable Documents

[AD1] Herschel/Planck Instrument Interface document Part A, SCI-PT-IIDA-04624 Issue 3.3

[AD2] Herschel/Planck Instrument Interface document Part B, SCI-PT-IIDB-04142 Issue 3.1

[AD3] Herschel/Planck Instrument Interface document Part B, SCI-PT-IIDB-04142 Issue 3.1, Annex 3, ICD 750800115

[AD4] Herschel/Planck Instrument Interface document Part A, SCI-PT-IIDA-04624 Issue 3.3 Annex 10

[AD5] Data analysis and scientific performance of the LFI FM instrument, PL-LFI-PST-AN-006 3.0

[AD6] Planck-LFI TV-TB test report: executive summary, PL-LFI-PST-RP-040 1.1

[AD7] Testing plan of the LFI instrument during the Planck Commissioning and CPV phase, PL-LFI-PST-PL-043 (4.2)

2.2 Reference Documents

[RD1] Planck Instrument Testing at PFM S/C levels, H-P-3-ASP-TN-0676, Issue 1.0

[RD2] Planck LFI User Manual, PL-LFI-PST-MA-001 Issue 2.1

[RD3] Estimate of Planck-LFI in flight performance, PL-LFI-PST-RP-040 1.0

[RD4] Planck-LFI CPV: 1 Hz frequency spikes, PL-LFI-PST-RP-061

3 Introduction

This test consists in a 12-hours data acquisition performed with the instrument set with "CRYO" biases, i.e. the biases that have been obtained in CSL after the tuning activities (see details in Section 4.3.3). The objective of this test is to verify readiness of the instrument for the CPV bias tuning activity from the signal stability point of view. In particular we want to verify that:

- no current drops or abrupt variations are observed in FEM drain currents;
- no frequency spikes are observed besides those already characterised during the SPIKE-02 test;
- no pop-corn noise is detected in radiometer voltage outputs;
- 1/f noise knee frequencies calculated from differenced datastreams are much less than those calculated from undifferenced data and, in general, less than 1 Hz.

Important notice. As during this test the 4K temperature was still around 20 K and the stability was not optimised yet the check on knee frequency is meaningful just from the functionality point of view. No comparison is done between the calculated knee frequencies and the LFI scientific requirements.

4 Test Execution

4.1 Test configuration

The test configuration is the following

SCOS 2K EGSE 3.1 Release 1.2
RTSILib version 1.0
RTSI Client version 1.2
LEVEL1 (TMH/TQL) version 5.1
LIFE Machine version OM 3.00
IDIS 2.7.3.4

LFI Personnel involved during the test is:

LFI Instrument Operation Manager	Anna Gregorio (UniTs anna.gregorio@ts.infn.it)
LFI Calibration Scientist	Aniello Mennella (UniMi aniello.mennella@fisica.unimi.it)
LFI CPV Manager	Francesco Cuttaia (IASF-BO cuttaia@iasfbo.inaf.it)
Test leader	Maura Sandri
LFI IOT	Anna Gregorio, Aniello Mennella, Cristian Franceschet, Chris Butler, Marco Frailis, Samuele Galeotta, Andrea Zacchei, Maura Sandri, Luca Terenzi, Francesco Cuttaia
Industry support	Paola Battaglia

4.2 Pass-fail criteria, verification matrix

CPV **P_PVP_LFI_0102_01**

June, 18 2009 07:35z **DoY 169** **OD 35-36**

Duration **12:00:00**

Test name: **Stability check**

Test objectives: Check for instabilities (Scientific signal and HK) in undisturbed conditions to verify no un-expected features (Pop-corn noise, spike, current drops) are present.

Verification matrix

Check	Passed?			Recovered?	
	Yes	No	Notes	Yes	No
No unexpected events packets	Yes				
TC procedure			N/A		
No unexpected features		No	An unexpected drain current instability has been noticed in the LFI21M1 channel		
Data saved and stored at DPC	Yes				

4.3 Procedure/ Test sequence and environmental conditions

4.3.1 Test procedure

The test consisted in a 12 hours data acquisition with the instrument running in stable conditions: no telecommands were uploaded to the instrument. Test started at about 1624001700 (June 18th, 7:35 UTC, OD35) and ended at about 1624044900 (June 18th, 19:35 UTC, OD36).

4.3.2 Temperatures

In Figures 1, 2 and 3 we report the behaviour of the back-end, front-end and 4K cooler temperatures, respectively. In Figure 2 it may be noticed a small (~ 5 mK) rise of the front-end unit temperature during the first part of the test, which was caused by the instrument bias setting just before the start of the test.

Furthermore the 4K cooler temperature was characterised by a ~200 mK drift and fluctuations of the order of 15 mK peak to peak.

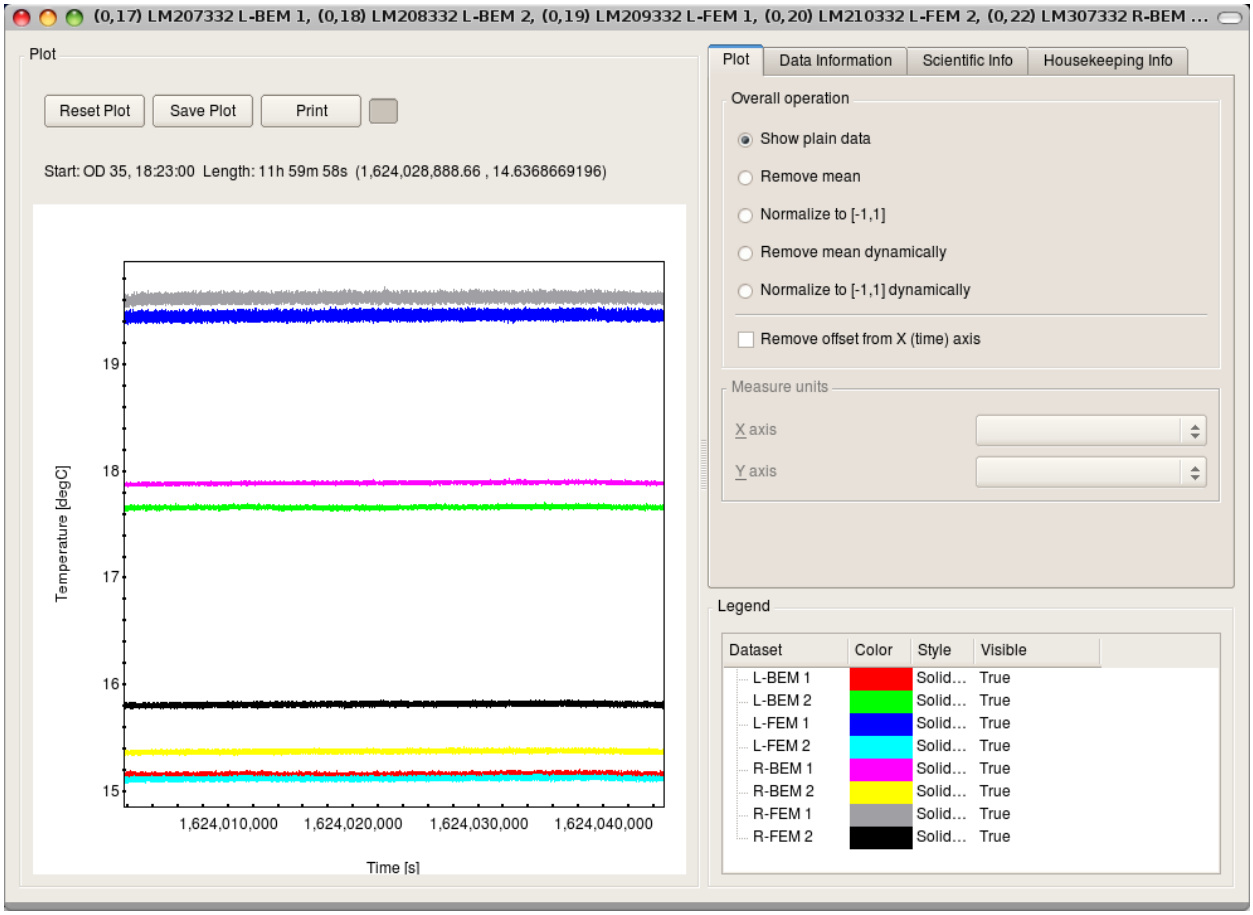

Figure 1 – BEU temperatures during the test.

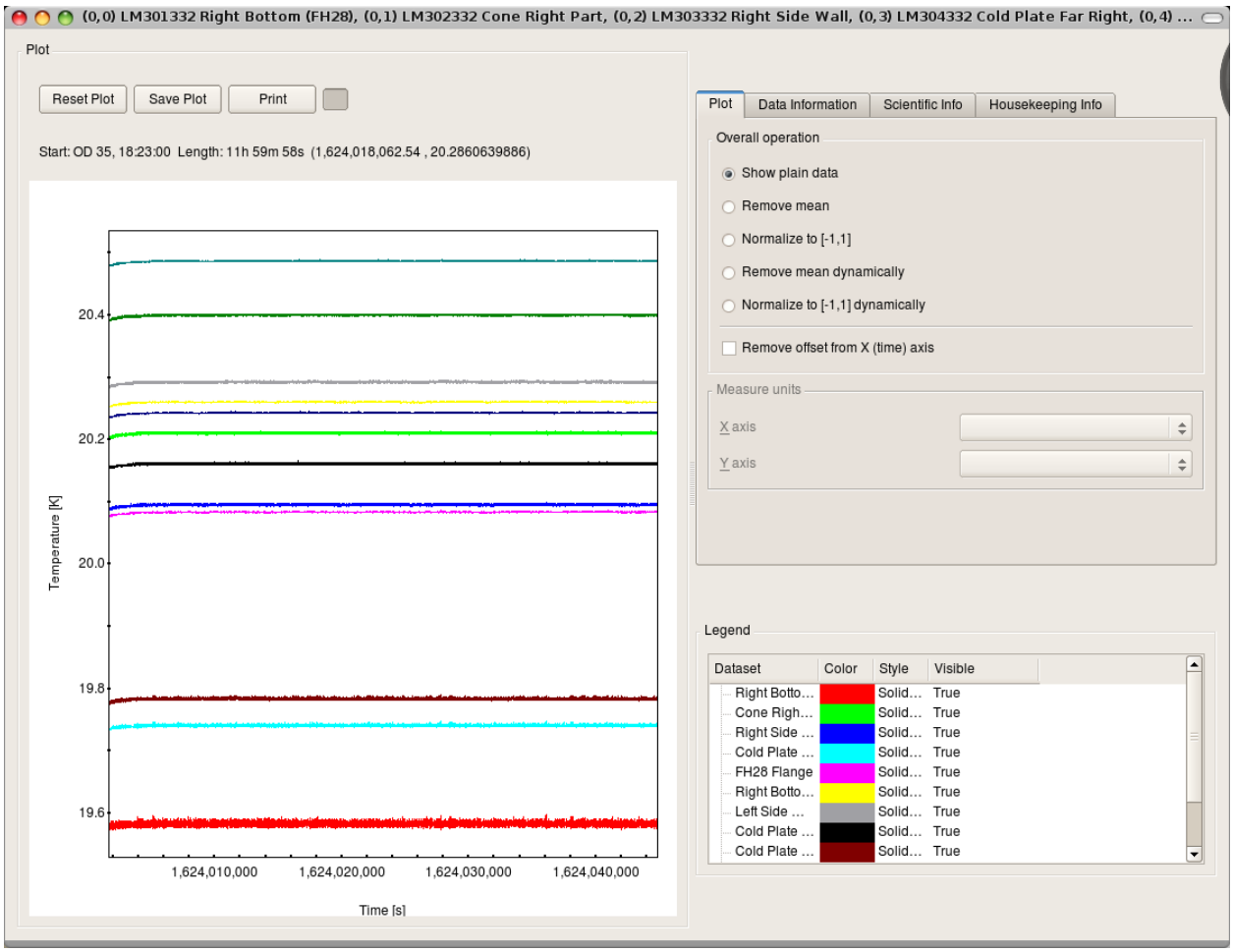

Figure 2 – FEU temperatures during the test.

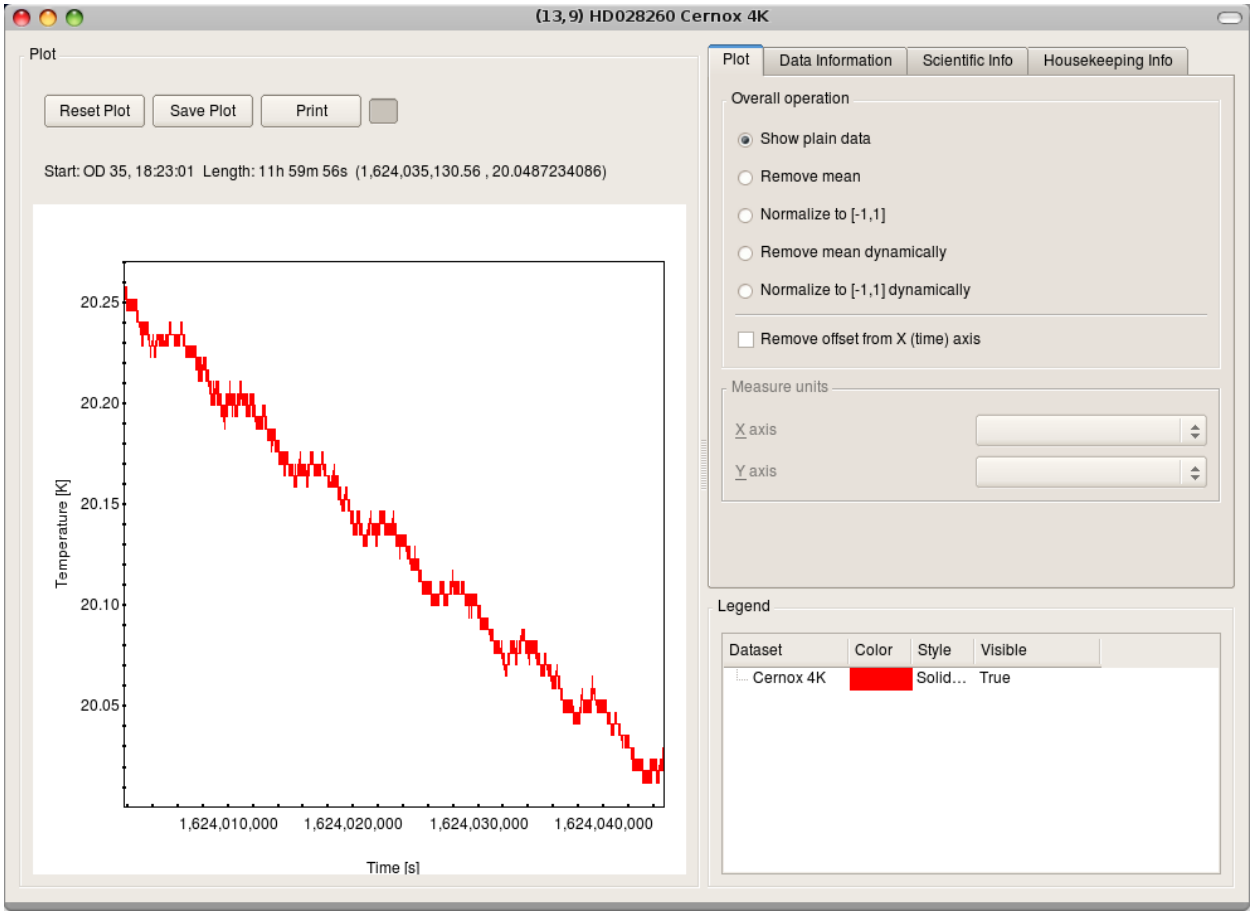

Figure 3 – 4K temperature during the test.

4.3.3 Bias, phase switch and DAE configuration

The test has been run with the "CRYO" biases resulting from the tuning activity performed in CSL. The only exception is the drain voltage of LFI24M1 that was set to 183 as the value used in CSL (200) was later found to be a wrong value that very likely was the cause of the poor noise performance measured in CSL for the LFI24M radiometer. The biases for all 44 ACAs and phase switches are reported in the following table.

RCA	FEM arm	vg1	vg2	vd	I1	I2
LFI18	S2	208	205	114	255	255
	S1	192	197	138	255	255
	M1	190	194	126	255	255
	M2	198	201	125	255	255
LFI19	S2	204	216	125	255	255
	S1	215	209	120	255	255
	M1	213	206	124	255	255
	M2	211	208	126	255	255
LFI20	S2	188	201	127	255	255
	S1	199	221	132	255	255
	M1	209	219	121	255	255
	M2	215	221	127	255	255
LFI21	S2	216	223	132	255	255
	S1	181	197	136	255	255
	M1	198	207	141	255	255
	M2	196	197	136	255	255
LFI22	S2	206	204	130	255	255
	S1	204	189	128	255	255
	M1	203	194	125	255	255
	M2	178	176	130	255	255
LFI23	S2	190	208	122	255	255
	S1	181	211	118	255	255
	M1	207	192	120	255	255
	M2	210	195	119	255	255
LFI24	M2	227	213	183	91	255
	M1	219	217	183	128	250
	S2	225	213	152	86	215
	S1	219	219	157	84	235
LFI25	M1	227	212	184	174	235
	M2	219	212	185	89	250
	S1	224	216	167	93	255
	S2	223	212	166	119	225
LFI26	M2	226	217	170	153	210
	M1	232	209	169	98	245
	S2	232	217	169	93	230
LFI27	S1	228	226	172	135	230
	M1	240	108	156	178	180
	M2	244	90	157	144	214
LFI28	S1	237	102	157	138	192
	S2	246	114	156	128	200
	M1	243	101	157	132	162
	M2	240	112	156	117	188

S1	240	84	157	111	168
S2	245	121	158	99	173

The DAE offsets were optimised in order to avoid saturation while some values of the DAE gain was set to a value different from zero in order to obtain proper noise resolution. The DAE gain and offset values (in DAE units) used in this test are listed in the following table.

RCA	DAE channel	DAE gain	DAE offset
LFI18	M-00	0	0
	M-01	0	0
	S-10	0	128
	S-11	1	128
LFI19	M-00	0	214
	M-01	0	204
	S-10	0	220
	S-11	0	224
LFI20	M-00	0	128
	M-01	0	128
	S-10	0	128
	S-11	0	128
LFI21	M-00	0	195
	M-01	0	204
	S-10	0	180
	S-11	0	180
LFI22	M-00	0	255
	M-01	0	255
	S-10	0	255
	S-11	0	255
LFI23	M-00	1	100
	M-01	0	100
	S-10	0	180
	S-11	8	180
LFI24	M-00	3	255
	M-01	3	255
	S-10	9	255
	S-11	9	255
LFI25	M-00	2	255
	M-01	2	255
	S-10	2	255
	S-11	2	255
LFI26	M-00	9	255
	M-01	9	255
	S-10	2	255
	S-11	8	255
LFI27	M-00	0	0
	M-01	0	0
	S-10	0	0
	S-11	0	0
LFI28	M-00	0	60
	M-01	0	41
	S-10	0	60
	S-11	0	143

The used switching configuration was the nominal one, reported in the following table

RC	A/C	B/D	A/C	B/D pos

A	4KHz	4KHz	pos	
LFI18	0	1	1	0
LFI19	0	1	1	0
LFI20	0	1	1	0
LFI21	0	1	1	0
LFI22	0	1	1	0
LFI22	0	1	1	0
LFI23	1	0	1	0
LFI24	0	1	1	0
LFI25	0	1	1	0
LFI26	0	1	1	0
LFI27	0	1	1	0
LFI28	0	1	1	0

4.3.4 Results and Conclusions

The test was executed in the scheduled time and no non-nominal features were observed from the point of view of the test conduction.

5 Data Analysis

5.1 Drain current stability

To characterise drain current stability we have calculated the standard deviation for Id in all channels. Values reported in Table 19 show that the stability is very good, with variations that are less than 1% for all channels. Three channels, however, display variations of the order of 0.1% which are larger that the other channels, for which variations are of the order of 0.02% - 0.04%. These channels are LFI18M1, LFI21M1 and LFI22S2.

Table 19 – Drain current average values and standard deviation

		Idrain		
		Mean	Std-Dev	%
18	M1	13.506181	0.017434	0.13
	M2	14.461901	0.007091	0.05
	S1	19.852057	0.008057	0.04
	S2	21.473844	0.004042	0.02
19	M1	18.173356	0.007965	0.04
	M2	19.827996	0.008162	0.04
	S1	17.884434	0.008286	0.05
	S2	16.923038	0.008304	0.05
20	M1	20.625001	0.004615	0.02
	M2	20.628464	0.004581	0.02
	S1	18.759894	0.008097	0.04
	S2	18.581814	0.008014	0.04
21	M1	18.796397	0.022832	0.12
	M2	19.776468	0.006998	0.04
	S1	16.357825	0.006859	0.04
	S2	20.414910	0.005918	0.03
22	M1	14.245209	0.006699	0.05
	M2	14.945102	0.007336	0.05
	S1	16.601957	0.007159	0.04
	S2	15.422569	0.017499	0.11
23	M1	15.005848	0.007792	0.05
	M2	14.637226	0.009712	0.07
	S1	20.796225	0.005150	0.02
	S2	15.073960	0.007843	0.05
24	M1	11.283840	0.007691	0.07
	M2	9.955510	0.006618	0.07
	S1	12.773828	0.007414	0.06
	S2	9.864146	0.007149	0.07
25	M1	9.373331	0.007131	0.08
	M2	9.975986	0.008103	0.08
	S1	11.223737	0.007865	0.07
	S2	9.579777	0.007670	0.08
26	M1	8.127130	0.007198	0.09
	M2	11.724655	0.006752	0.06
	S1	13.389905	0.007109	0.05

	S2	10.435533	0.007196	0.07
27	**M1**	8.163221	0.005636	0.07
	M2	7.258037	0.005509	0.08
	S1	8.516431	0.005887	0.07
	S2	8.046167	0.005693	0.07
28	**M1**	9.622442	0.006495	0.07
	M2	9.173459	0.006968	0.08
	S1	9.096832	0.006543	0.07
	S2	10.471940	0.006315	0.06

The case of LFI18M1 is known since tests in CSL, where in all cases the drain current has always shown variations like those displayed in Fig. 4.

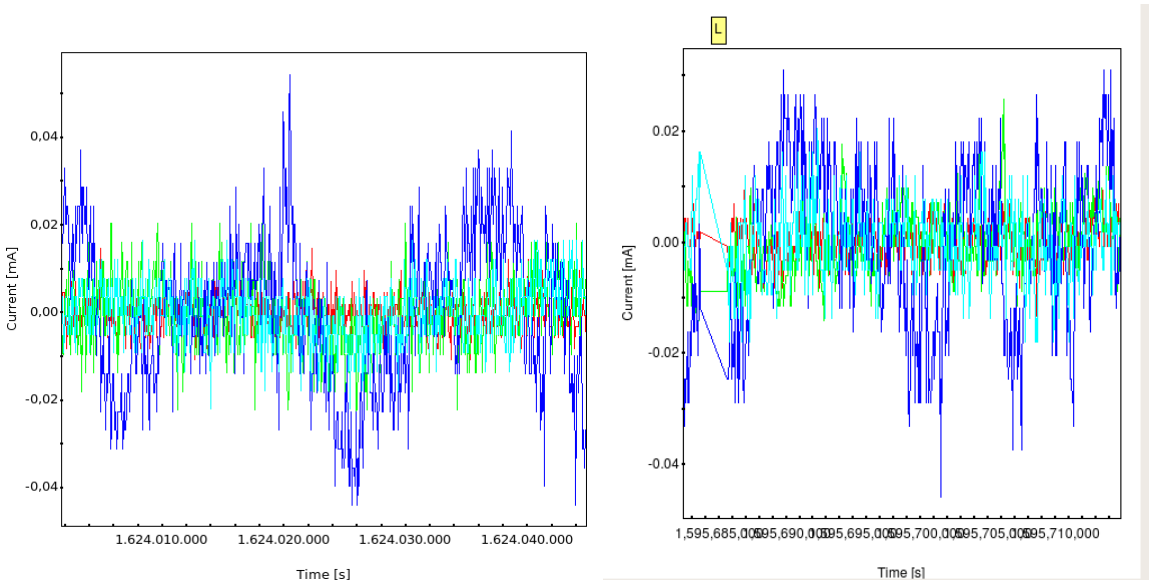

Figure 4 – Feed 18 FEM Id S2 (red), Id S1 (green), Id M1 (blue), and Id M2 (cyan). Left panel: CPV stability check. Right panel CSL test XXX_0203

The case of LFI22 is also a known case of drain current variations greater than the average, as shown in Fig. 5.

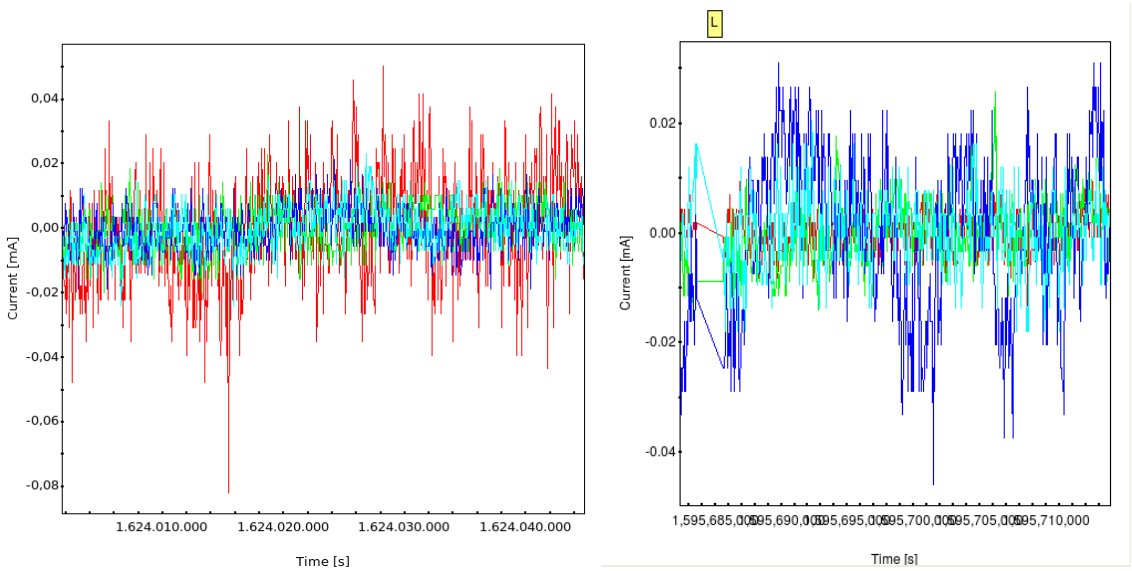

Figure 5 – Feed 22 FEM Id S2 (red), Id S1 (green), Id M1 (blue), and Id M2 (cyan). Left panel: CPV stability check. Right panel CSL test XXX_0203. On the right panel the S2 drain current is shown in blue

The case of LFI21M1, shown in Fig. 6, is the most peculiar of the three instabilitites. In fact they display a typical two state instability, with current drops of the order of 0.05 mA. This effect has never been seen in CSL tests as well during pre-launch warm tests in Kourou.

A preliminary analysis suggests that the onset of this effect is during the CRYO-01 test during CPV, but investigations are still ongoing.

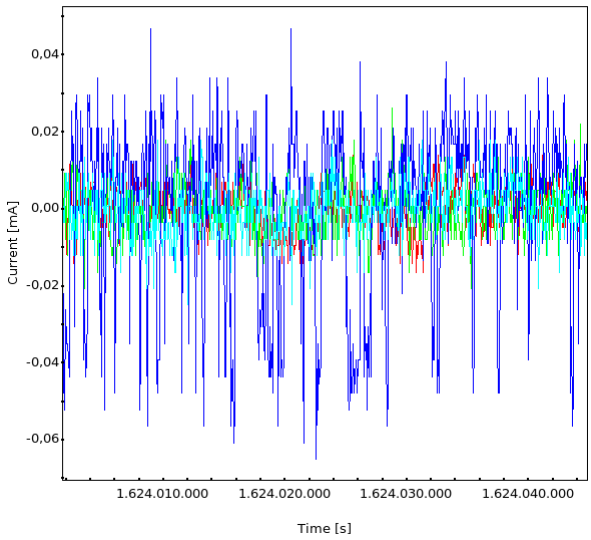

Figure 6 – Feed 21 FEM Id S2 (red), Id S1 (green), Id M1 (blue), and Id M2 (cyan).

It must be stressed that in all three cases the instabilities are small and the effect on the differential output signal is practically negligible. The effect, however, will be monitored in the

next tests, in particular during the reference functionality test, during which bias conditions similar to those experienced during the CRYO-01 test will be reproduced.

5.2 Output signal stability

In Table 20 we summarise average voltage outputs and corresponding standard deviations. In yellow we highlight the voltage outputs corresponding to the channels displaying the drain current instability discussed above.

Table 20 – Average voltage outputs and standard deviations. In yellow we indicate the channels affected by the drain current instability discussed above

		Sky			Ref		
		Mean	Std-Dev	%	Mean	Std-Dev	%
18	M-00	2.286087	0.011941	0.52	3.544921	0.019061	0.54
	M-01	2.994476	0.015058	0.50	4.661827	0.024255	0.52
	S-10	1.302273	0.001880	0.14	2.045111	0.005064	0.25
	S-11	1.136228	0.001620	0.14	1.667549	0.004010	0.24
19	M-00	1.410022	0.001162	0.08	2.143736	0.002974	0.14
	M-01	1.497931	0.001133	0.08	2.359151	0.003295	0.14
	S-10	0.861597	0.000675	0.08	1.331925	0.001865	0.14
	S-11	1.076465	0.000874	0.08	1.603701	0.002288	0.14
20	M-00	1.642502	0.001228	0.07	2.498324	0.004807	0.19
	M-01	1.594553	0.001098	0.07	2.419931	0.004562	0.19
	S-10	1.521321	0.001742	0.11	2.219871	0.004345	0.20
	S-11	1.511425	0.001636	0.11	2.208710	0.004193	0.19
21	M-00	0.902587	0.000997	0.11	1.499708	0.002968	0.20
	M-01	0.866529	0.001010	0.12	1.373929	0.002566	0.19
	S-10	1.302349	0.002269	0.17	1.798244	0.004755	0.26
	S-11	1.348878	0.002372	0.18	1.798393	0.004633	0.26
22	M-00	0.595780	0.000654	0.11	0.915944	0.001567	0.17
	M-01	0.652815	0.000574	0.09	0.995888	0.001764	0.18
	S-10	0.686273	0.001118	0.16	1.012926	0.001695	0.17
	S-11	0.866764	0.001359	0.16	1.246176	0.002078	0.17
23	M-00	1.138716	0.001450	0.13	1.671059	0.002666	0.16
	M-01	1.352273	0.001736	0.13	2.074248	0.003325	0.16
	S-10	1.275856	0.002254	0.18	1.900300	0.003720	0.20
	S-11	0.677788	0.001263	0.19	1.019608	0.002106	0.21
24	M-00	0.074342	0.000033	0.04	0.127161	0.000201	0.16
	M-01	0.075406	0.000038	0.05	0.135772	0.000243	0.18
	S-10	0.107250	0.000057	0.05	0.184823	0.000317	0.17
	S-11	0.114329	0.000052	0.05	0.195435	0.000334	0.17
25	M-00	0.162719	0.000057	0.04	0.270040	0.000383	0.14
	M-01	0.152957	0.000055	0.04	0.261137	0.000378	0.14
	S-10	0.164639	0.000062	0.04	0.292902	0.000456	0.16
	S-11	0.141485	0.000051	0.04	0.248302	0.000387	0.16
26	M-00	0.101878	0.000048	0.05	0.178184	0.000259	0.15
	M-01	0.125999	0.000051	0.04	0.207549	0.000278	0.13

	S-10	0.145764	0.000052	0.04	0.260311	0.000406	0.16
	S-11	0.157197	0.000044	0.03	0.270689	0.000383	0.14
27	**M-00**	1.254842	0.000397	0.03	2.477550	0.004383	0.18
	M-01	1.360505	0.000425	0.03	2.658601	0.004566	0.17
	S-10	1.287030	0.000376	0.03	2.447550	0.004120	0.17
	S-11	1.054729	0.000330	0.03	2.049112	0.003685	0.18
28	**M-00**	1.143043	0.000356	0.03	2.025477	0.003684	0.18
	M-01	1.452922	0.000487	0.03	2.563907	0.004487	0.18
	S-10	1.052867	0.000331	0.03	1.938088	0.003539	0.18
	S-11	0.923581	0.000300	0.03	1.735037	0.003202	0.18

In Figures 7, 8 and 9 we show the output voltage plots for the affected channels where it is possible to appreciate the signal instability corresponding to the drain current instability. Once again it is useful to stress that these instability become completely negligible in the sky-ref differenced signal. The complete set of plots for all detectors is reported in Appendix 1.

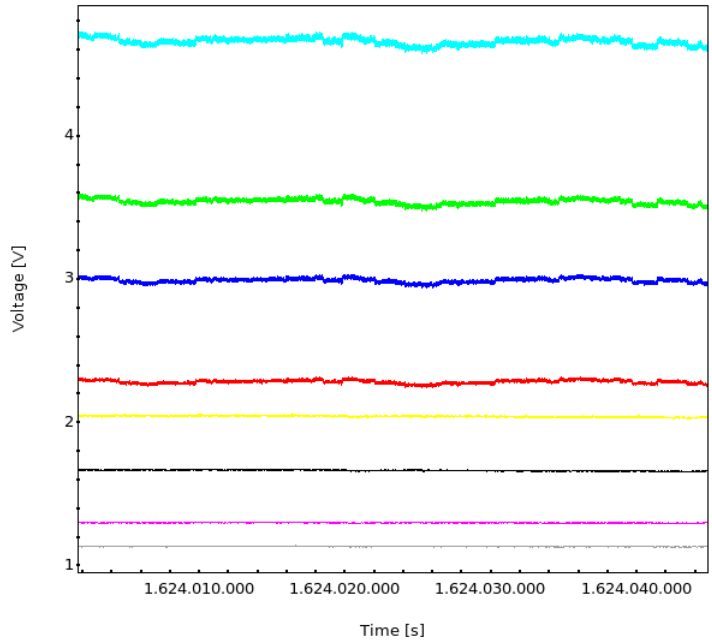

Figure 7 – Feed 18: M-00 sky (red), M-00 ref (green), M-01sky (blue), M-01 ref (cyan), S-10 sky (pink), S-10 ref (yellow), S-11 sky (grey), S-11 ref (black)

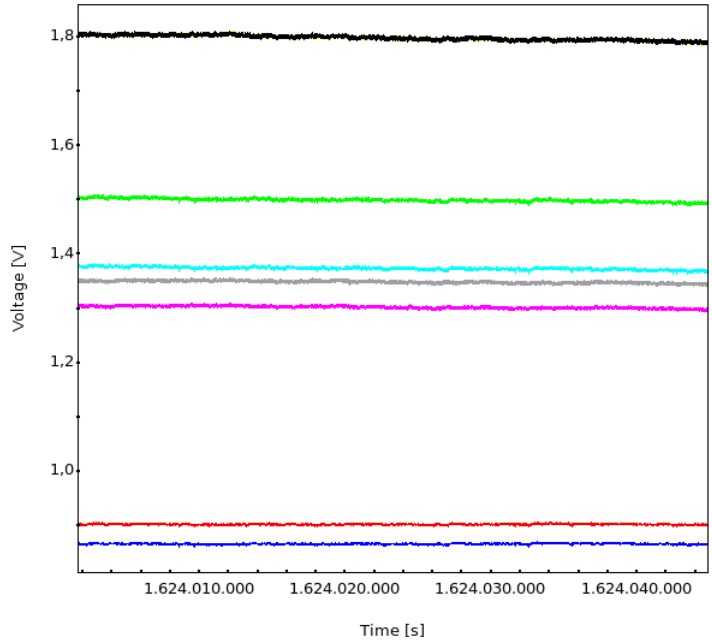

Figure 8 – Feed 21: M-00 sky (red), M-00 ref (green), M-01sky (blue), M-01 ref (cyan), S-10 sky (pink), S-10 ref (yellow), S-11 sky (grey), S-11 ref (black)

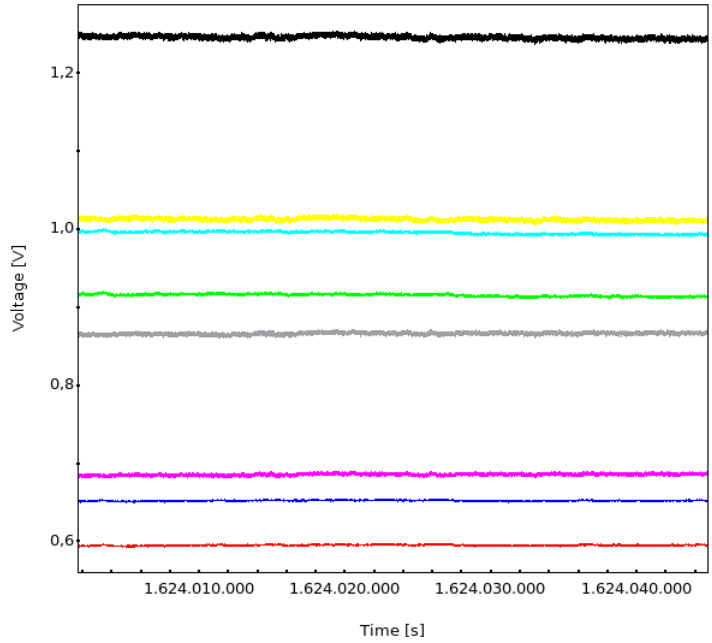

Figure 9 – Feed 22: M-00 sky (red), M-00 ref (green), M-01sky (blue), M-01 ref (cyan), S-10 sky (pink), S-10 ref (yellow), S-11 sky (grey), S-11 ref (black)

		Sky			Ref			Diff	
		Mean	Std-Dev	%	Mean	Std-Dev	%	Mean	Std-Dev
18	M-00	2.286087	0.011941	0.52	3.544921	0.019061	0.54	-9.091156E-08	0.003570
	M-01	2.994476	0.015058	0.50	4.661827	0.024255	0.52	-1.219480E-07	0.004693
	S-10	1.302273	0.001880	0.14	2.045111	0.005064	0.25	-5.278139E-08	0.001911
	S-11	1.136228	0.001620	0.14	1.667549	0.004010	0.24	-4.297255E-08	0.001526
19	M-00	1.410022	0.001162	0.08	2.143736	0.002974	0.14	-5.685869E-08	0.002074
	M-01	1.497931	0.001133	0.08	2.359151	0.003295	0.14	-6.348563E-08	0.002281
	S-10	0.861597	0.000675	0.08	1.331925	0.001865	0.14	-3.435155E-08	0.001285
	S-11	1.076465	0.000874	0.08	1.603701	0.002288	0.14	-4.059665E-08	0.001531
20	M-00	1.642502	0.001228	0.07	2.498324	0.004807	0.19	-6.697648E-08	0.002444
	M-01	1.594553	0.001098	0.07	2.419931	0.004562	0.19	-6.606589E-08	0.002432
	S-10	1.521321	0.001742	0.11	2.219871	0.004345	0.20	-5.863147E-08	0.002068
	S-11	1.511425	0.001636	0.11	2.208710	0.004193	0.19	-5.765006E-08	0.002050
21	M-00	0.902587	0.000997	0.11	1.499708	0.002968	0.20	-4.065843E-08	0.001552
	M-01	0.866529	0.001010	0.12	1.373929	0.002566	0.19	-3.990168E-08	0.001450
	S-10	1.302349	0.002269	0.17	1.798244	0.004755	0.26	-3.132882E-08	0.001413
	S-11	1.348878	0.002372	0.18	1.798393	0.004633	0.26	-3.027860E-08	0.001366
22	M-00	0.595780	0.000654	0.11	0.915944	0.001567	0.17	-2.546570E-08	0.000906
	M-01	0.652815	0.000574	0.09	0.995888	0.001764	0.18	-2.679500E-08	0.001010
	S-10	0.686273	0.001118	0.16	1.012926	0.001695	0.17	-2.808725E-08	0.001047
	S-11	0.866764	0.001359	0.16	1.246176	0.002078	0.17	-3.581285E-08	0.001299
23	M-00	1.138716	0.001450	0.13	1.671059	0.002666	0.16	-4.234956E-08	0.001617
	M-01	1.352273	0.001736	0.13	2.074248	0.003325	0.16	-5.130777E-08	0.001922
	S-10	1.275856	0.002254	0.18	1.900300	0.003720	0.20	-4.849303E-08	0.001828
	S-11	0.677788	0.001263	0.19	1.019608	0.002106	0.21	-2.557291E-08	0.000990
24	M-00	0.074342	0.000033	0.04	0.127161	0.000201	0.16	-3.031358E-09	0.000114
	M-01	0.075406	0.000038	0.05	0.135772	0.000243	0.18	-3.383574E-09	0.000119
	S-10	0.107250	0.000057	0.05	0.184823	0.000317	0.17	-4.282533E-09	0.000158
	S-11	0.114329	0.000052	0.05	0.195435	0.000334	0.17	-4.676980E-09	0.000160
25	M-00	0.162719	0.000057	0.04	0.270040	0.000383	0.14	-6.211718E-09	0.000217
	M-01	0.152957	0.000055	0.04	0.261137	0.000378	0.14	-5.924099E-09	0.000207
	S-10	0.164639	0.000062	0.04	0.292902	0.000456	0.16	-6.376542E-09	0.000241
	S-11	0.141485	0.000051	0.04	0.248302	0.000387	0.16	-5.700386E-09	0.000210
26	M-00	0.101878	0.000048	0.05	0.178184	0.000259	0.15	-4.447828E-09	0.000137
	M-01	0.125999	0.000051	0.04	0.207549	0.000278	0.13	-4.848747E-09	0.000146
	S-10	0.145764	0.000052	0.04	0.260311	0.000406	0.16	-7.142459E-09	0.000218
	S-11	0.157197	0.000044	0.03	0.270689	0.000383	0.14	-7.250841E-09	0.000210
27	M-00	1.254842	0.000397	0.03	2.477550	0.004383	0.18	-5.978291E-08	0.002125
	M-01	1.360505	0.000425	0.03	2.658601	0.004566	0.17	-6.189077E-08	0.002254
	S-10	1.287030	0.000376	0.03	2.447550	0.004120	0.17	-5.961784E-08	0.002094
	S-11	1.054729	0.000330	0.03	2.049112	0.003685	0.18	-5.198813E-08	0.001809
28	M-00	1.143043	0.000356	0.03	2.025477	0.003684	0.18	-5.871257E-08	0.001956
	M-01	1.452922	0.000487	0.03	2.563907	0.004487	0.18	-7.228483E-08	0.002317
	S-10	1.052867	0.000331	0.03	1.938088	0.003539	0.18	-5.421252E-08	0.001736
	S-11	0.923581	0.000300	0.03	1.735037	0.003202	0.18	-4.529374E-08	0.001527

5.3 Frequency spikes

From the complete set of power spectra displayed in Appendix 2 we see that 1Hz frequency spikes are present in some of the total power and differenced channels. If we compare this result with that obtained during the SPIKE-02 test [RD4] we see that more spikes are visible during this test than in the SPIKE-02 test. This is because of the much longer acquisition of the stability check (12 hours) compared to the SPIKE-02 test (1 hour).

This is shown in Fig. 10 that shows the amplitude spectral density of the same channel (LFI18S-10, sky data) using the first hour of data or the complete 12 hours dataset. It is apparent that spikes are not visible if the spectrum is calculated with a short acquisition time.

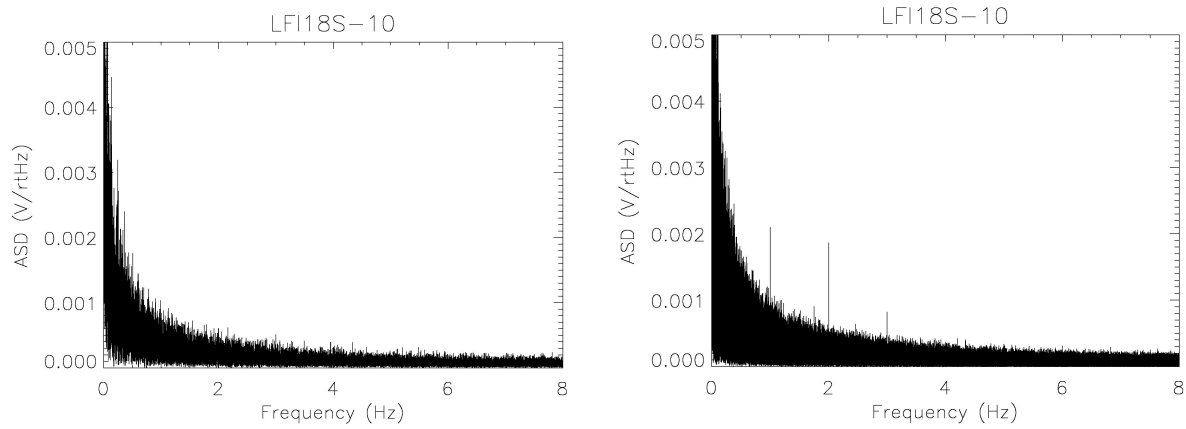

Fig. 10 – Amplitude spectral density of LFI18S-10 (sky data). Left panel: from a 1-hour data stream. Right panel: from the complete 12 hours dataset.

5.4 Noise Properties

In Table 21 we report 1/f knee frequencies and slopes measured for differenced data during the stability check test. We can notice, in particular that all knee frequencies are well below 1 Hz with the single exception of LFI24S-10, which is marginally above 1 Hz.

It is of key importance to stress that non of these values have scientific relevance, as this measurement has been performed with the 4K cooler far from nominal conditions both for temperature level and stability.

The check in this case has been performed only to verify the receiver ability to reduce the knee frequency of the total power datastreams (sky and reference load) when the difference is taken.

The complete set of difference power spectra with the 1/f noise fit results is provided in Appendix 3. Notice from the power spectra the big peak at ~16 mHz, corresponding to the sky signal.

Table 21 – Knee frequency and slope during the stability check test

	Knee Frequency				Slope			
	M-00	M-01	S-10	S-11	M-00	M-01	S-10	S-11
18	0.023921	0.036708	0.158654	0.083535	-1.799142	-1.667211	-1.257107	-1.322264
19	0.050763	0.075388	0.072735	0.168526	-1.379871	-1.267729	-1.338787	-1.123585
20	0.054642	0.073771	0.022769	0.020301	-1.290931	-1.129944	-1.451747	-1.696513
21	0.243918	0.364286	0.126583	0.101900	-1.333013	-1.227208	-1.551706	-1.579242
22	0.040049	0.155836	0.114319	0.414903	-1.583183	-1.333887	-1.251901	-0.947424
23	0.048261	0.149804	0.570988	0.402203	-1.517916	-1.048242	-1.048546	-1.162712
24	0.076818	0.178881	1.172567	0.175072	-1.005346	-0.937630	-0.693986	-0.909346
25	0.044138	0.014981	0.053841	0.035306	-1.172891	-1.582400	-1.102388	-1.341777
26	0.040949	0.034620	0.025489	0.044693	-1.275496	-1.301756	-1.528762	-1.218077
27	0.046597	0.102116	0.026456	0.031562	-1.221287	-1.026062	-1.423635	-1.299297
28	0.046621	0.037772	0.024554	0.026980	-1.163093	-1.216908	-1.417922	-1.250116

In Table 22 we summarise the uncalibrated white noise limit and its standard deviation for all channels. Considering that the white noise limit is (at first order) independent from the absolute temperature of the reference load we have calibrated these values using the CSL calibration constants and compared the calibrated sensitivity with the one derived in CSL and extrapolated at 2.7 K [RD3]. This comparison is shown in Fig. 11 that shows how the calibrated white noise is essentially consistent with CSL measurements. The only noticeable exception is LFI24M-01 that shows a much lesser noise, as a result of the correction in drain voltage that was set to a wrong value in CSL.

It is worth stressing, however, that the calibrated white noise calculations must not be considered as the final scientific performance of the instrument, but only as a verification that the instrument is working as it did before launch.

Table 22 – Uncalibrated white noise and standard deviations (V/rtHz)

	White Noise							
	M-00		M-01		S-10		S-11	
	Mean	Std-Dev	Mean	Std-Dev	Mean	Std-Dev	Mean	Std-Dev
18	7.42E-05	1.57E-06	9.68E-05	2.11E-06	3.81E-05	6.55E-07	2.83E-05	5.51E-07
19	4.43E-05	8.49E-07	4.71E-05	7.03E-07	2.59E-05	5.85E-07	3.09E-05	7.39E-07
20	4.75E-05	9.80E-07	4.82E-05	8.36E-07	4.58E-05	9.42E-07	4.34E-05	7.67E-07
21	2.61E-05	4.55E-07	2.47E-05	4.08E-07	3.71E-05	8.48E-07	4.25E-05	8.04E-07
22	1.68E-05	3.62E-07	1.84E-05	3.63E-07	2.03E-05	6.01E-07	2.53E-05	8.07E-07
23	3.26E-05	6.01E-07	3.57E-05	7.76E-07	3.45E-05	7.06E-07	1.90E-05	3.62E-07
24	3.20E-06	6.92E-08	4.00E-06	7.80E-08	4.64E-06	1.11E-07	4.32E-06	9.73E-08
25	6.61E-06	1.29E-07	6.32E-06	1.14E-07	7.66E-06	1.45E-07	5.61E-06	9.45E-08
26	4.86E-06	9.58E-08	5.76E-06	1.10E-07	6.92E-06	1.22E-07	5.94E-06	1.02E-07
27	4.70E-05	7.88E-07	5.20E-05	1.06E-06	4.59E-05	8.05E-07	4.15E-05	8.43E-07
28	4.46E-05	8.80E-07	5.85E-05	1.07E-06	3.61E-05	6.66E-07	3.29E-05	5.51E-07

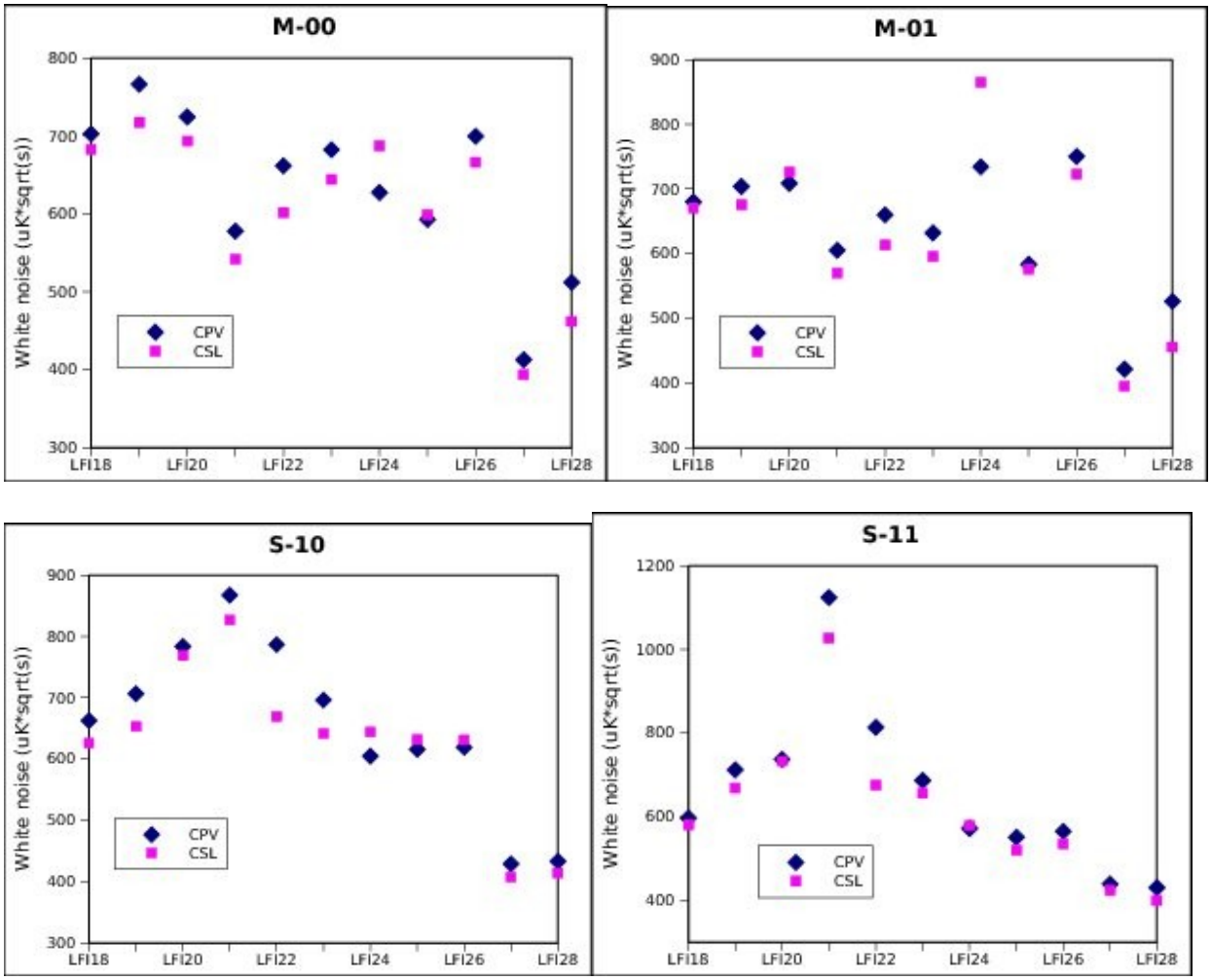

Fig 11 – Comparison of calibrated white noise between CPV and CSL with the instrument set at CSL optimal biases and reference load at ~20 K

6 Conclusions and recommendations

The stability check has been correctly run and the data have been analysed. We can summarise the results as follows:

- drain currents showed a stability comparable with that measured in CSL during a stable acquisition apart for the channel LFI21M1 that showed current drops never observed during the ground test campaign. Investigations are ongoing to understand the cause of the instability although they do not have an impact on the scientific quality of the signal.
- more frequency spikes are observed if compared with the SPIKE-02 test. This is not an anomaly but it is just the result of a much longer acquisition time. In fact on the same timescale of the SPIKE-02 test the spikes are the same. Furthermore the spikes observed during this test appear to be the usual well known 1 Hz spikes from the DAE housekeeping sequencer;
- no pop-corn noise is detected in radiometer voltage outputs, apart from variations correlated with the LFI21M drain current instability;
- 1/f noise knee frequencies calculated from differenced datastreams are much less than those calculated from undifferenced data and, in general, less than 1 Hz;
- calibrated white noise calculated using the CSL calibration constants are in line with CSL measurements.

Recommendations:

- the instability in LFI21M drain current will be monitored and previous CPV tests will be thoroughly analysed to identify the onset of the effect.

Appendix 1 – Voltage output plots for all channels

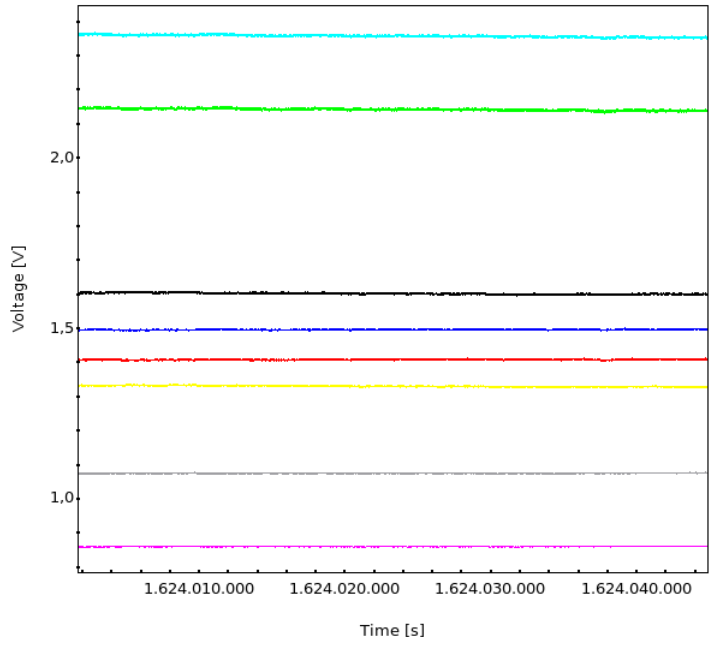

Figure 12 – Feed 19: M-00 sky (red), M-00 ref (green), M-01sky (blue), M-01 ref (cyan), S-10 sky (pink), S-10 ref (yellow), S-11 sky (grey), S-11 ref (black)

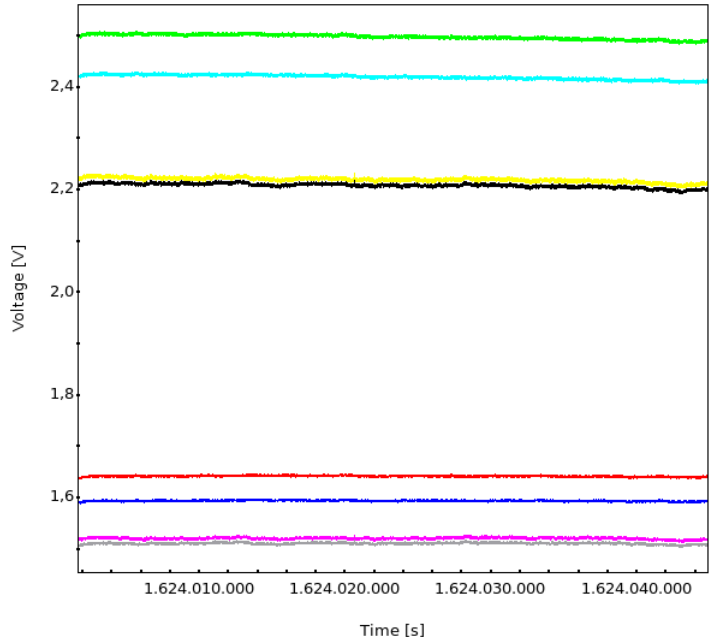

Figure 13 – Feed 20: M-00 sky (red), M-00 ref (green), M-01sky (blue), M-01 ref (cyan), S-10 sky (pink), S-10 ref (yellow), S-11 sky (grey), S-11 ref (black)

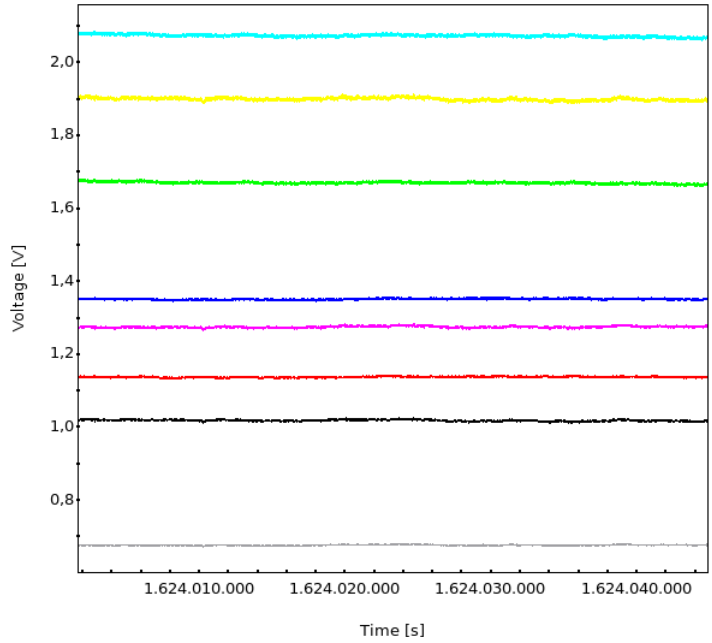

Figure 14 – Feed 23: M-00 sky (red), M-00 ref (green), M-01sky (blue), M-01 ref (cyan), S-10 sky (pink), S-10 ref (yellow), S-11 sky (grey), S-11 ref (black)

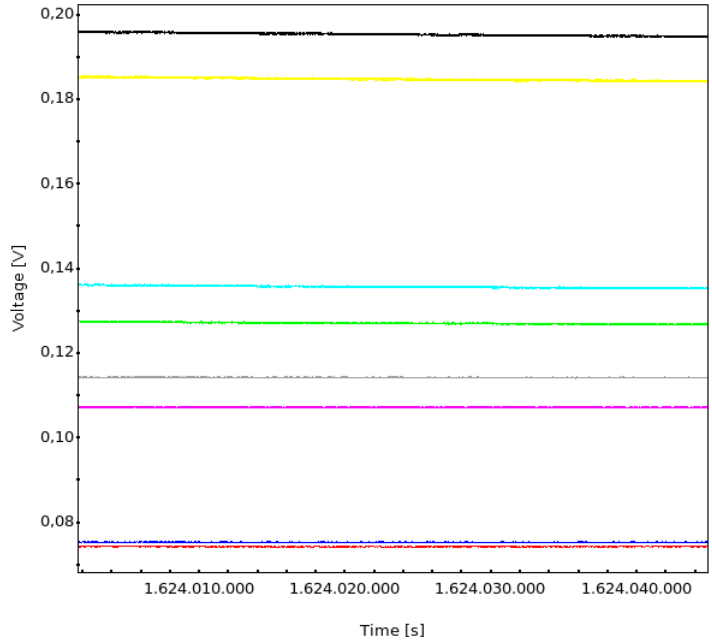

Figure 15 – Feed 24: M-00 sky (red), M-00 ref (green), M-01sky (blue), M-01 ref (cyan), S-10 sky (pink), S-10 ref (yellow), S-11 sky (grey), S-11 ref (black)

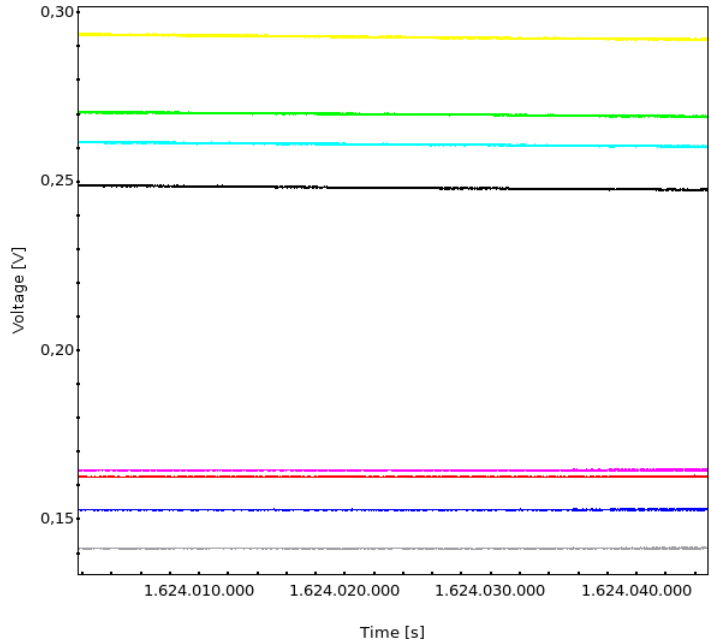

Figure 16 – Feed 25: M-00 sky (red), M-00 ref (green), M-01sky (blue), M-01 ref (cyan), S-10 sky (pink), S-10 ref (yellow), S-11 sky (grey), S-11 ref (black)

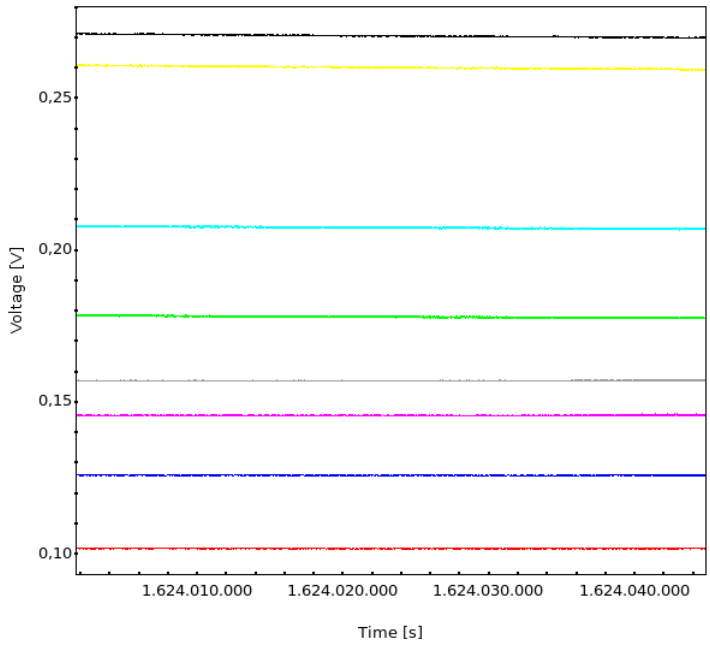

Figure 17 – Feed 26: M-00 sky (red), M-00 ref (green), M-01sky (blue), M-01 ref (cyan), S-10 sky (pink), S-10 ref (yellow), S-11 sky (grey), S-11 ref (black)

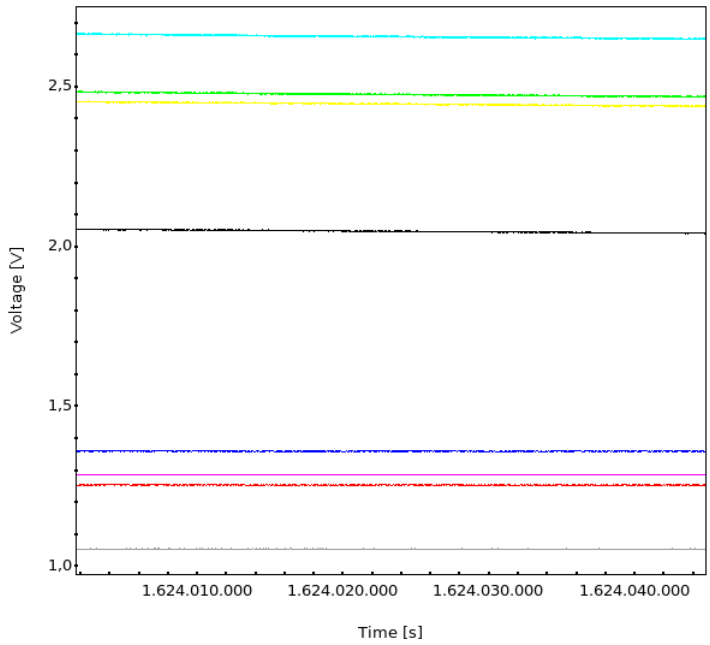

Figure 18 – Feed 27: M-00 sky (red), M-00 ref (green), M-01sky (blue), M-01 ref (cyan), S-10 sky (pink), S-10 ref (yellow), S-11 sky (grey), S-11 ref (black)

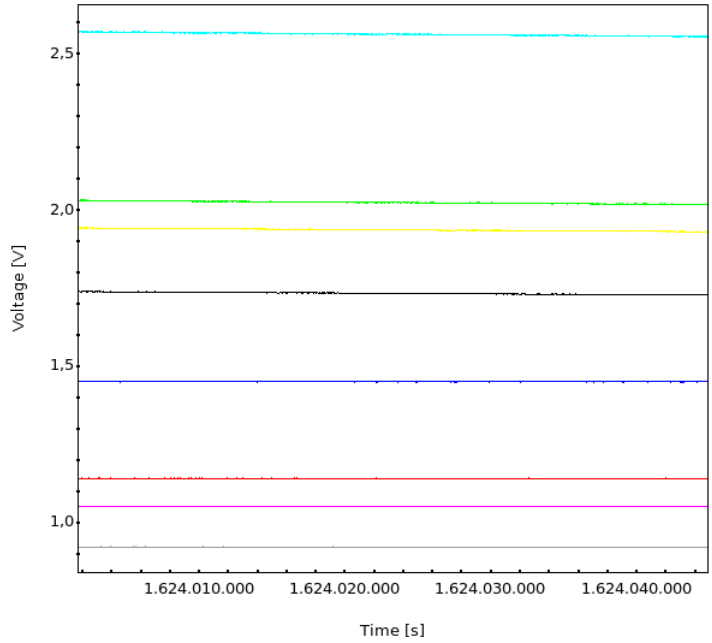

Figure 19 – Feed 28: M-00 sky (red), M-00 ref (green), M-01sky (blue), M-01 ref (cyan), S-10 sky (pink), S-10 ref (yellow), S-11 sky (grey), S-11 ref (black)

Appendix 2 – Power spectra with frequency spikes

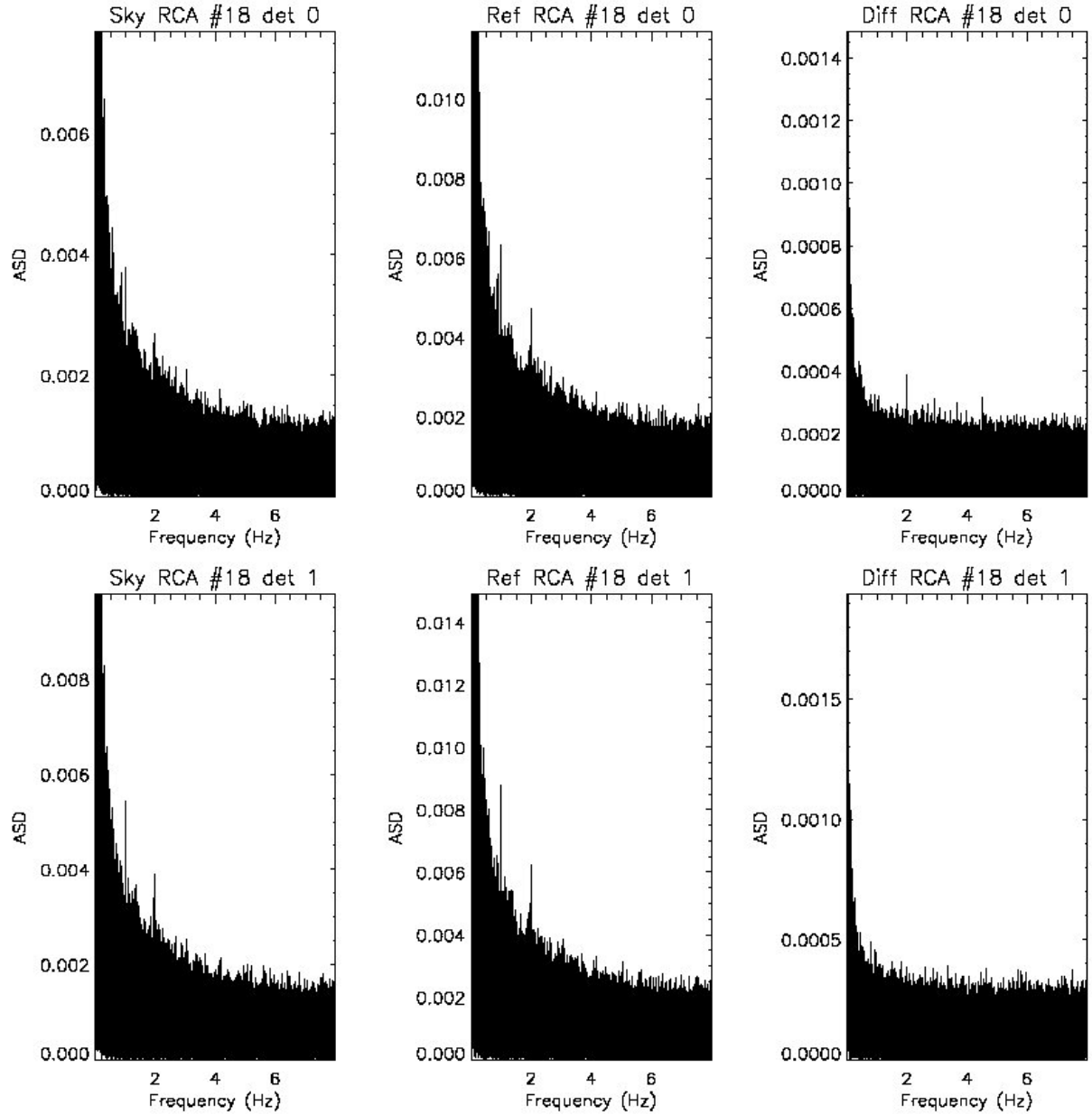

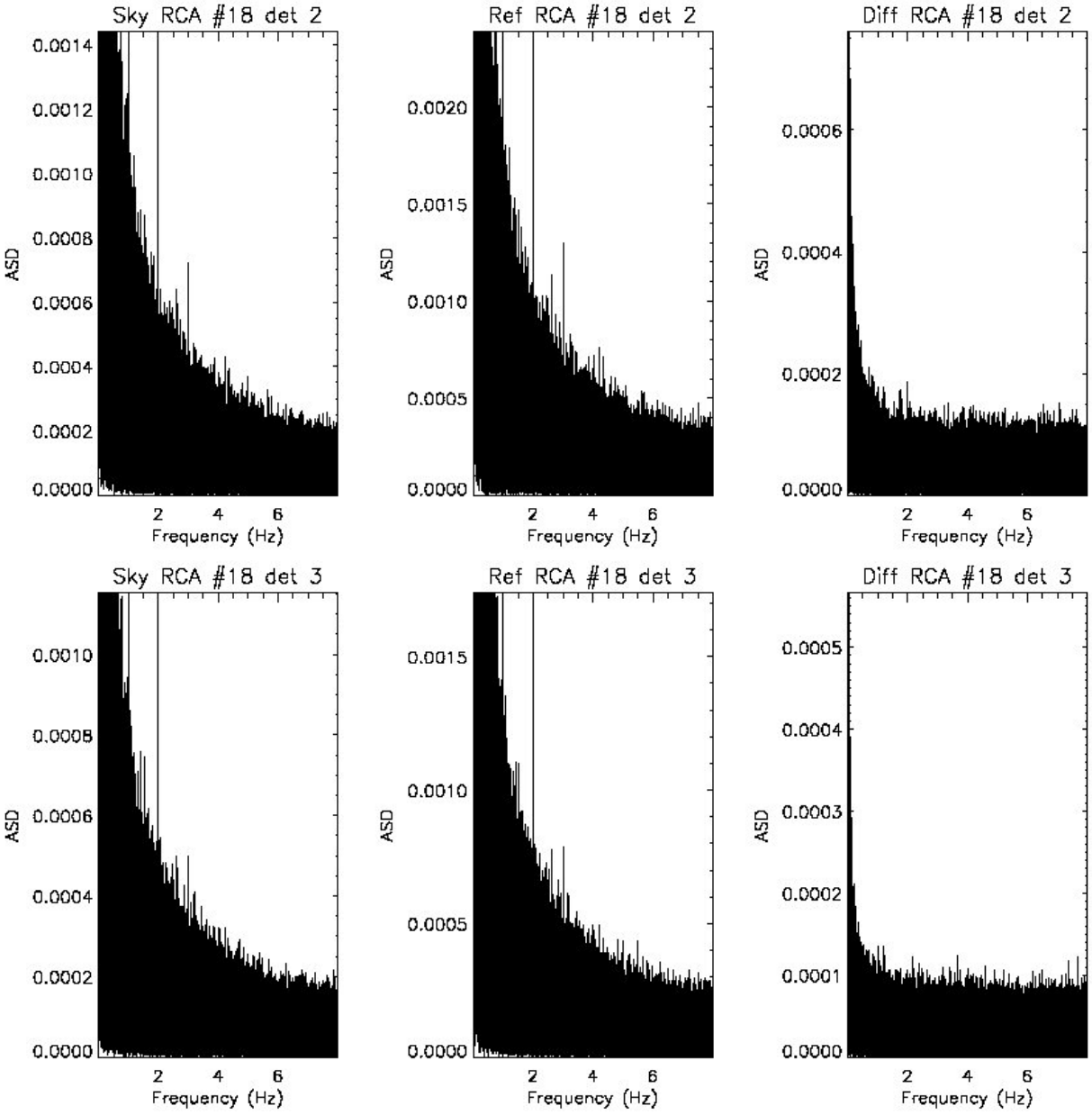
Sky RCA #18 det 2
Ref RCA #18 det 2
Diff RCA #18 det 2
Sky RCA #18 det 3
Ref RCA #18 det 3
Diff RCA #18 det 3
ASD
Frequency (Hz)

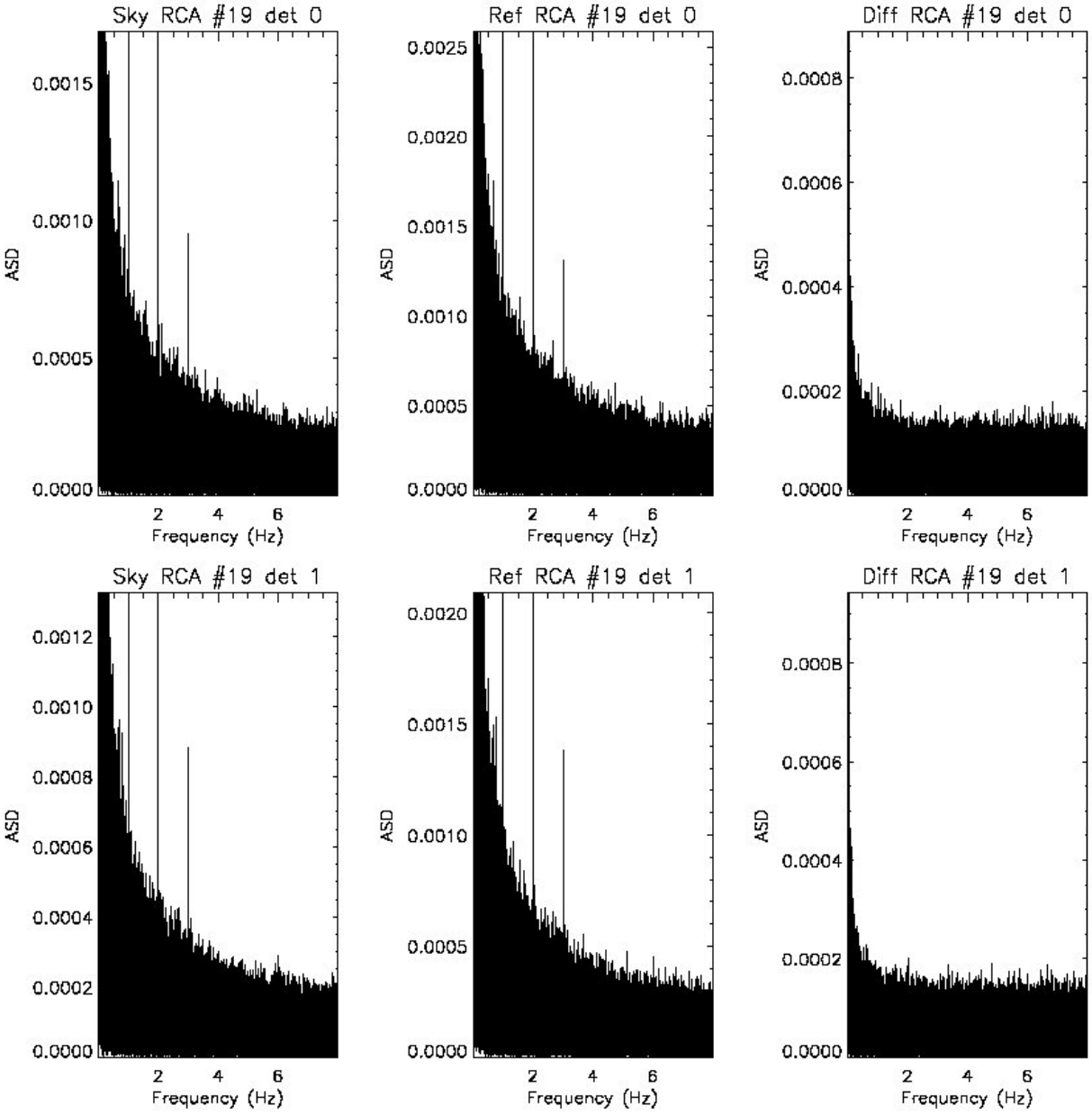
Sky RCA #19 det 0
Ref RCA #19 det 0
Diff RCA #19 det 0
Sky RCA #19 det 1
Ref RCA #19 det 1
Diff RCA #19 det 1
ASD
Frequency (Hz)

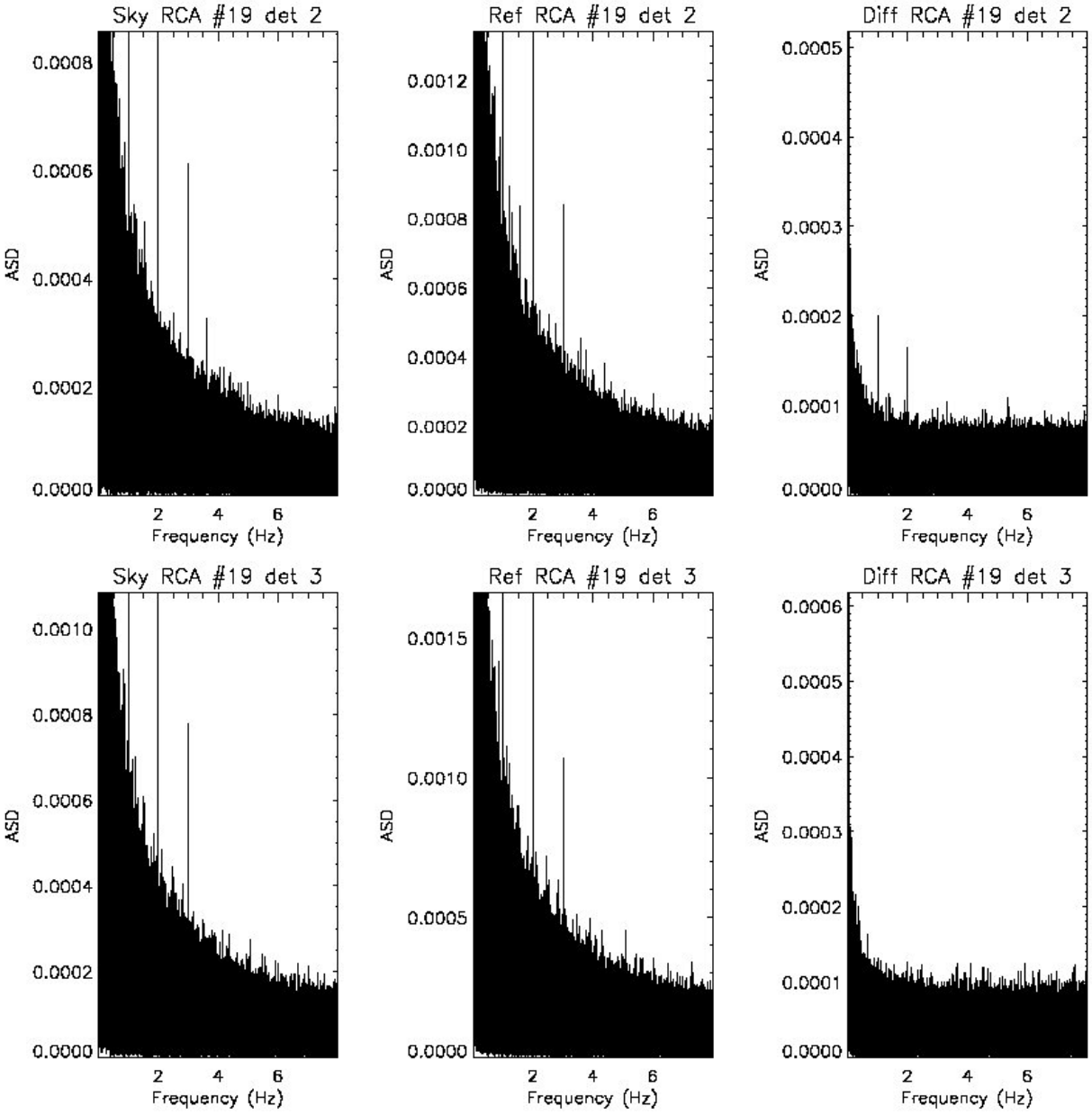
Sky RCA #19 det 2
Ref RCA #19 det 2
Diff RCA #19 det 2
Sky RCA #19 det 3
Ref RCA #19 det 3
Diff RCA #19 det 3
ASD
Frequency (Hz)

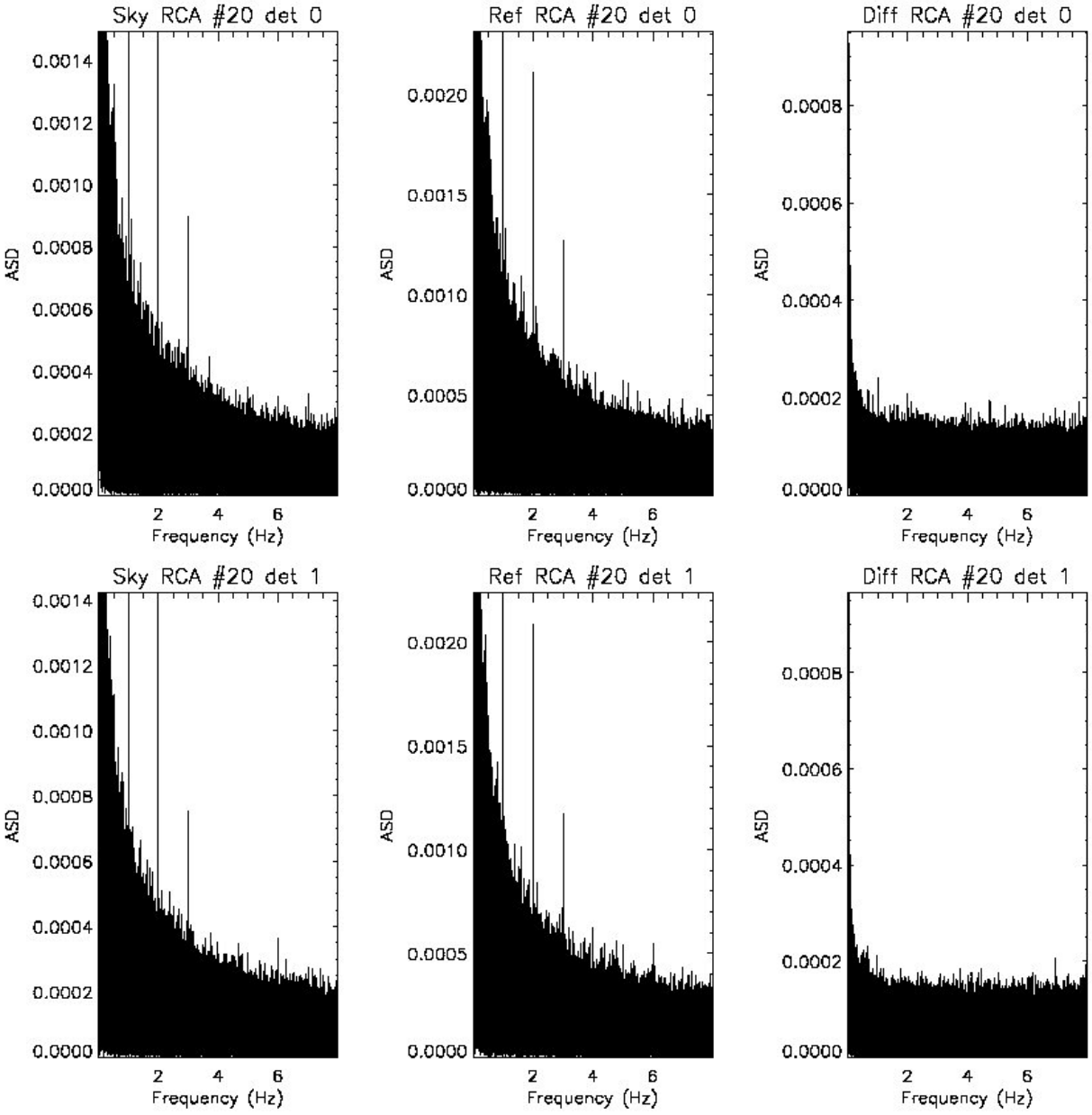
Sky RCA #20 det 0
Ref RCA #20 det 0
Diff RCA #20 det 0
Sky RCA #20 det 1
Ref RCA #20 det 1
Diff RCA #20 det 1
ASD
Frequency (Hz)

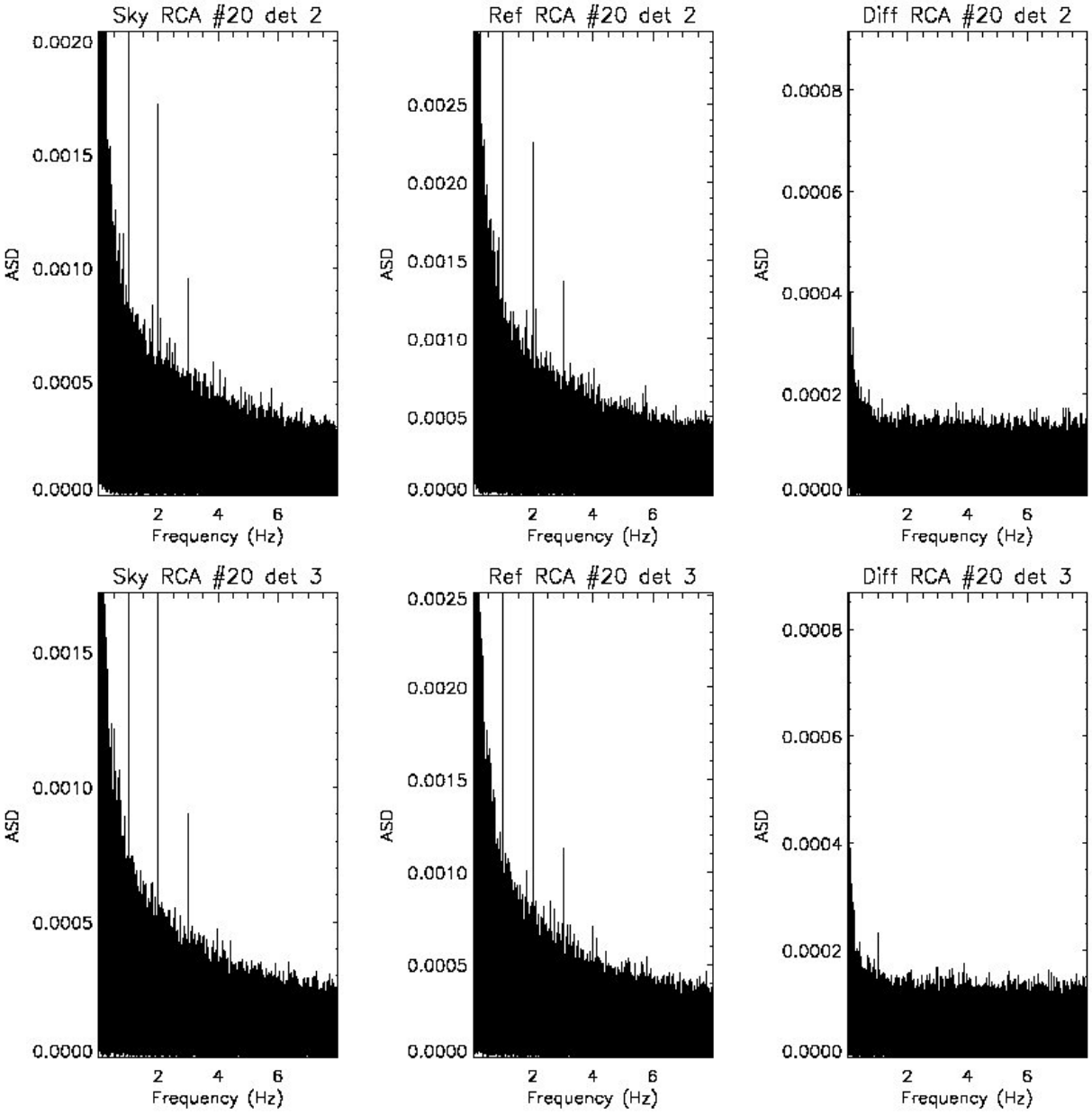
Sky RCA #20 det 2
Ref RCA #20 det 2
Diff RCA #20 det 2
Sky RCA #20 det 3
Ref RCA #20 det 3
Diff RCA #20 det 3
ASD
Frequency (Hz)

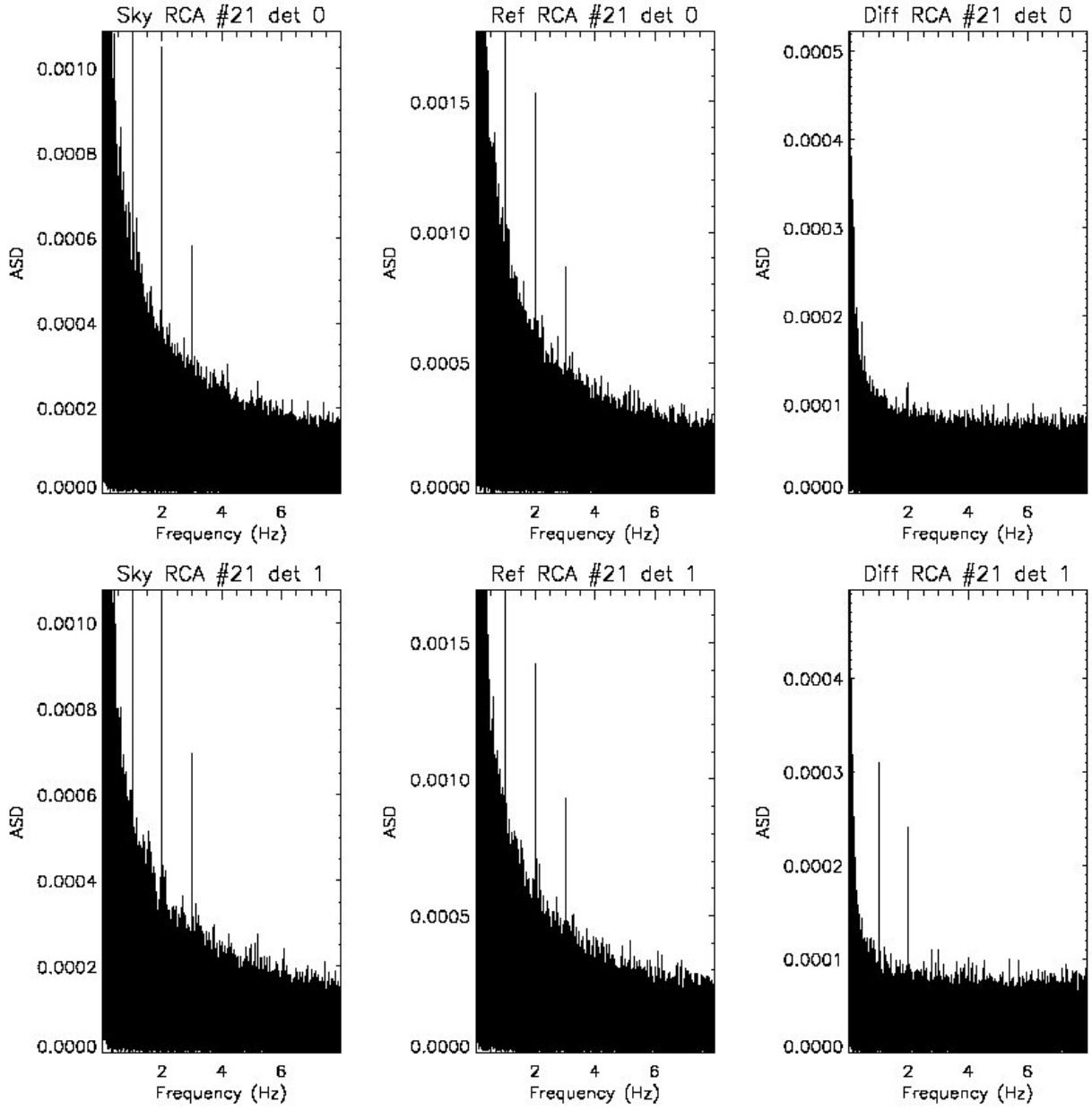
Sky RCA #21 det 0
Ref RCA #21 det 0
Diff RCA #21 det 0
Sky RCA #21 det 1
Ref RCA #21 det 1
Diff RCA #21 det 1
ASD
Frequency (Hz)

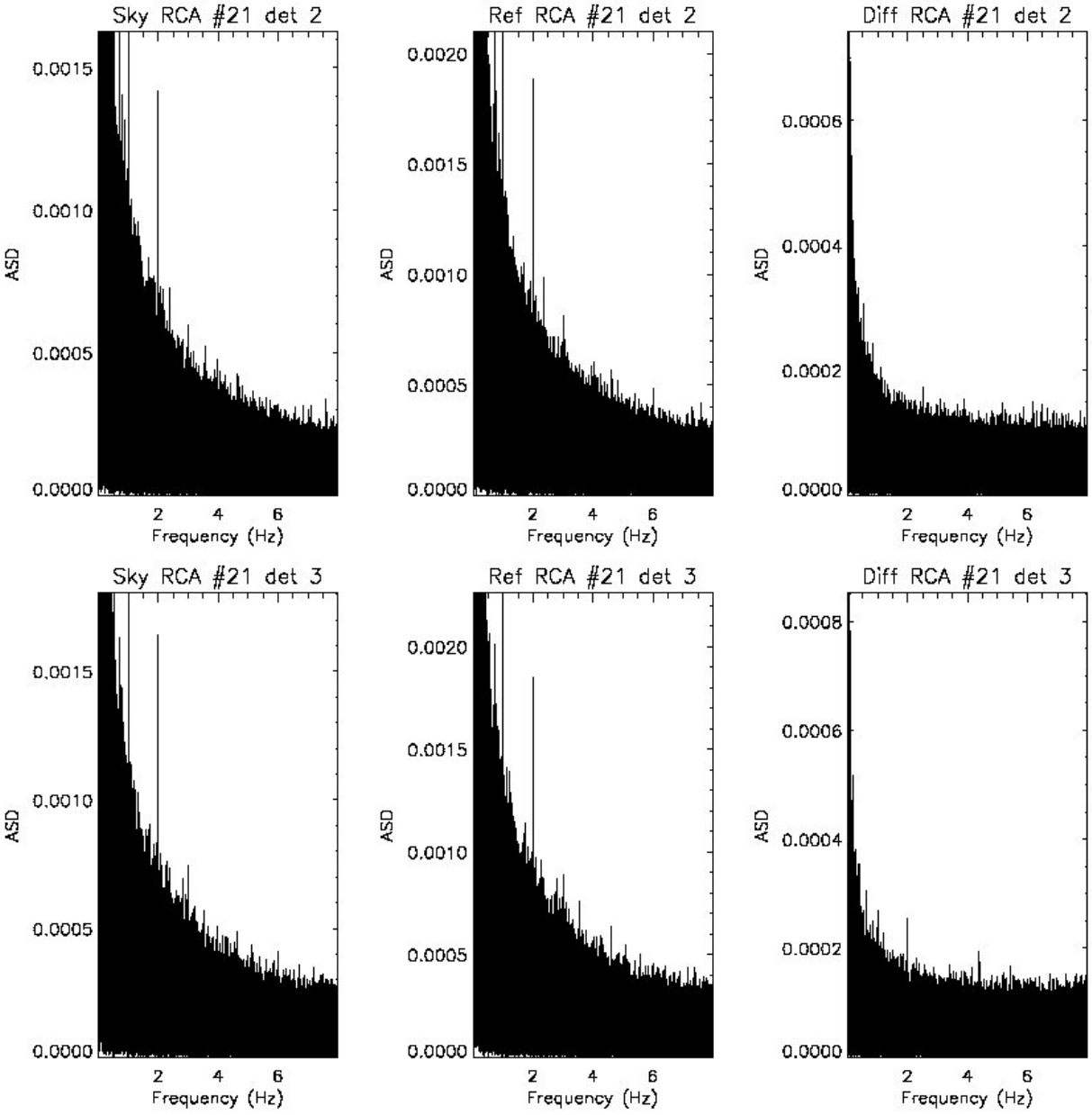
Sky RCA #21 det 2
Ref RCA #21 det 2
Diff RCA #21 det 2
Sky RCA #21 det 3
Ref RCA #21 det 3
Diff RCA #21 det 3
ASD
Frequency (Hz)
0.0000
0.0005
0.0010
0.0015
0.0020
0.0002
0.0004
0.0006
0.0008
2
4
6

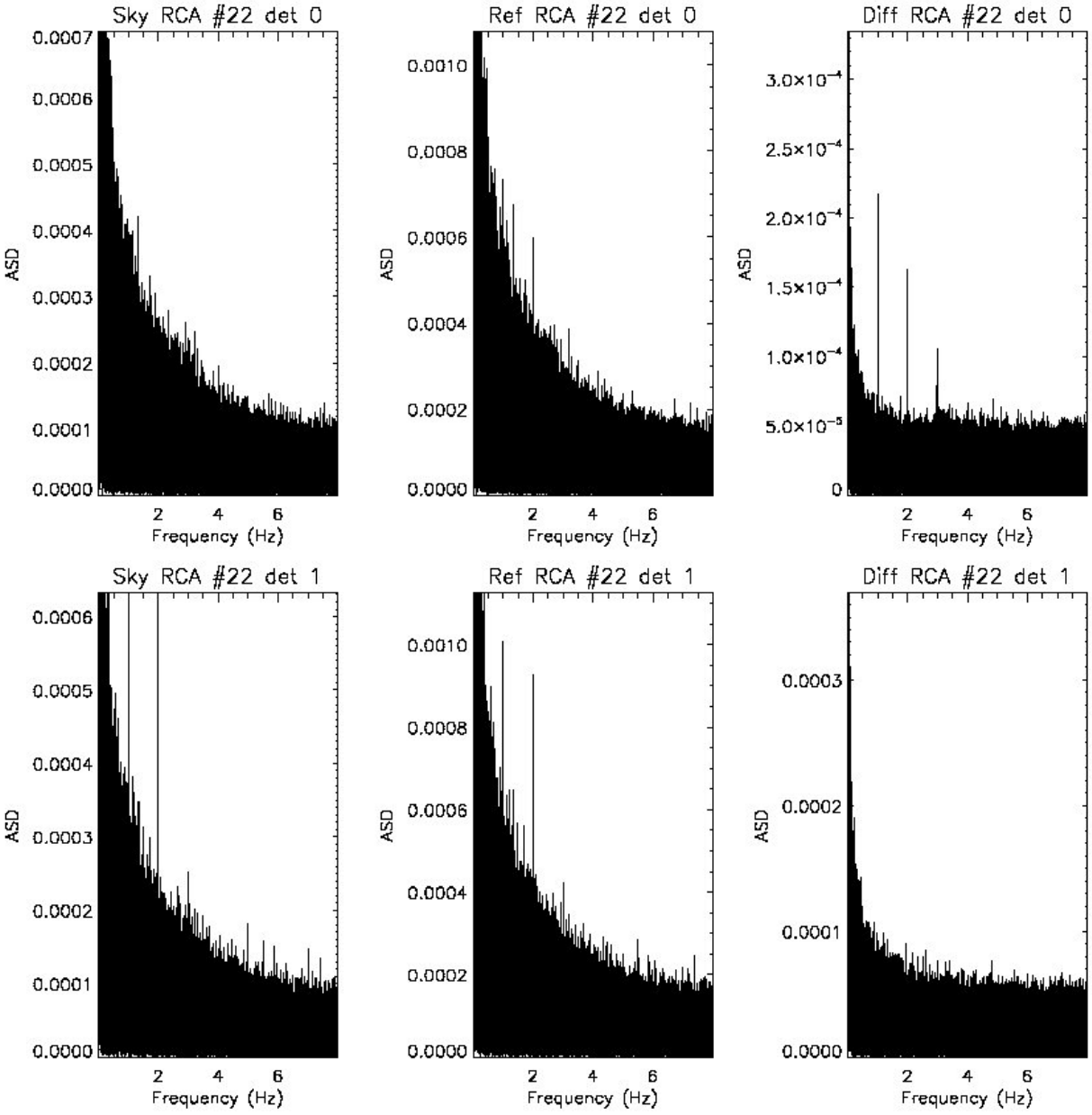
Sky RCA #22 det 0
Ref RCA #22 det 0
Diff RCA #22 det 0
Sky RCA #22 det 1
Ref RCA #22 det 1
Diff RCA #22 det 1
ASD
Frequency (Hz)

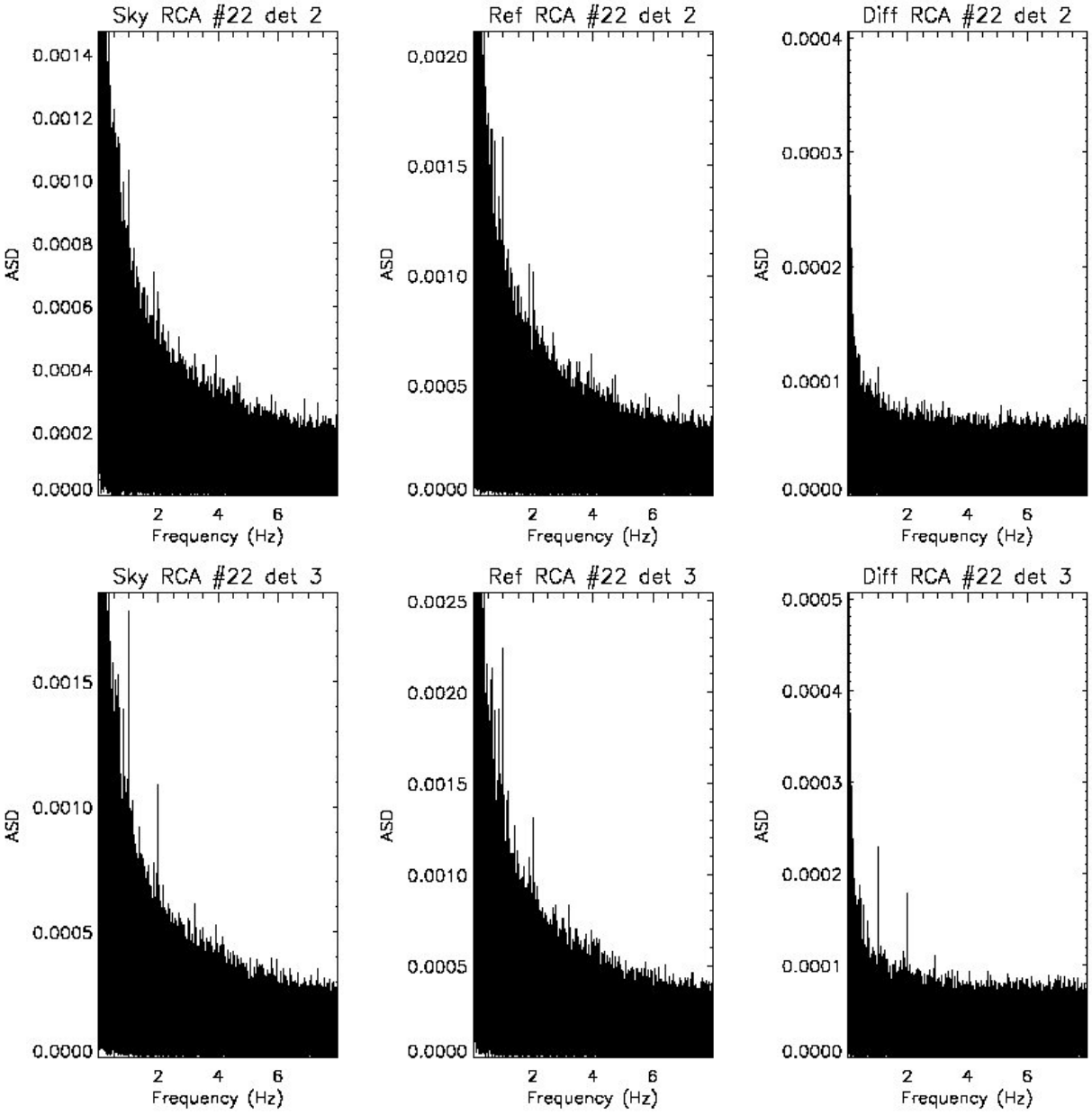
Sky RCA #22 det 2
Ref RCA #22 det 2
Diff RCA #22 det 2
Sky RCA #22 det 3
Ref RCA #22 det 3
Diff RCA #22 det 3
ASD
Frequency (Hz)

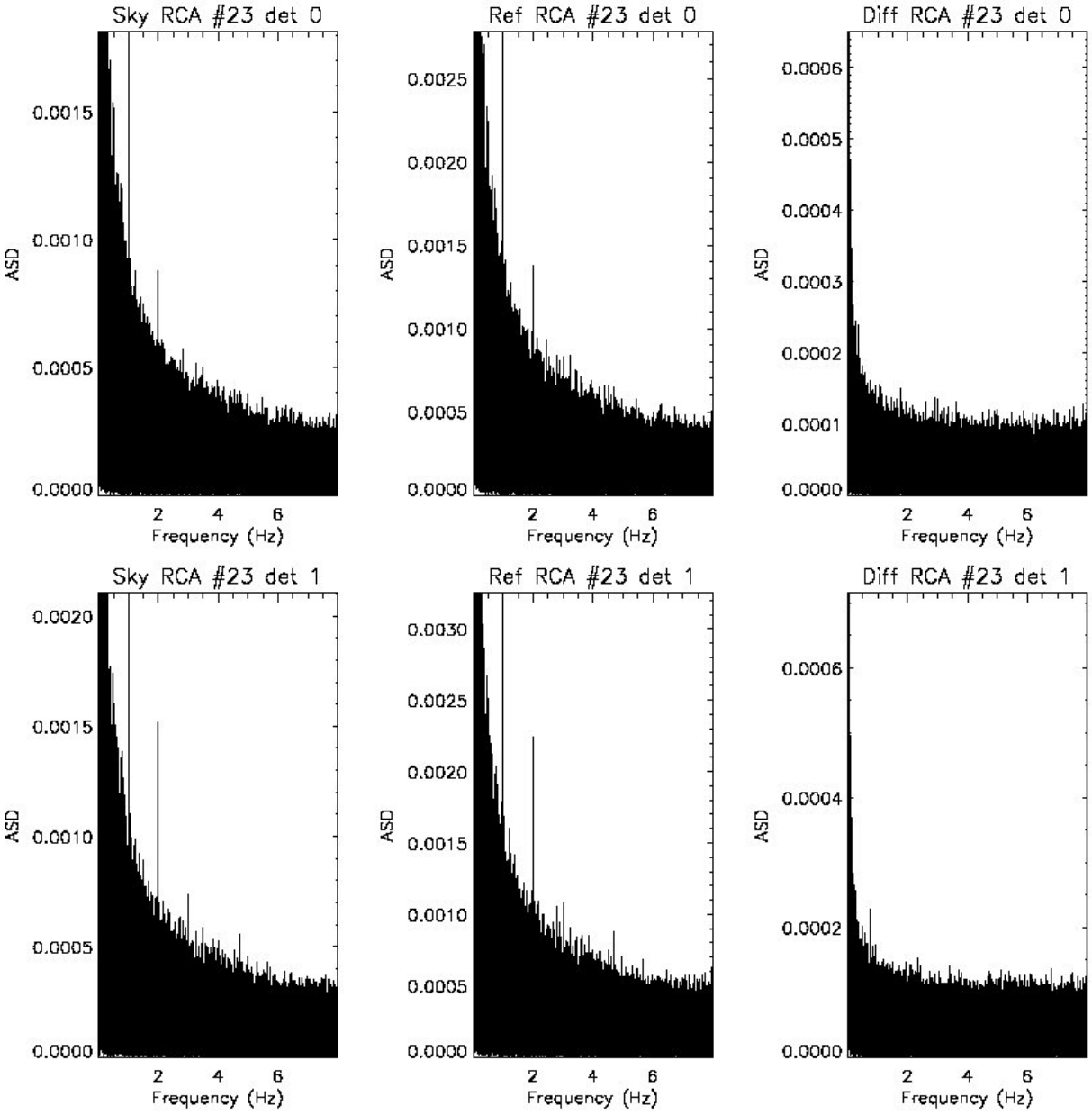
Sky RCA #23 det 0
Ref RCA #23 det 0
Diff RCA #23 det 0
Sky RCA #23 det 1
Ref RCA #23 det 1
Diff RCA #23 det 1
ASD
Frequency (Hz)

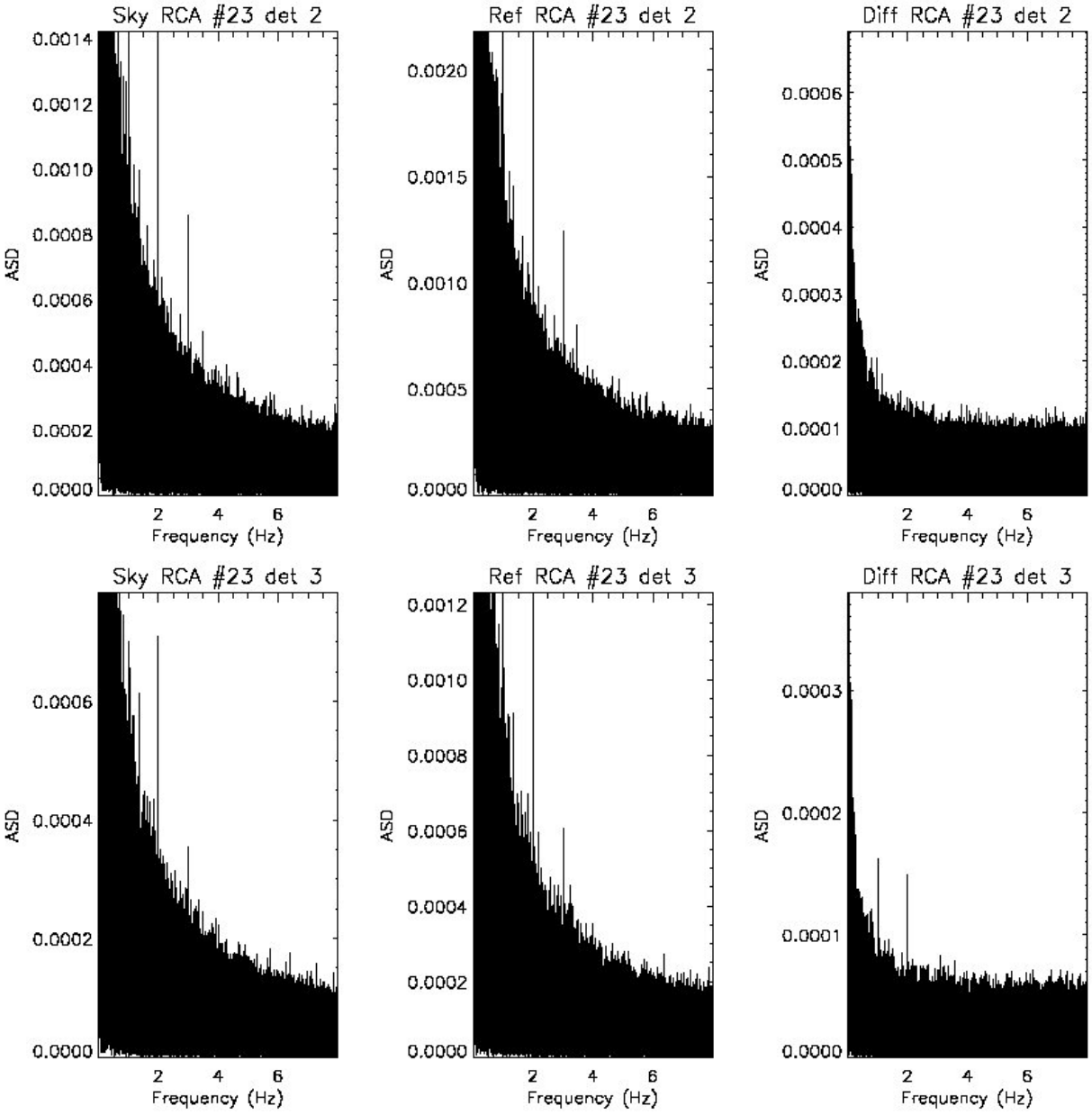
Sky RCA #23 det 2
Ref RCA #23 det 2
Diff RCA #23 det 2
Sky RCA #23 det 3
Ref RCA #23 det 3
Diff RCA #23 det 3
ASD
Frequency (Hz)

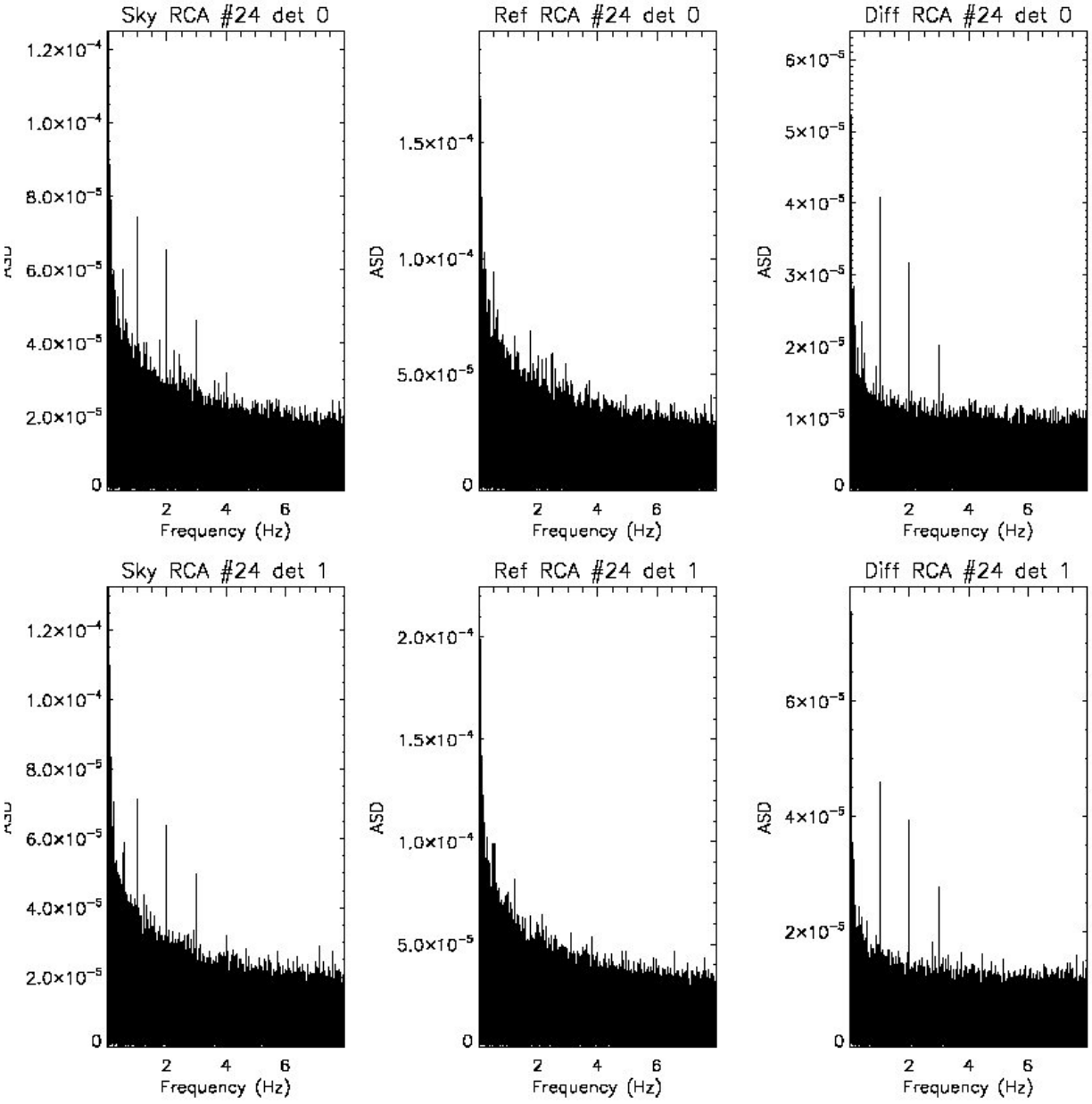
Sky RCA #24 det 0
Ref RCA #24 det 0
Diff RCA #24 det 0
Sky RCA #24 det 1
Ref RCA #24 det 1
Diff RCA #24 det 1
ASD
Frequency (Hz)

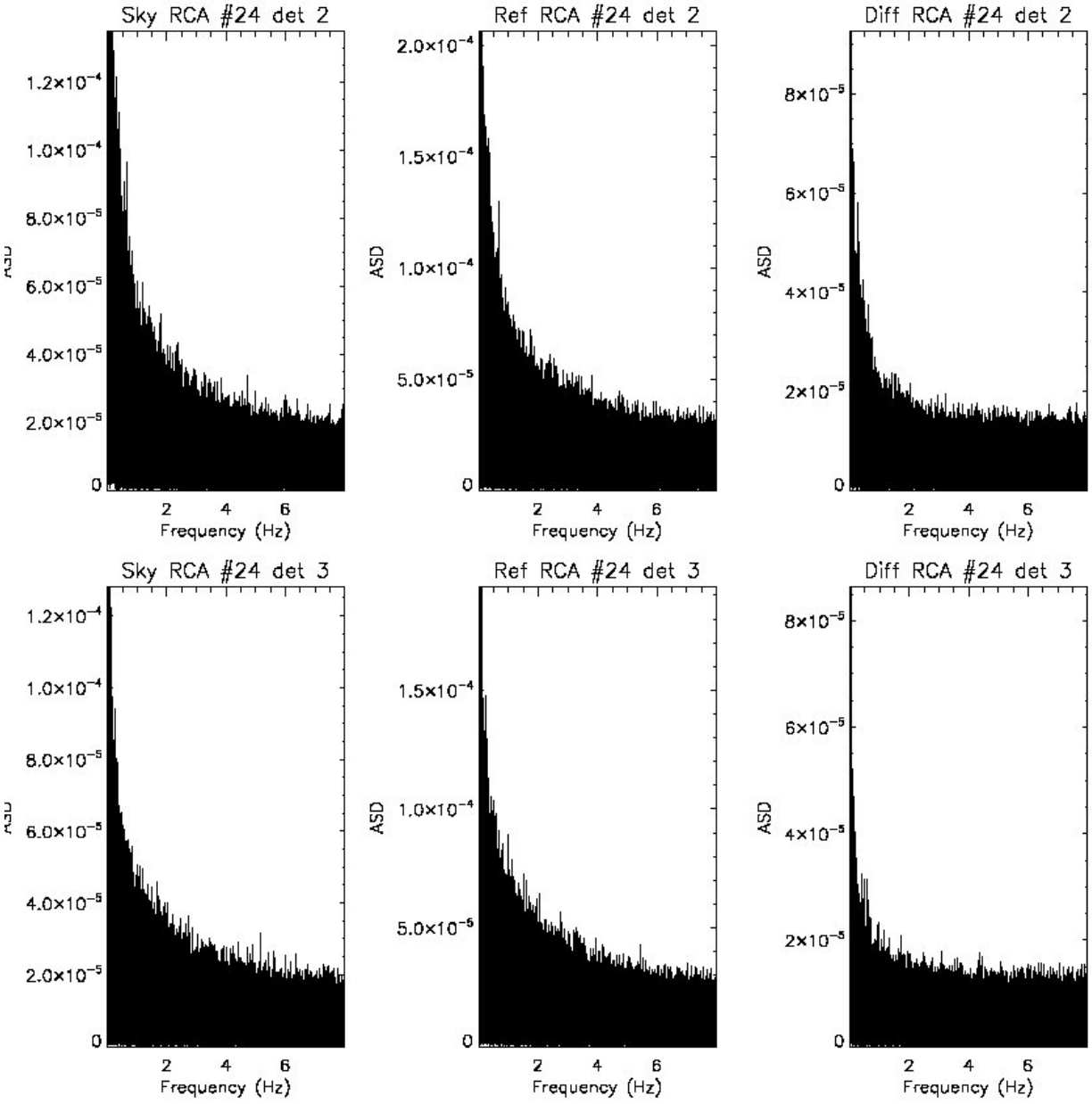
Sky RCA #24 det 2
Ref RCA #24 det 2
Diff RCA #24 det 2
Sky RCA #24 det 3
Ref RCA #24 det 3
Diff RCA #24 det 3
ASD
Frequency (Hz)

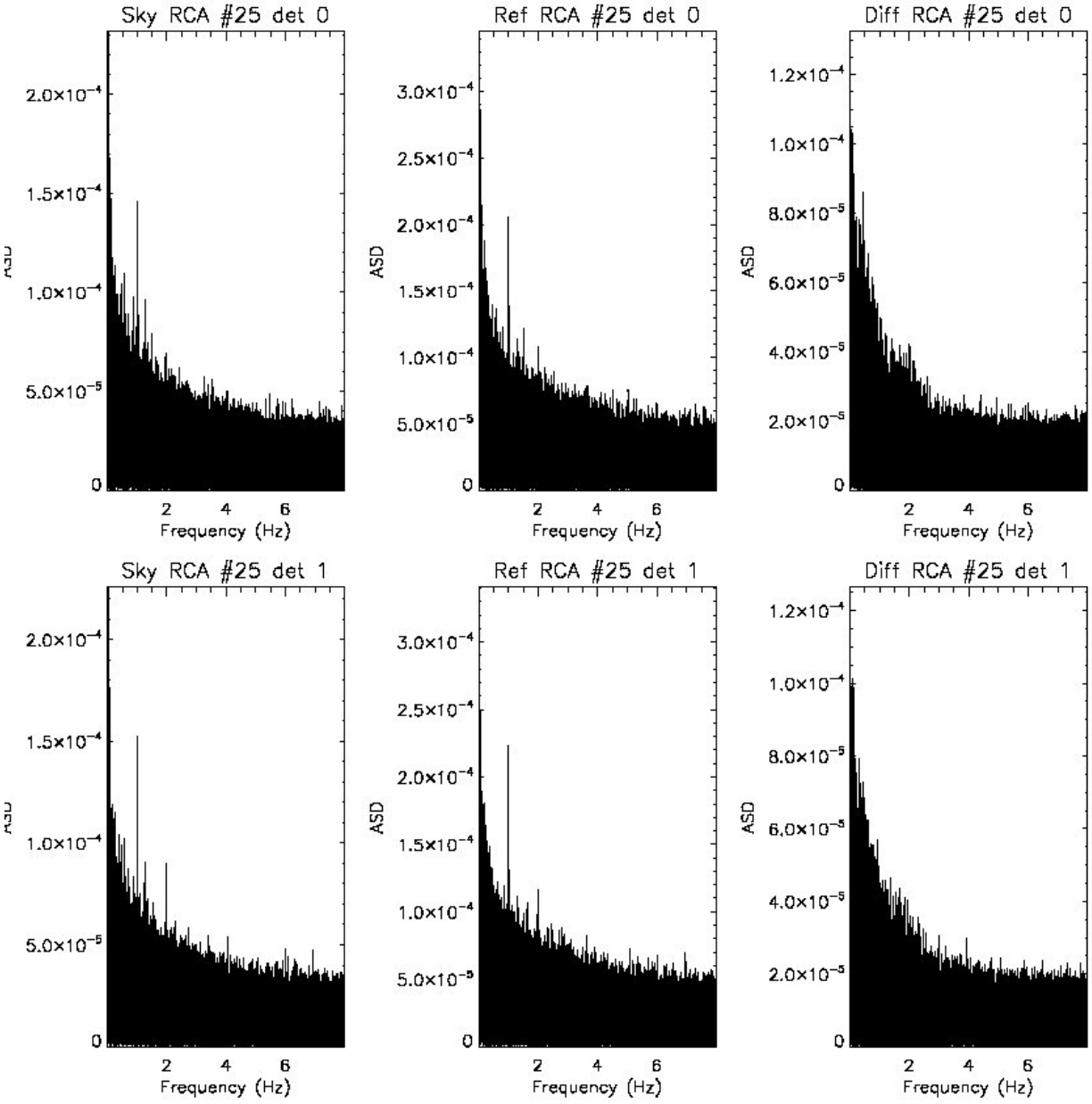
Sky RCA #25 det 0
Ref RCA #25 det 0
Diff RCA #25 det 0
Sky RCA #25 det 1
Ref RCA #25 det 1
Diff RCA #25 det 1
ASD
Frequency (Hz)

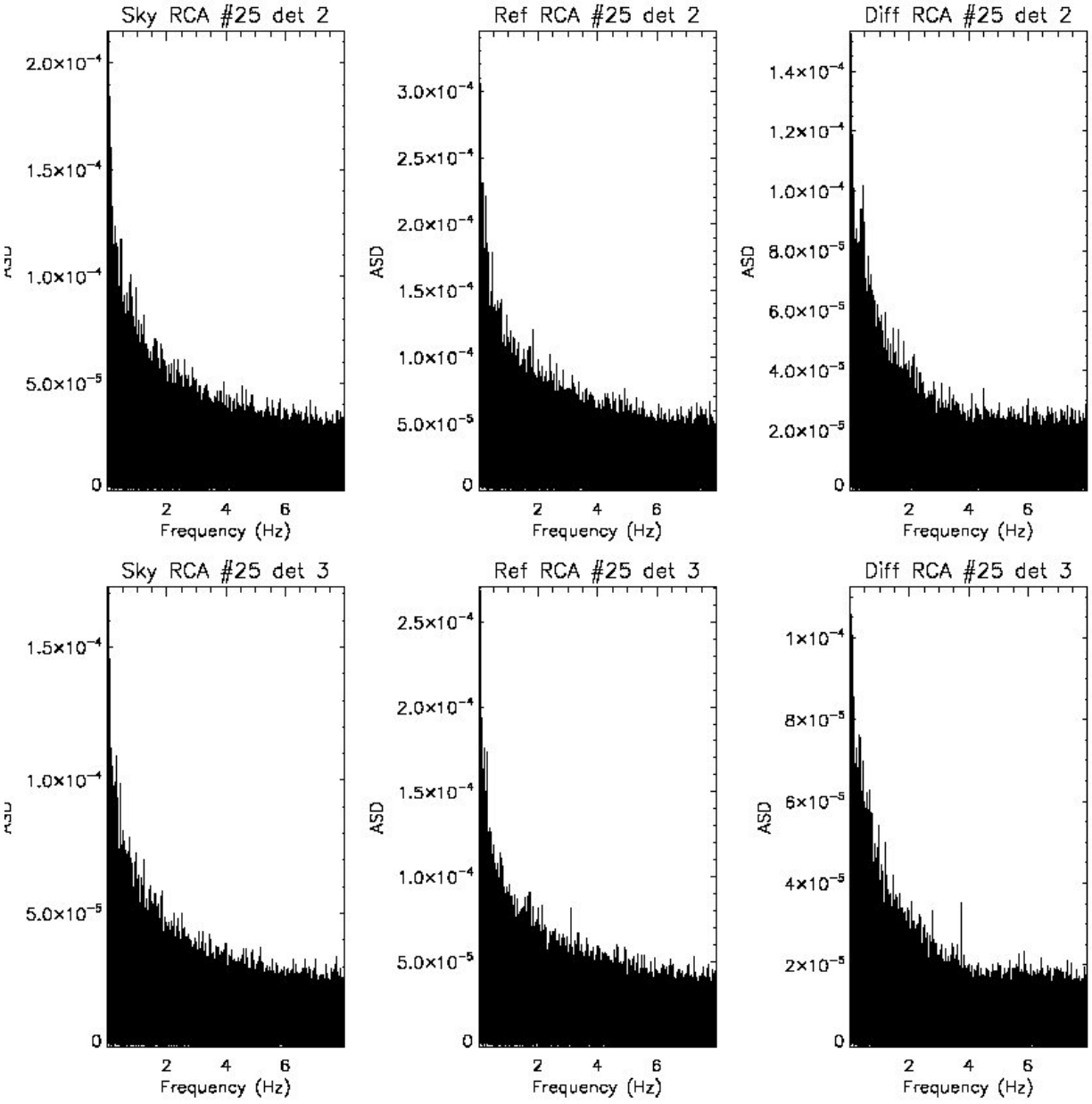
Sky RCA #25 det 2
Ref RCA #25 det 2
Diff RCA #25 det 2
Sky RCA #25 det 3
Ref RCA #25 det 3
Diff RCA #25 det 3
ASD
Frequency (Hz)

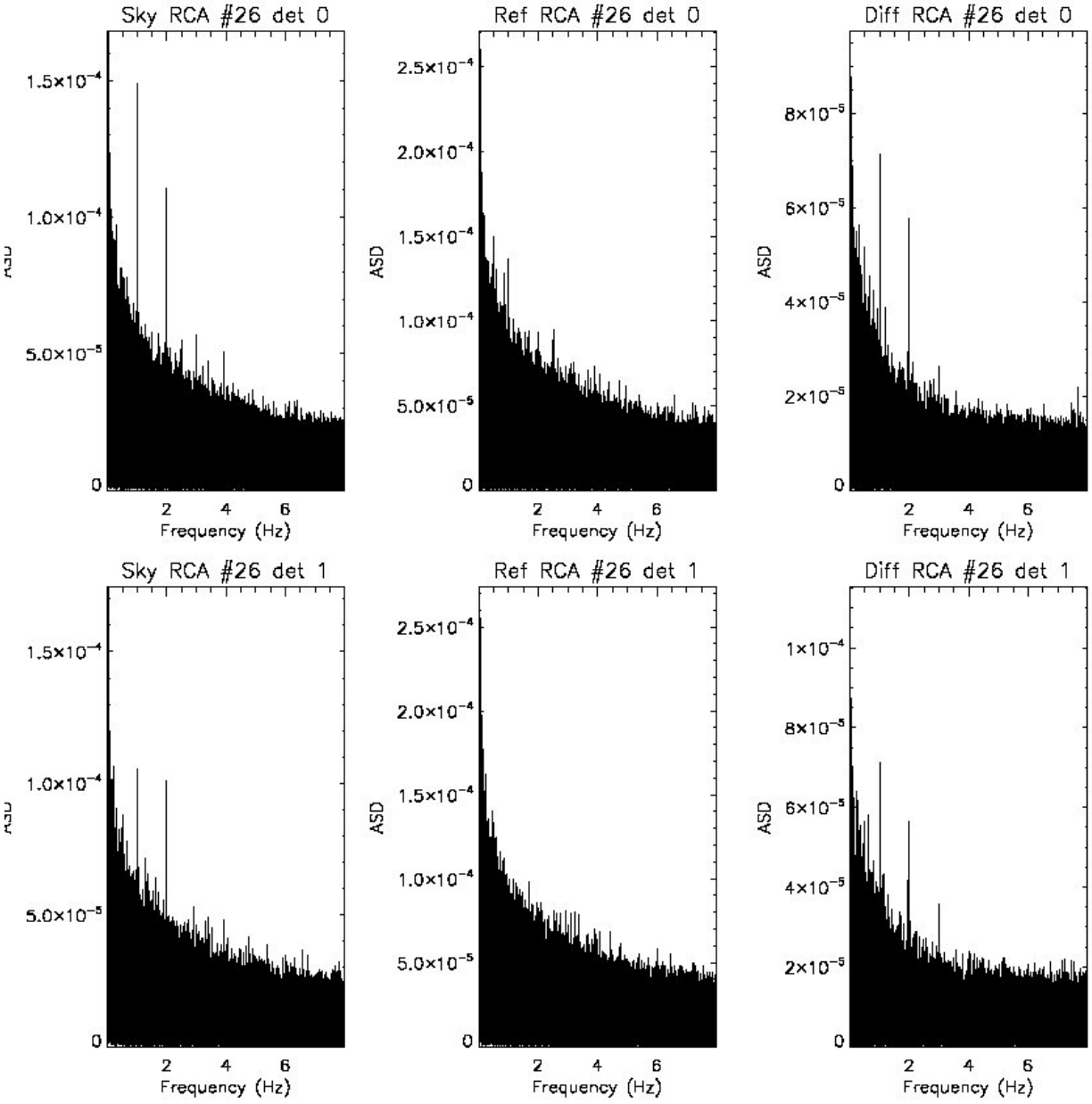
Sky RCA #26 det 0
Ref RCA #26 det 0
Diff RCA #26 det 0
Sky RCA #26 det 1
Ref RCA #26 det 1
Diff RCA #26 det 1
ASD
Frequency (Hz)

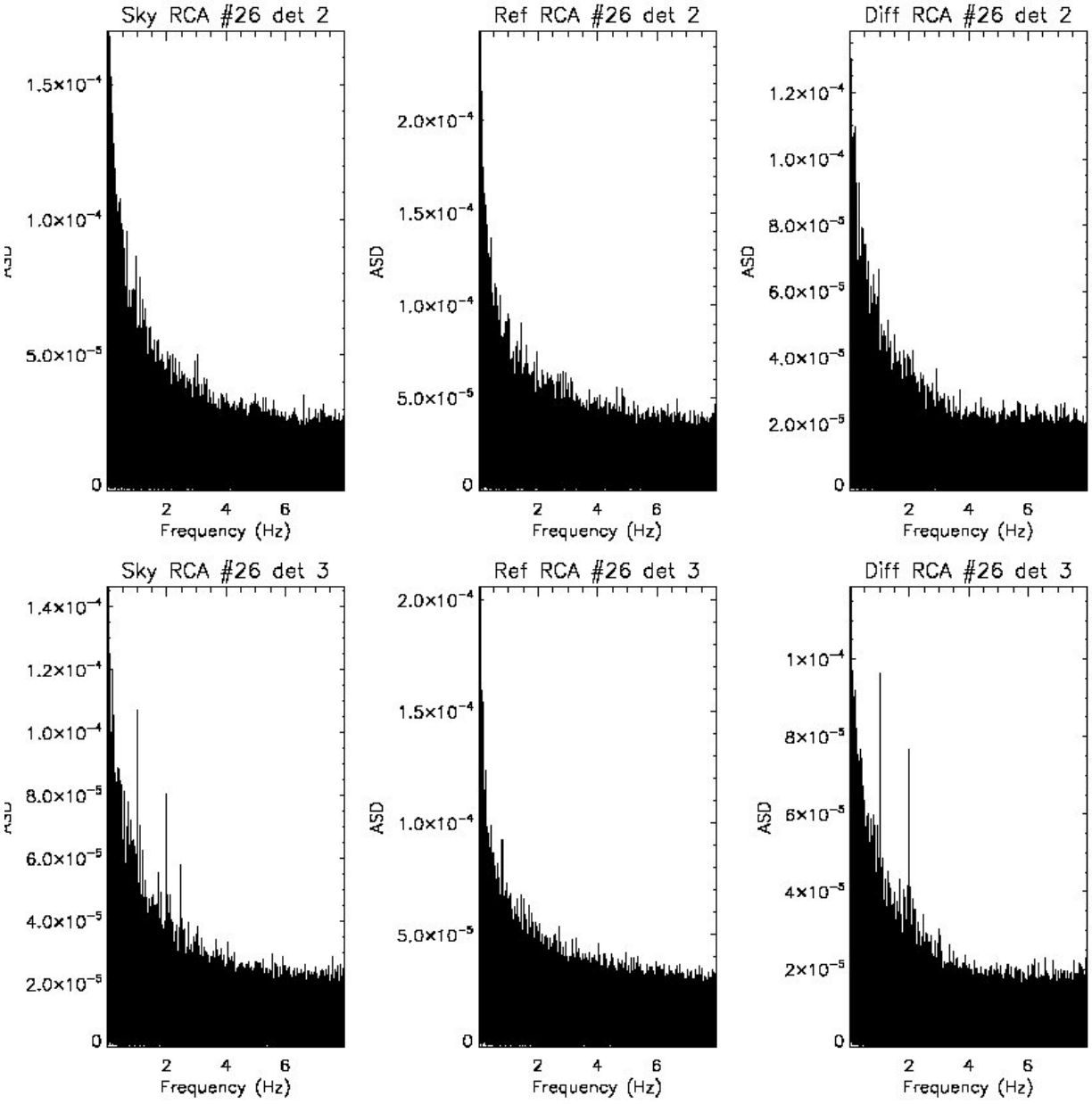
Sky RCA #26 det 2
Ref RCA #26 det 2
Diff RCA #26 det 2
Sky RCA #26 det 3
Ref RCA #26 det 3
Diff RCA #26 det 3
ASD
Frequency (Hz)

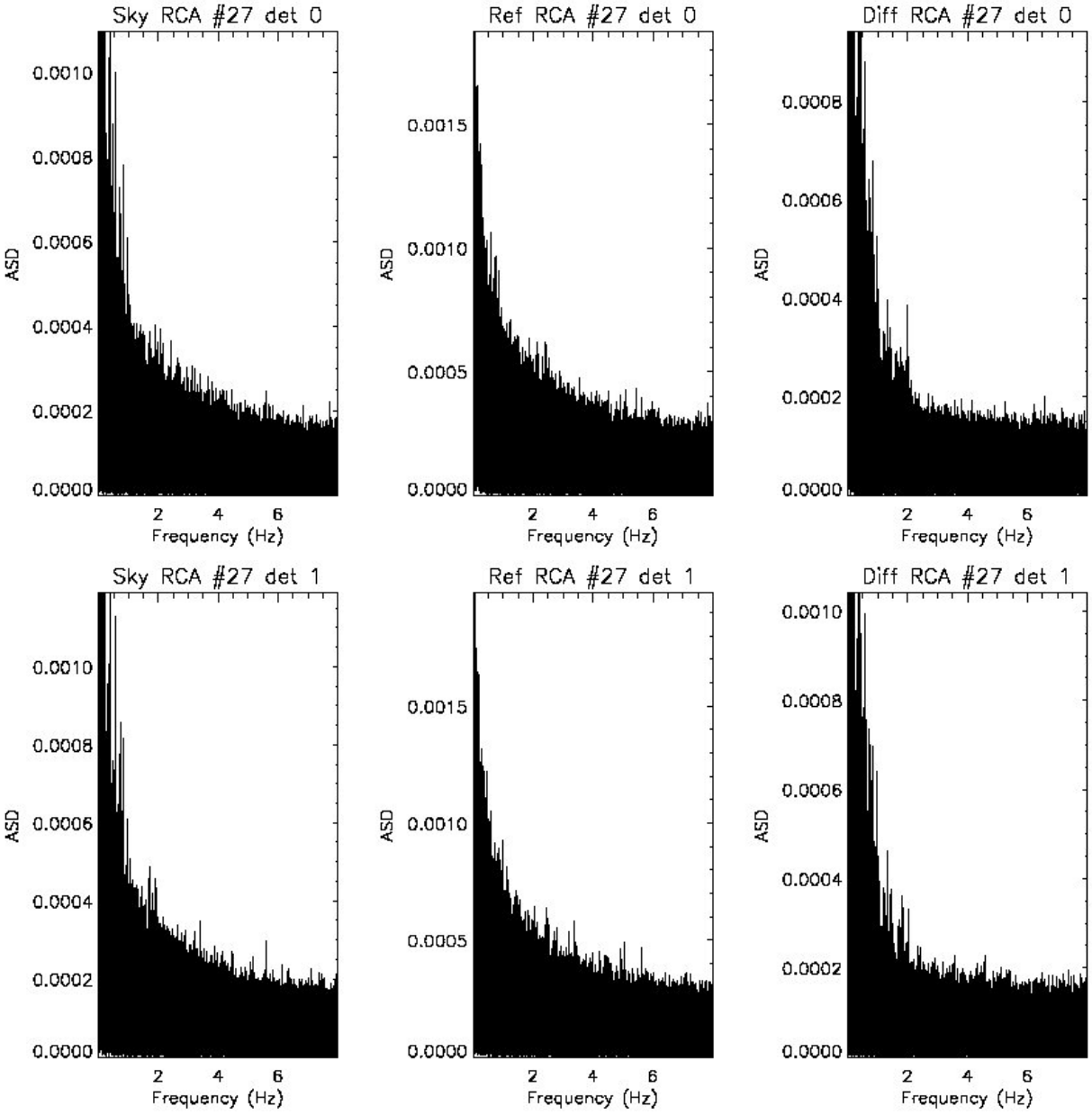
Sky RCA #27 det 0
Ref RCA #27 det 0
Diff RCA #27 det 0
Sky RCA #27 det 1
Ref RCA #27 det 1
Diff RCA #27 det 1
ASD
Frequency (Hz)

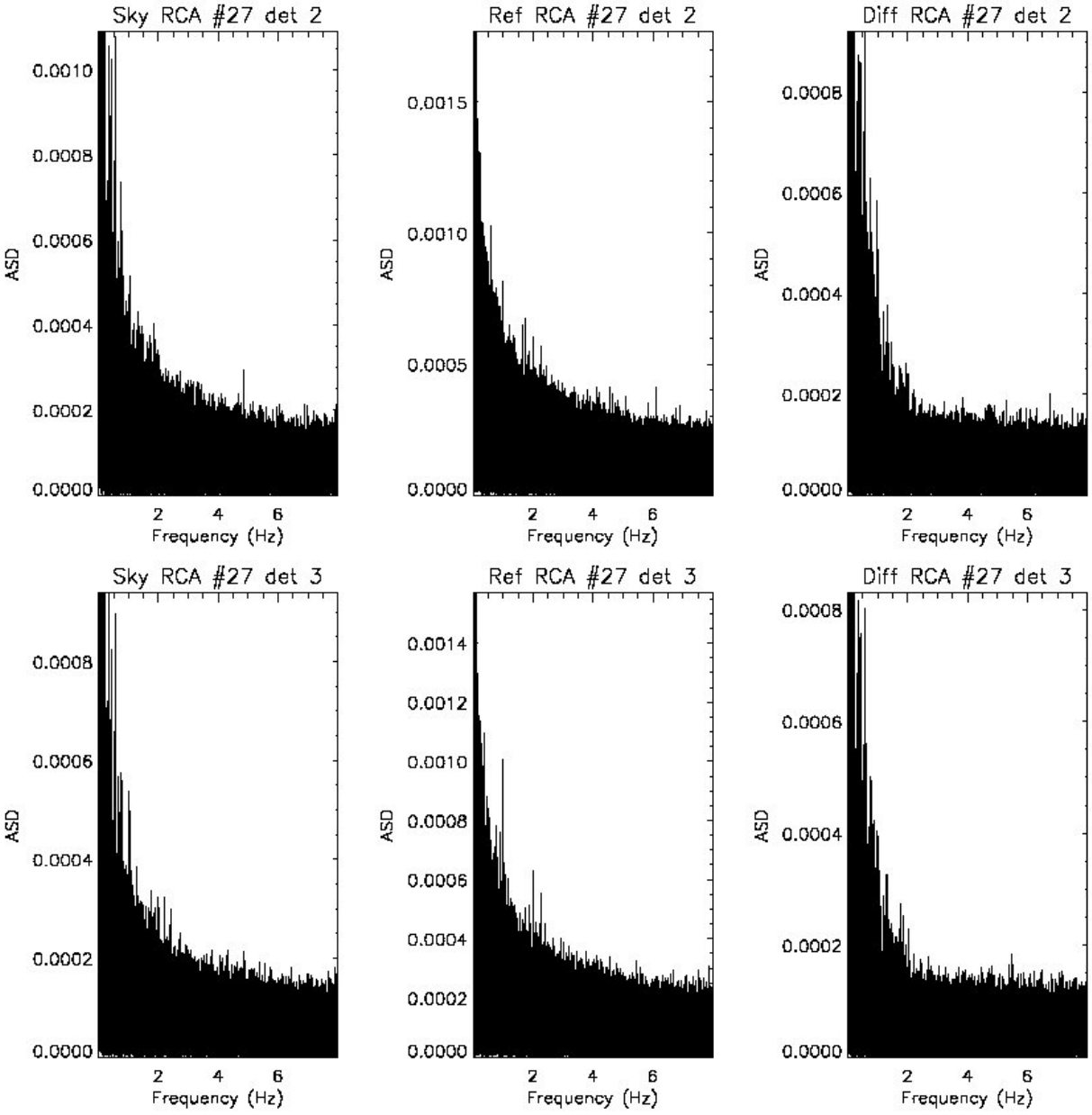
Sky RCA #27 det 2
Ref RCA #27 det 2
Diff RCA #27 det 2
Sky RCA #27 det 3
Ref RCA #27 det 3
Diff RCA #27 det 3
ASD
Frequency (Hz)

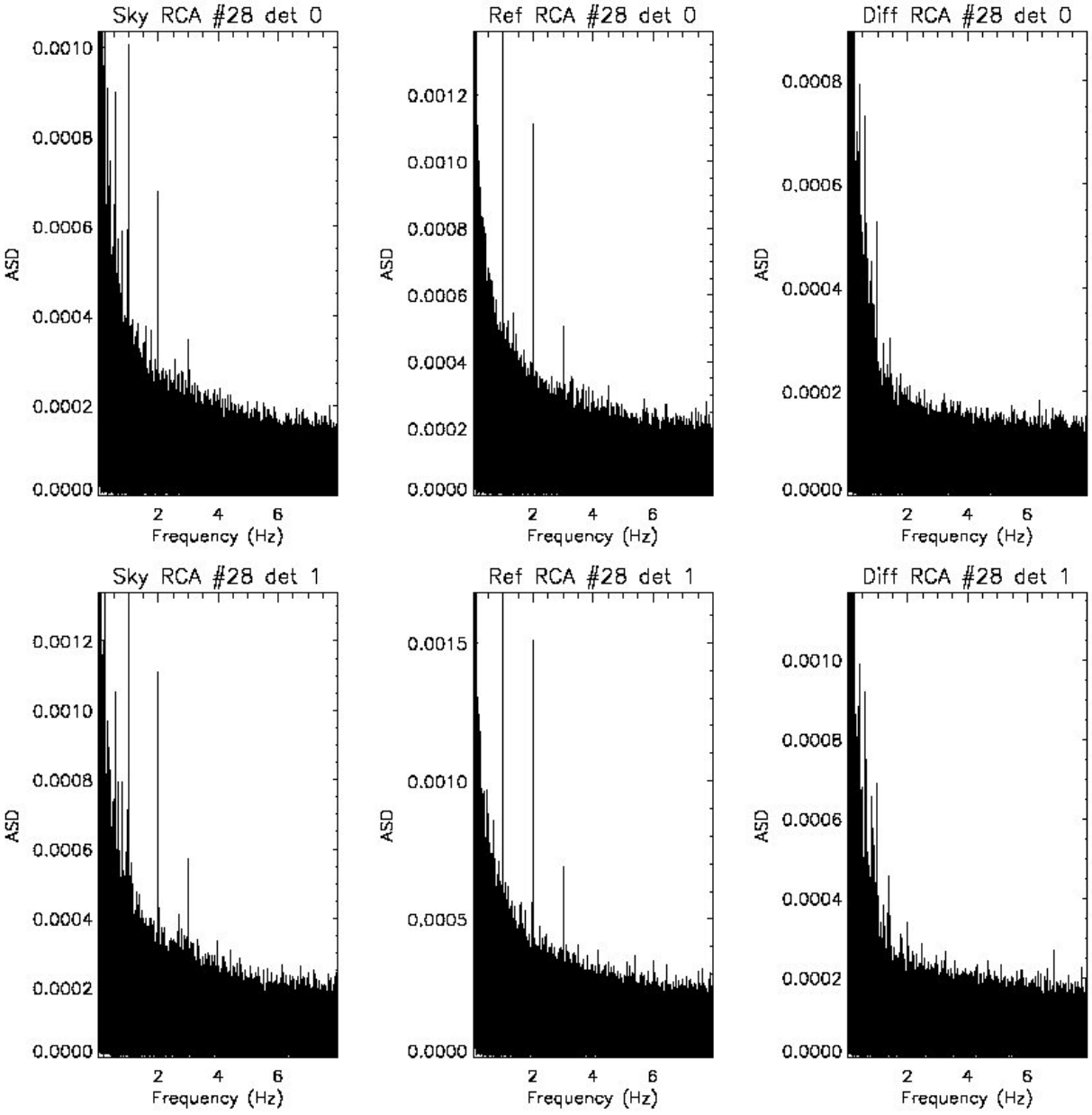
Sky RCA #28 det 0
Ref RCA #28 det 0
Diff RCA #28 det 0
Sky RCA #28 det 1
Ref RCA #28 det 1
Diff RCA #28 det 1
ASD
Frequency (Hz)

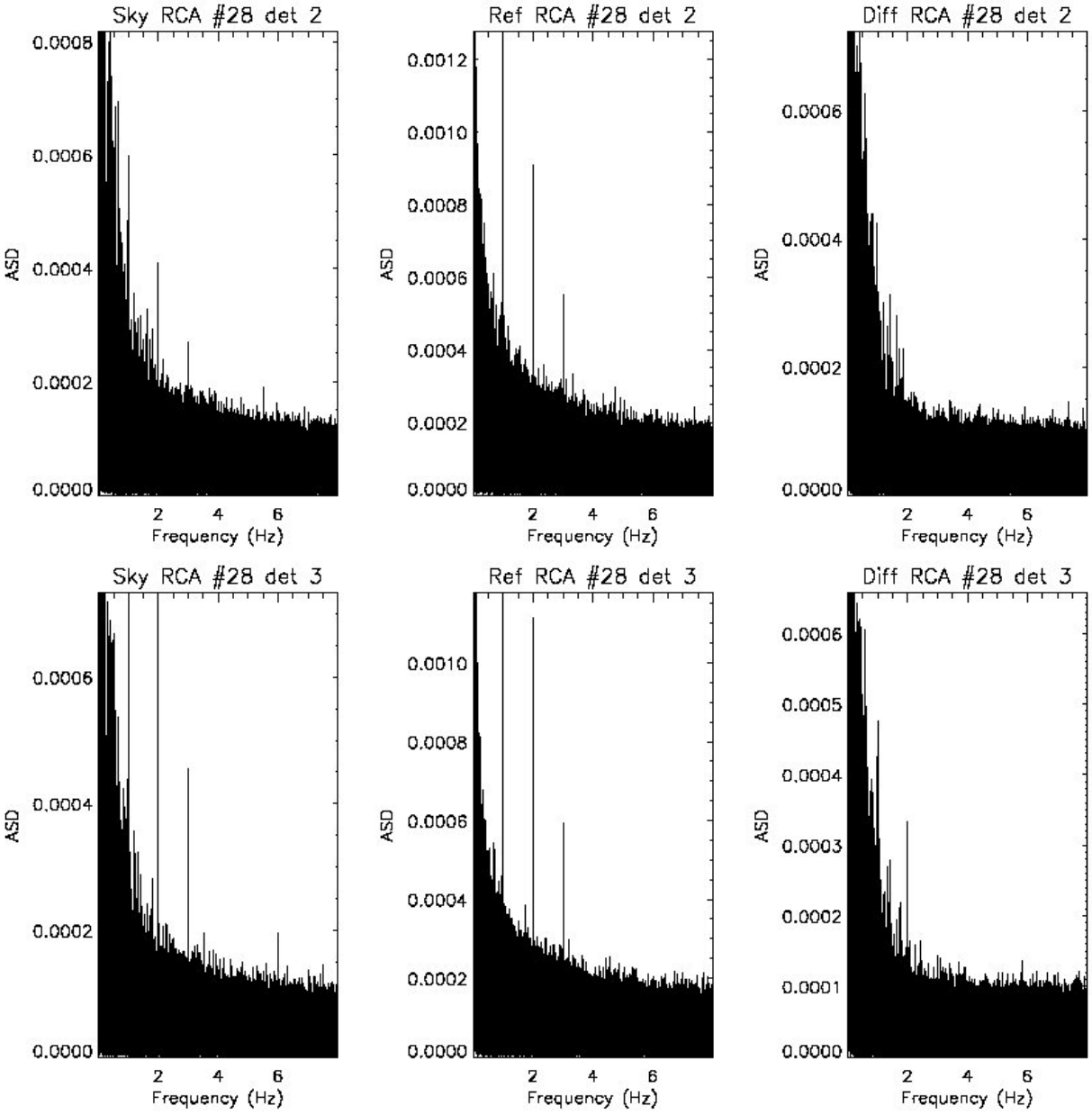
Sky RCA #28 det 2
Ref RCA #28 det 2
Diff RCA #28 det 2
Sky RCA #28 det 3
Ref RCA #28 det 3
Diff RCA #28 det 3
ASD
Frequency (Hz)

Appendix 3 – Power spectra of differenced datastreams

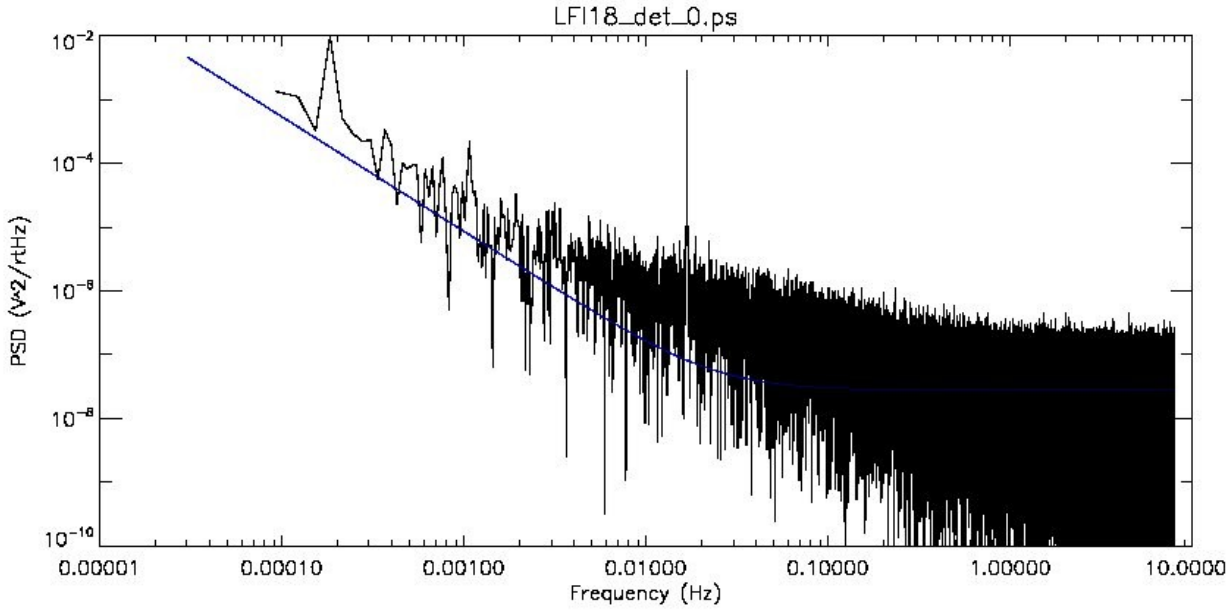

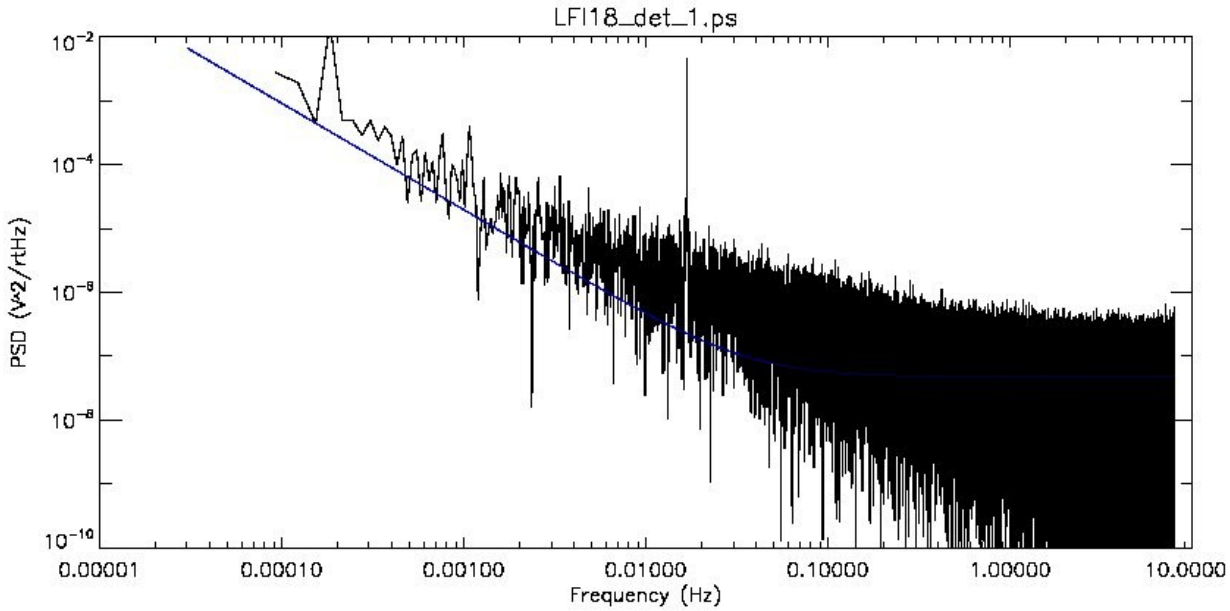

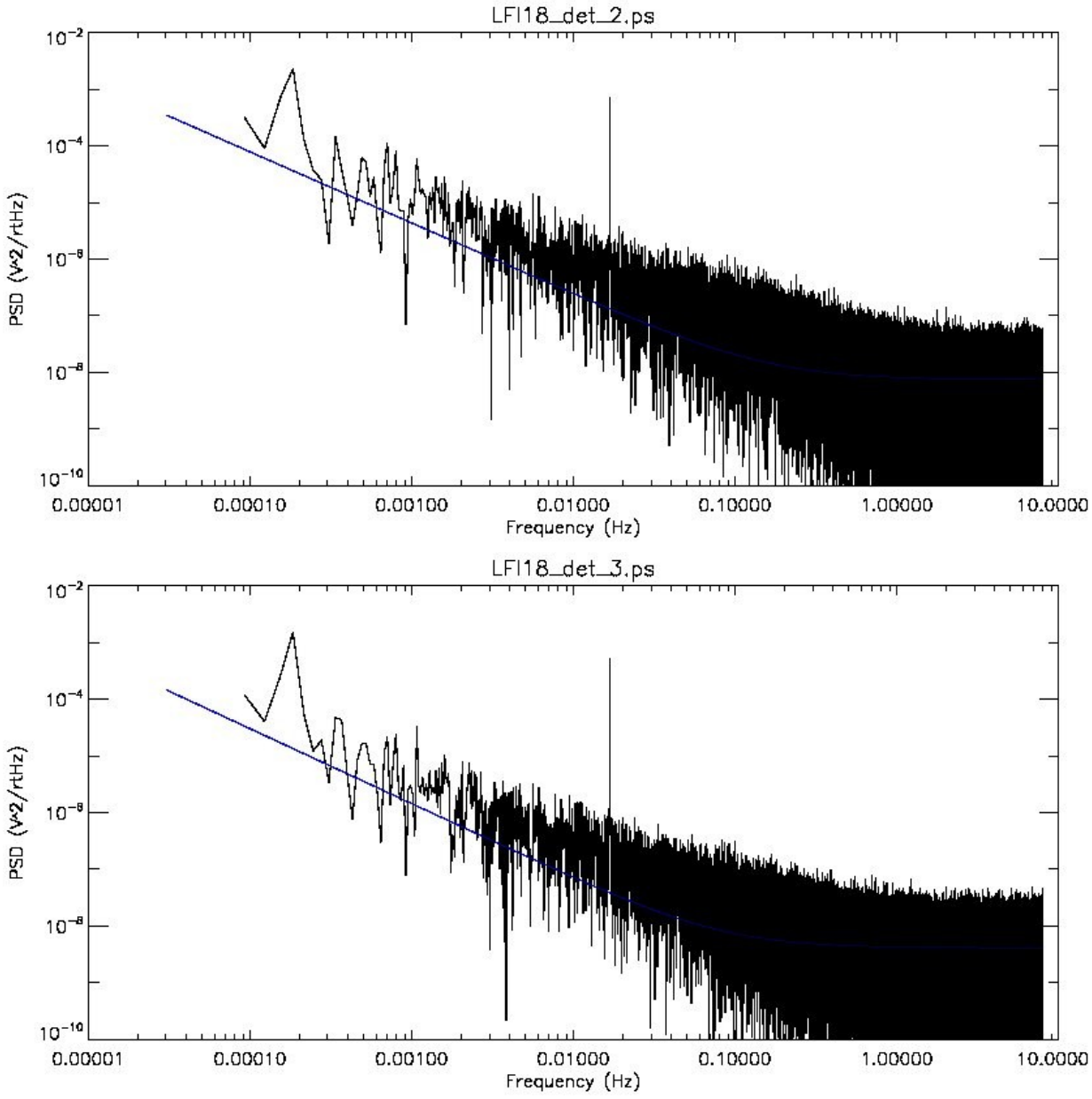
LFI18_det_2.ps
PSD (V^2/rtHz)
Frequency (Hz)
0.00001
0.00010
0.00100
0.01000
0.10000
1.00000
10.0000
LFI18_det_3.ps
PSD (V^2/rtHz)
Frequency (Hz)

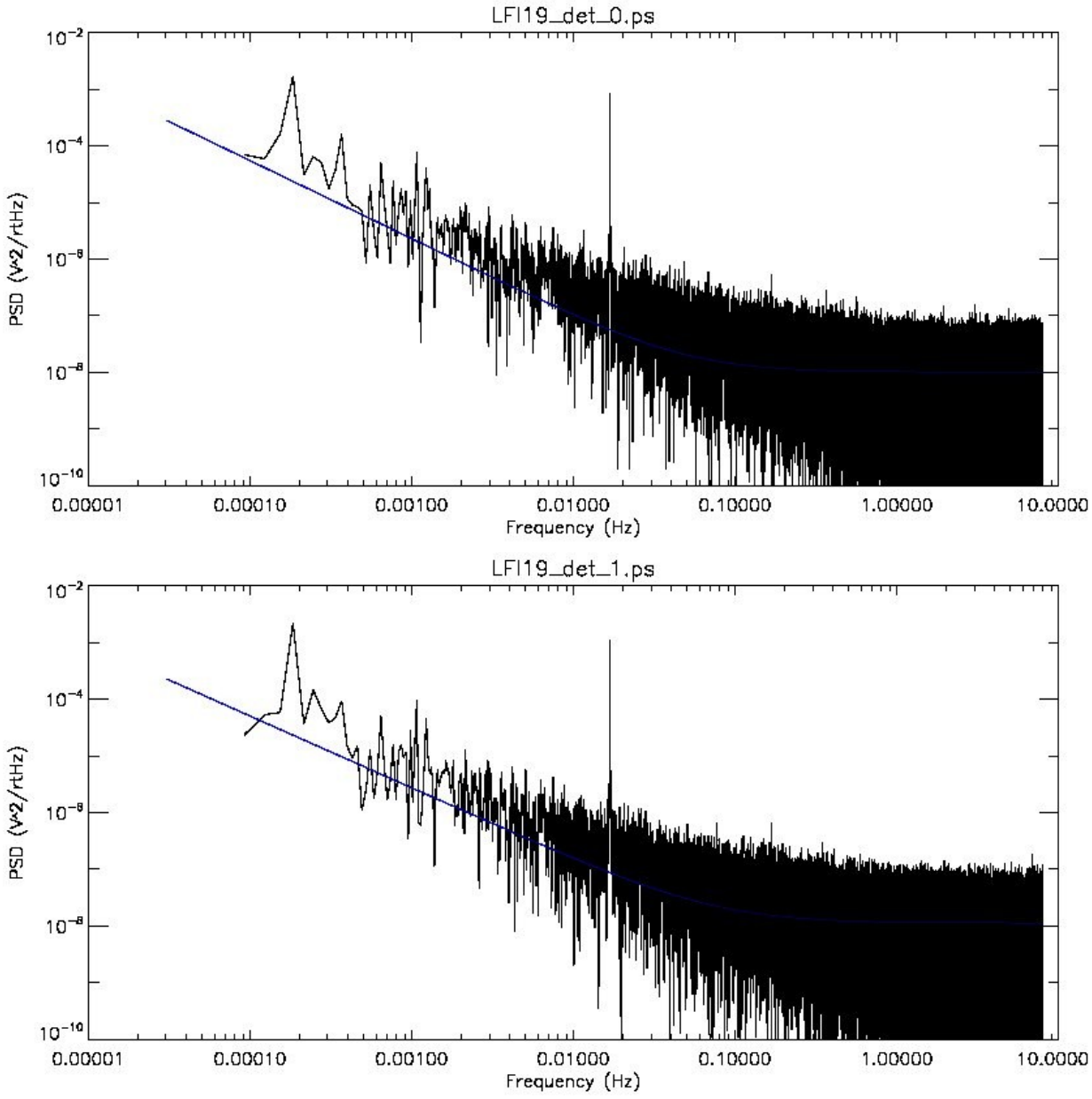
LFI19_det_0.ps
PSD (V^2/rtHz)
Frequency (Hz)
LFI19_det_1.ps
PSD (V^2/rtHz)
Frequency (Hz)

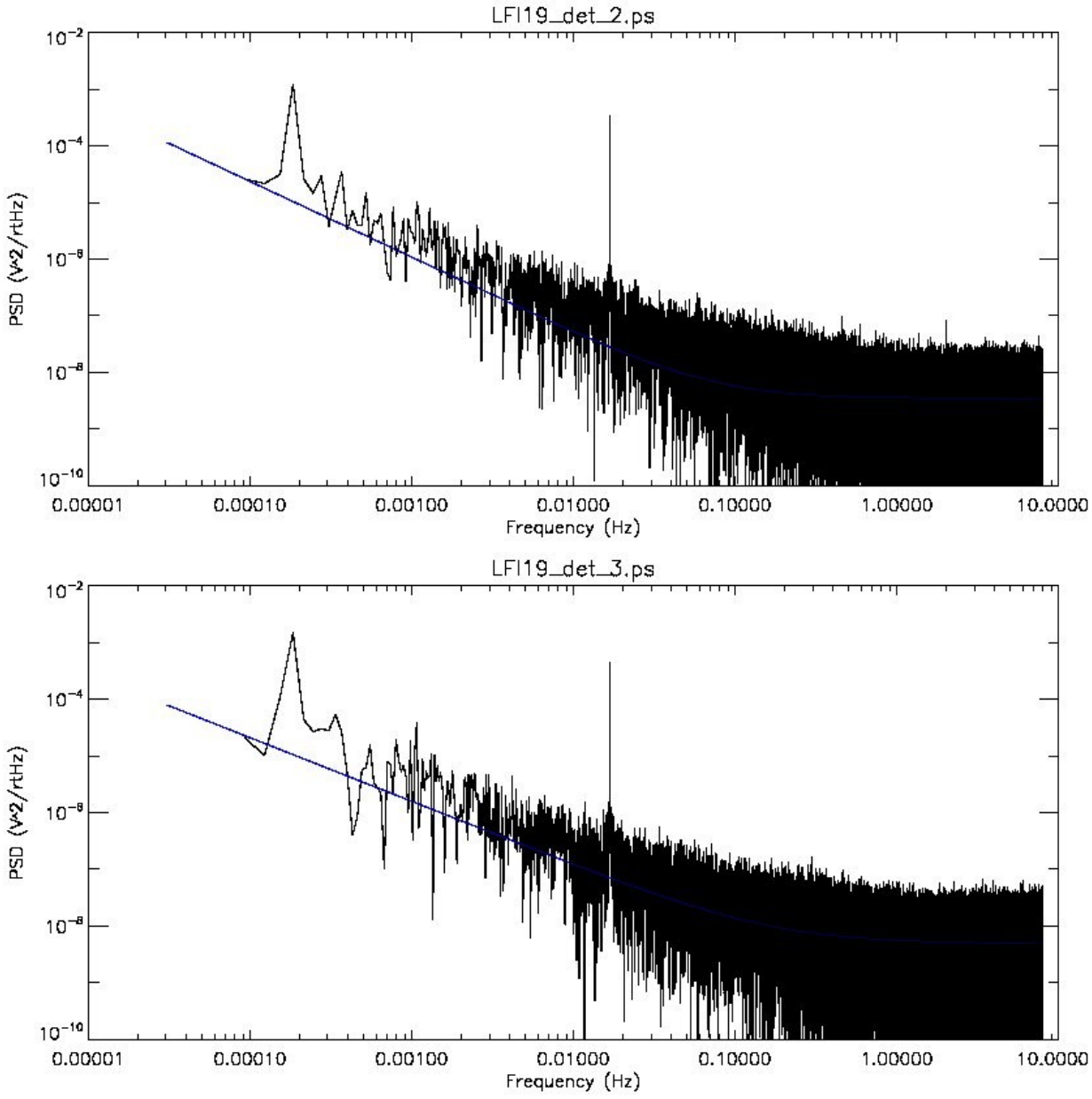
LFI19_det_2.ps
PSD (V^2/rtHz)
Frequency (Hz)
0.00001
0.00010
0.00100
0.01000
0.10000
1.00000
10.0000
LFI19_det_3.ps
PSD (V^2/rtHz)
Frequency (Hz)

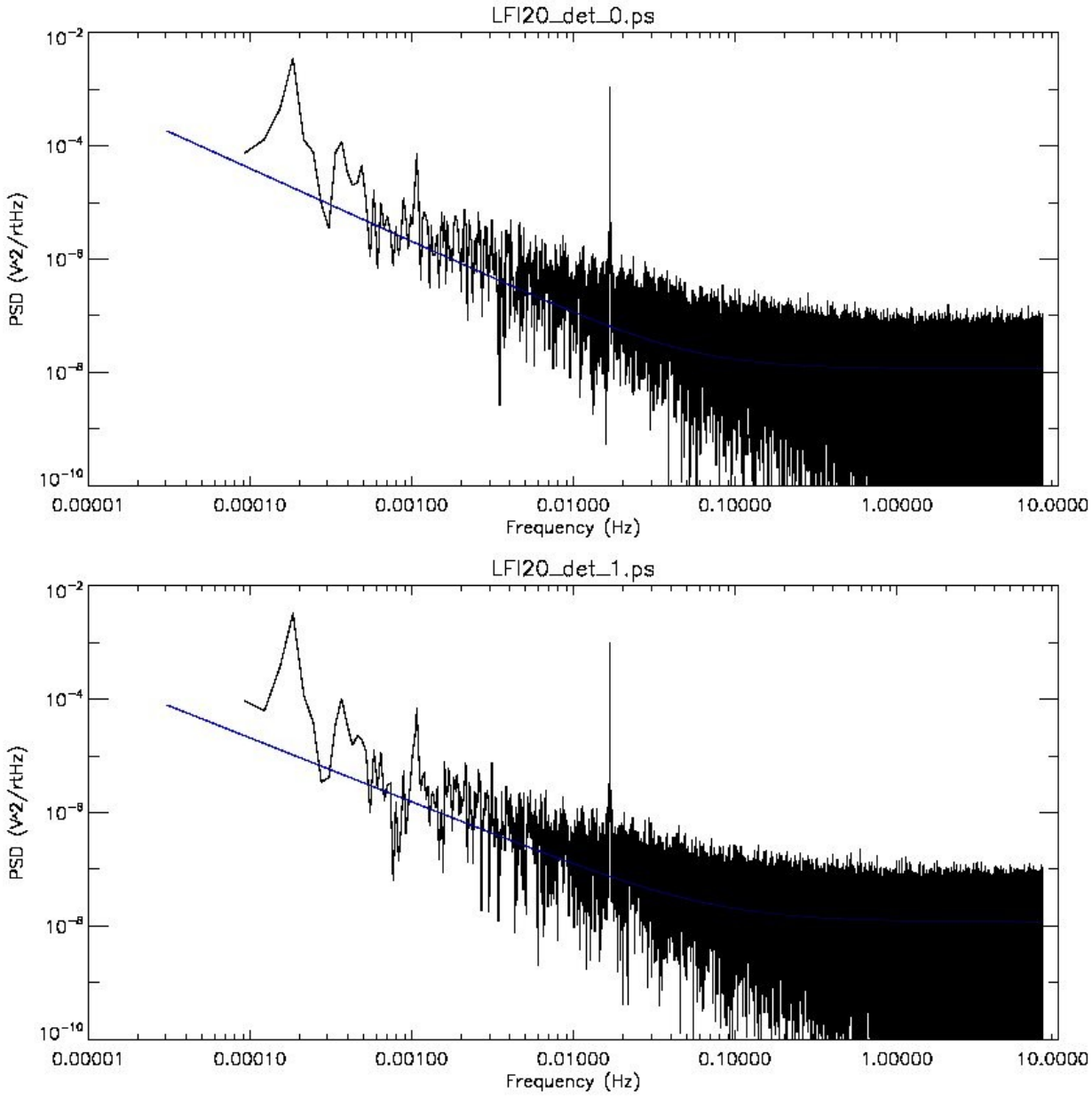
LFI20_det_0.ps
PSD (V^2/rtHz)
Frequency (Hz)
LFI20_det_1.ps
PSD (V^2/rtHz)
Frequency (Hz)

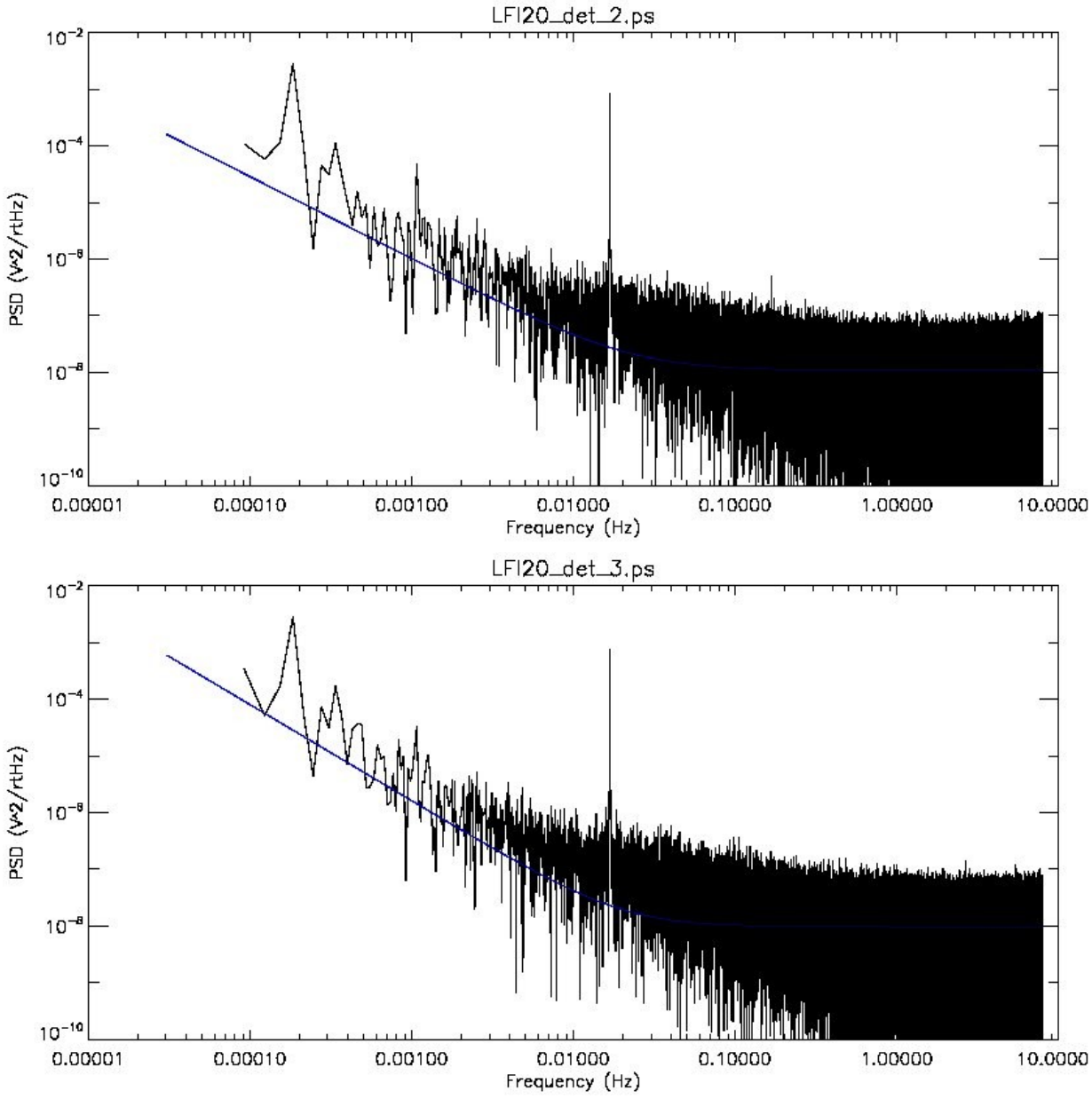
LFI20_det_2.ps
PSD (V^2/rtHz)
Frequency (Hz)
LFI20_det_3.ps
PSD (V^2/rtHz)
Frequency (Hz)

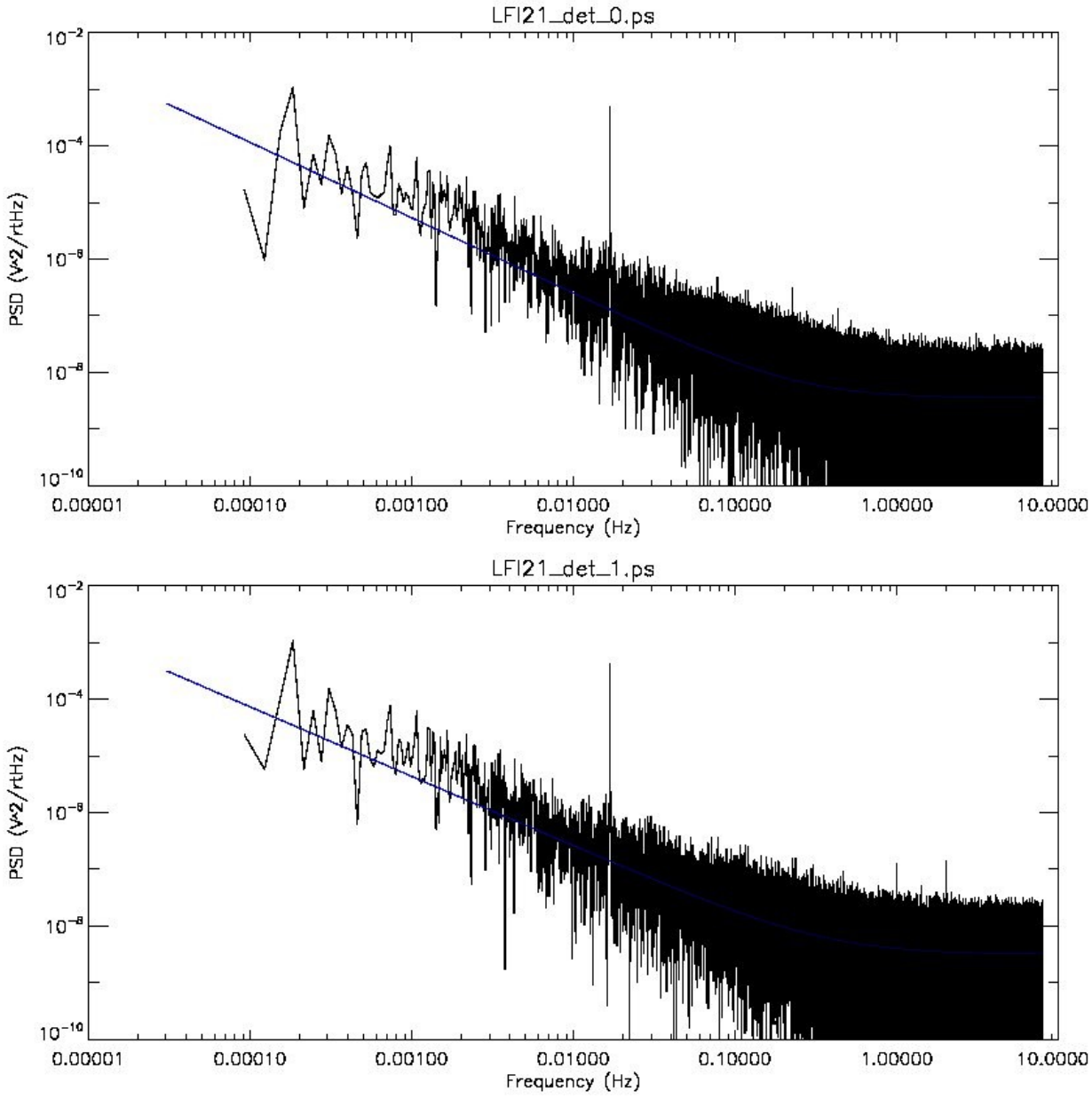
LFI21_det_0.ps
PSD (V^2/rtHz)
Frequency (Hz)
LFI21_det_1.ps
PSD (V^2/rtHz)
Frequency (Hz)

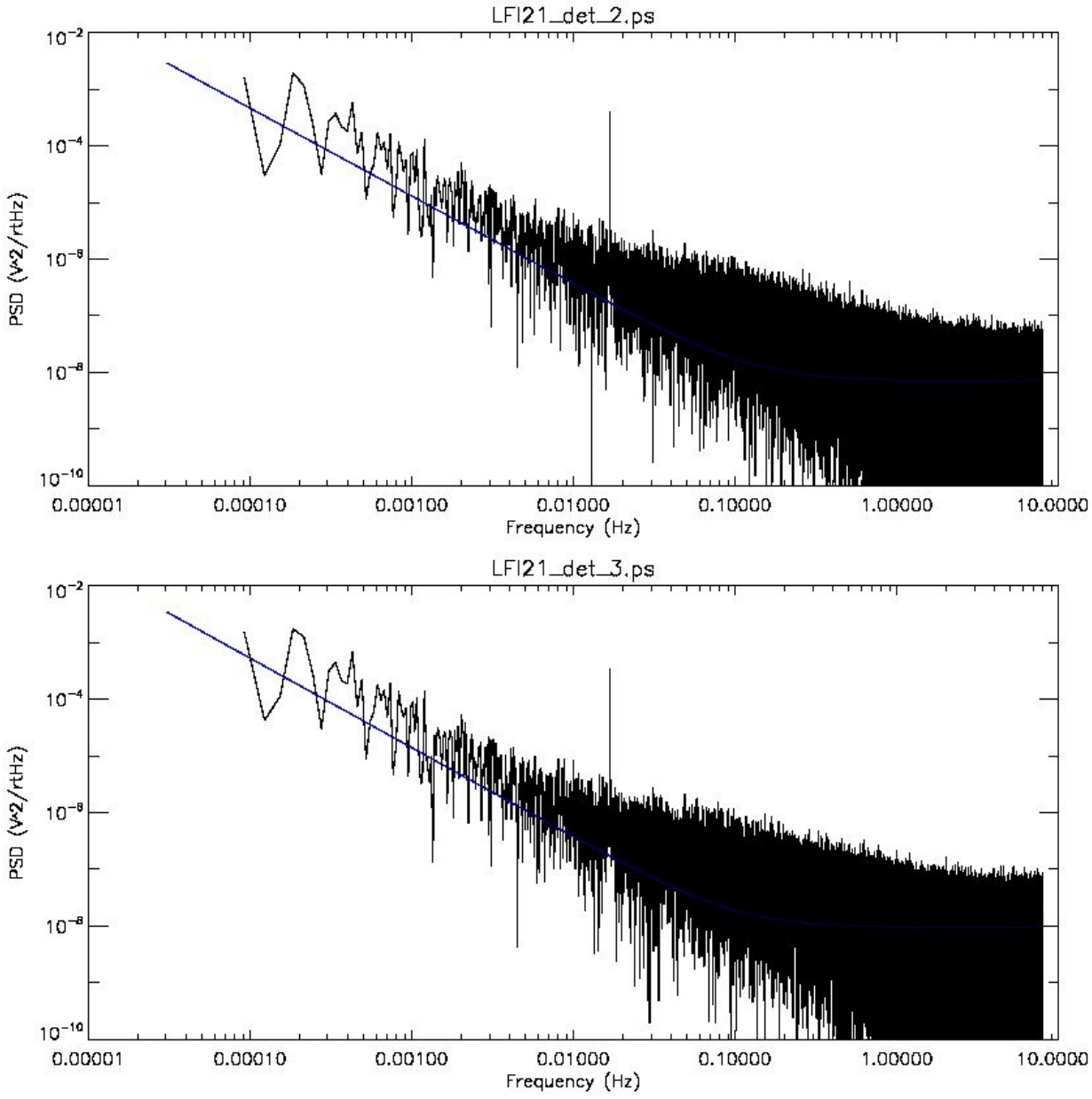
LFI21_det_2.ps
PSD (V^2/rtHz)
Frequency (Hz)
LFI21_det_3.ps
PSD (V^2/rtHz)
Frequency (Hz)

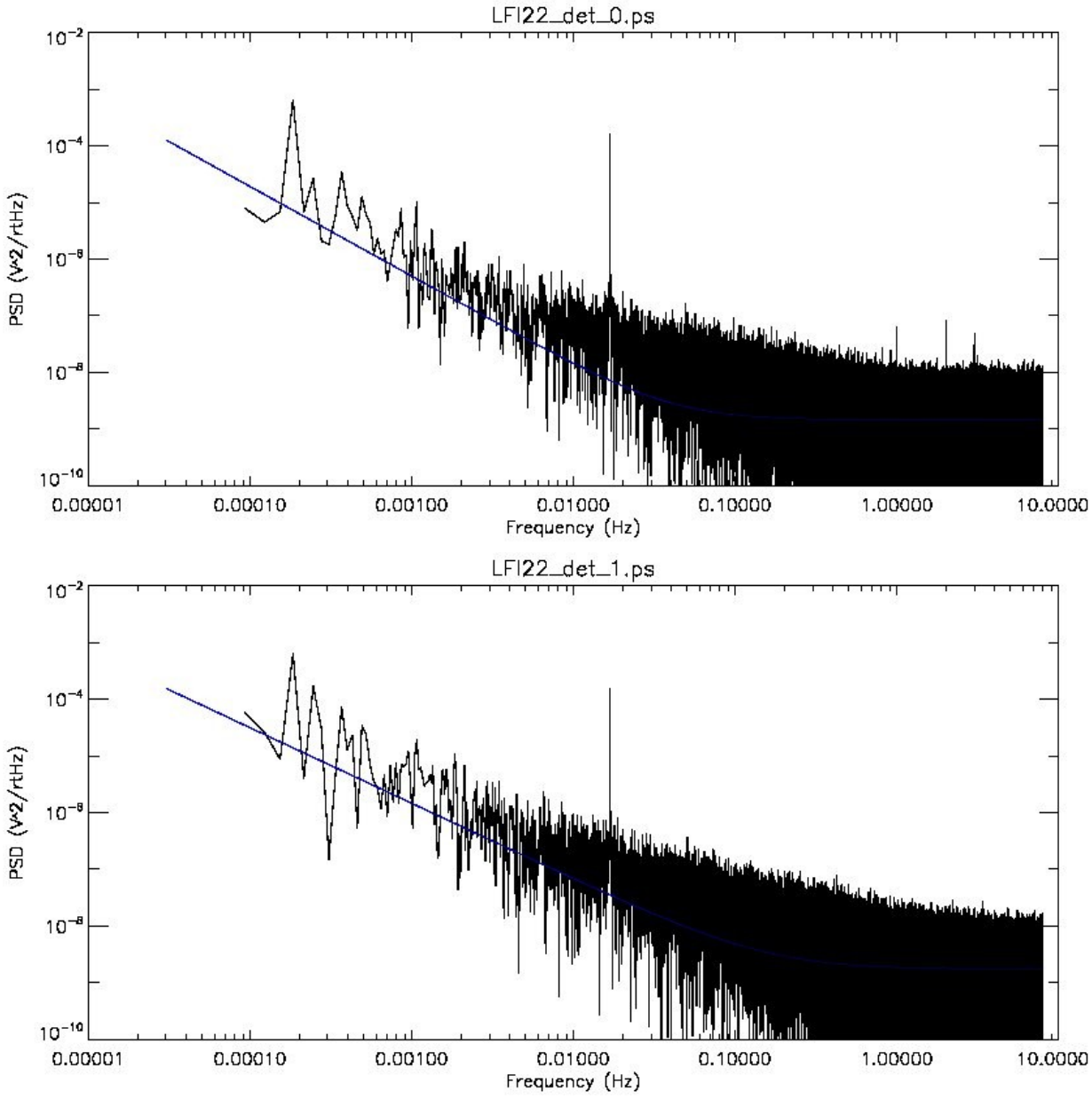
LFI22_det_0.ps
PSD (V^2/rtHz)
Frequency (Hz)
LFI22_det_1.ps
PSD (V^2/rtHz)
Frequency (Hz)

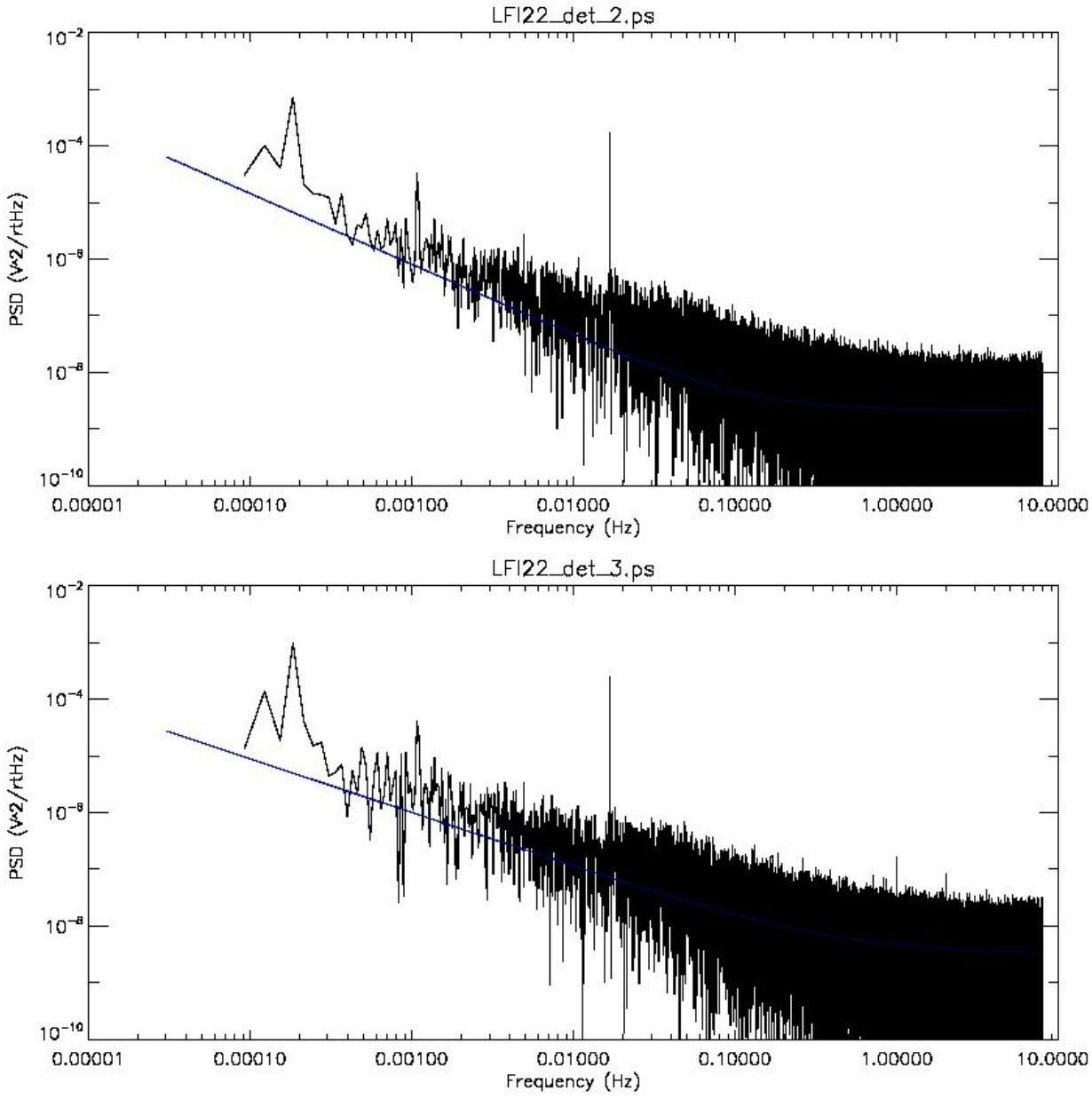
LFI22_det_2.ps
PSD (V^2/rtHz)
Frequency (Hz)
LFI22_det_3.ps
PSD (V^2/rtHz)
Frequency (Hz)

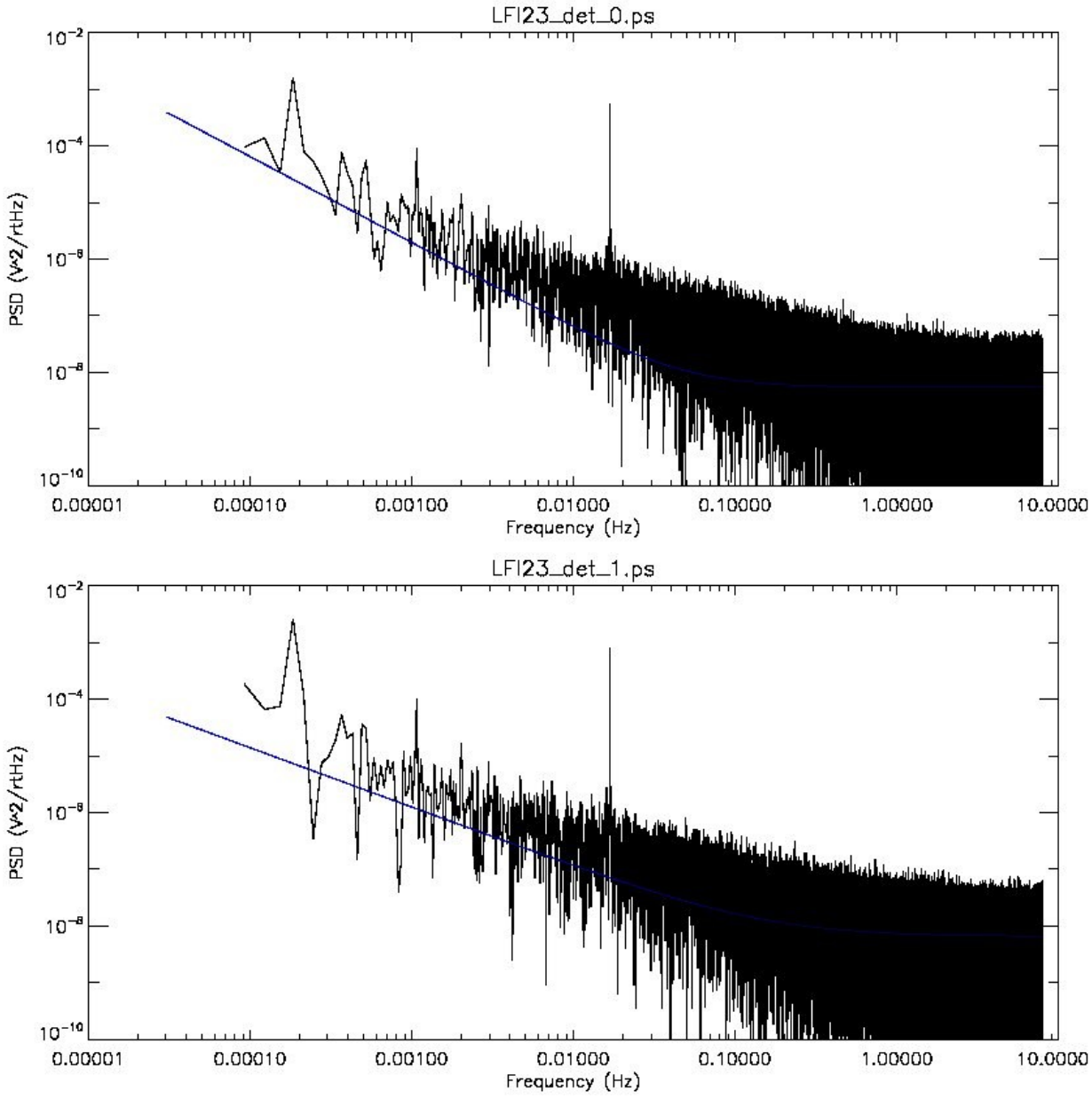
LFI23_det_0.ps
PSD (V^2/rtHz)
Frequency (Hz)
LFI23_det_1.ps
PSD (V^2/rtHz)
Frequency (Hz)

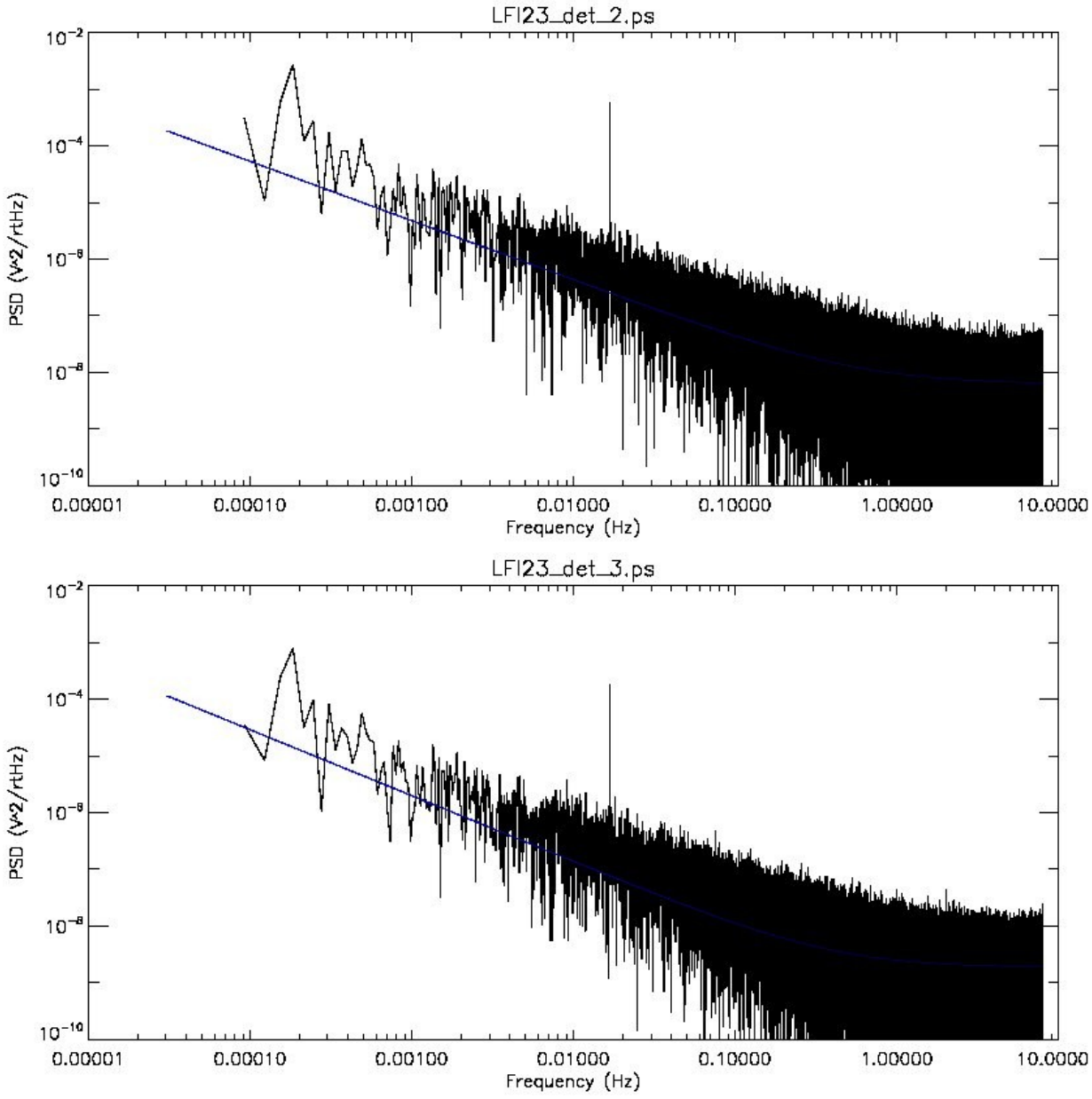
LFI23_det_2.ps
PSD (V^2/rtHz)
Frequency (Hz)
0.00001
0.00010
0.00100
0.01000
0.10000
1.00000
10.0000
LFI23_det_3.ps
PSD (V^2/rtHz)
Frequency (Hz)

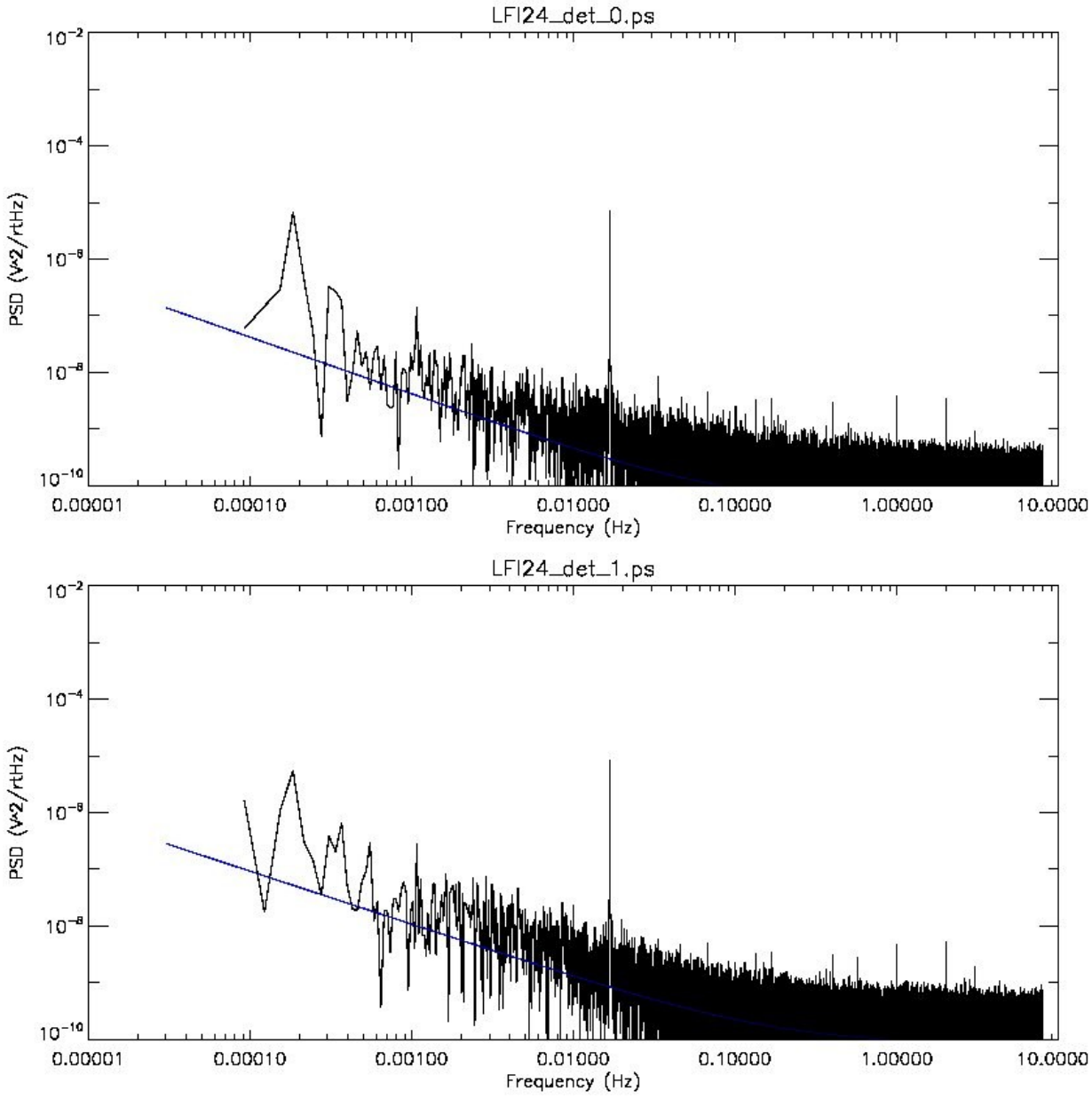
LFI24_det_0.ps
PSD (V^2/rtHz)
Frequency (Hz)
LFI24_det_1.ps
PSD (V^2/rtHz)
Frequency (Hz)

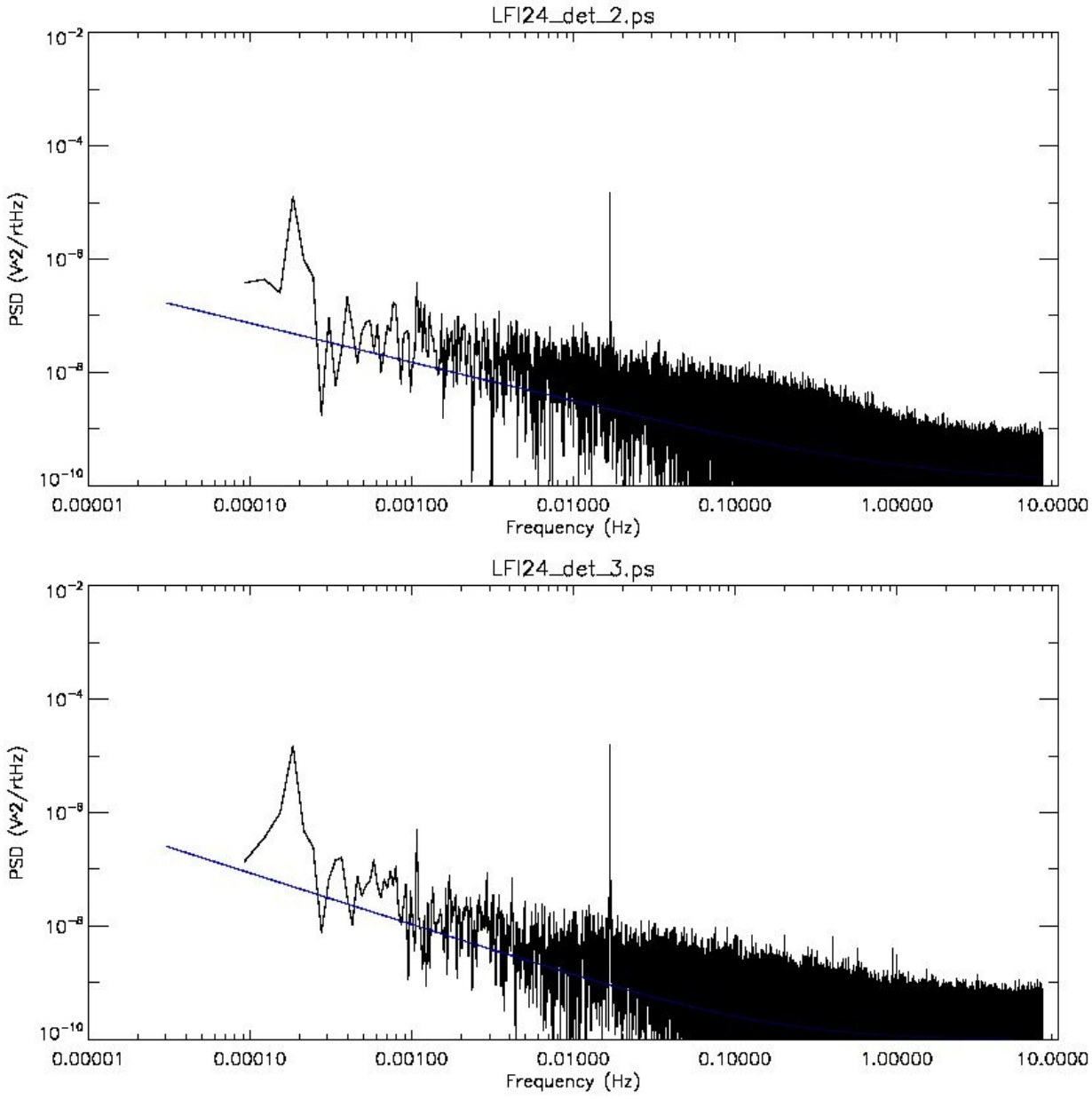
LFI24_det_2.ps
PSD (V^2/rtHz)
Frequency (Hz)
LFI24_det_3.ps
PSD (V^2/rtHz)
Frequency (Hz)

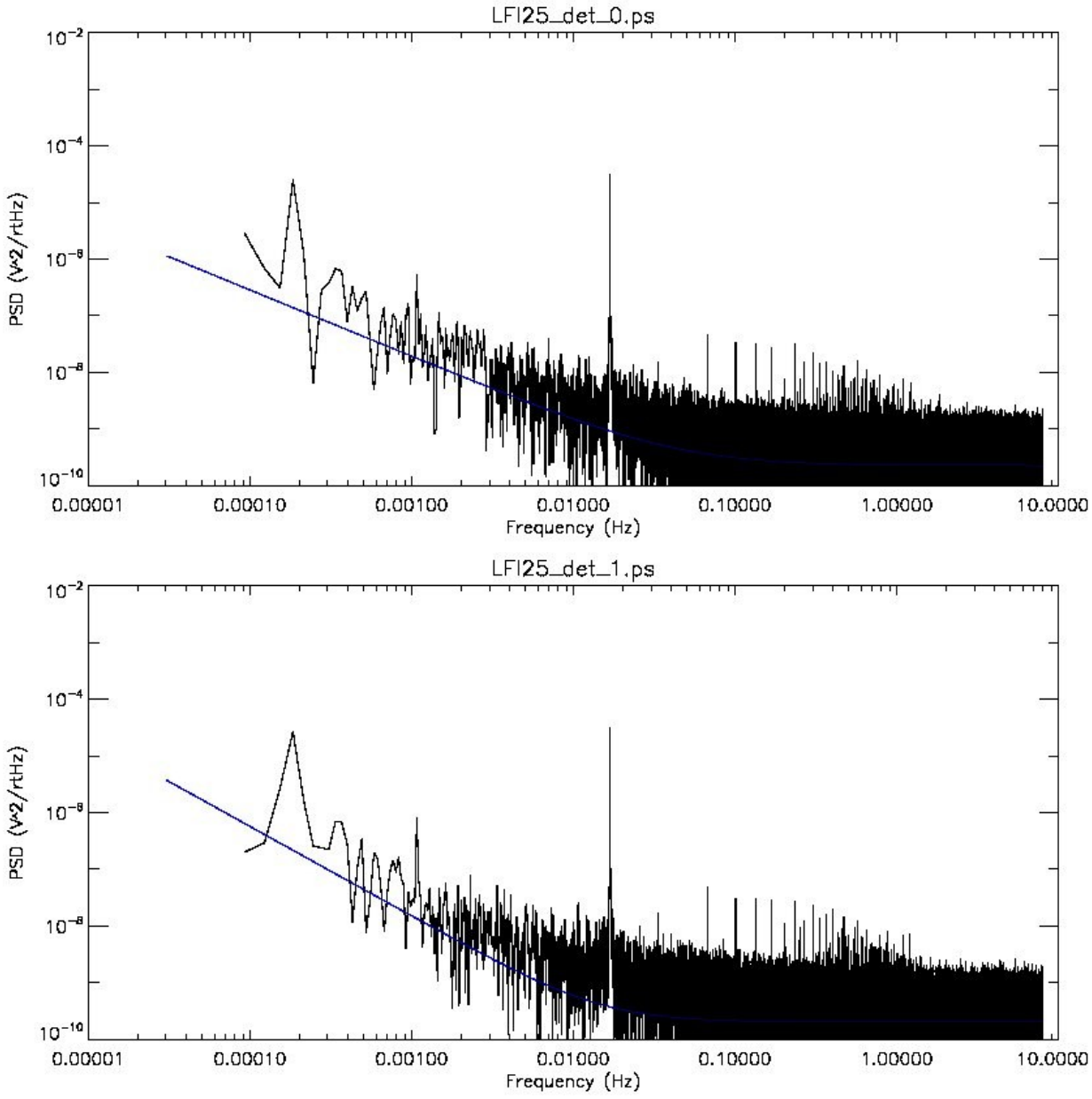
LFI25_det_0.ps
PSD (V^2/rtHz)
Frequency (Hz)
LFI25_det_1.ps
PSD (V^2/rtHz)
Frequency (Hz)

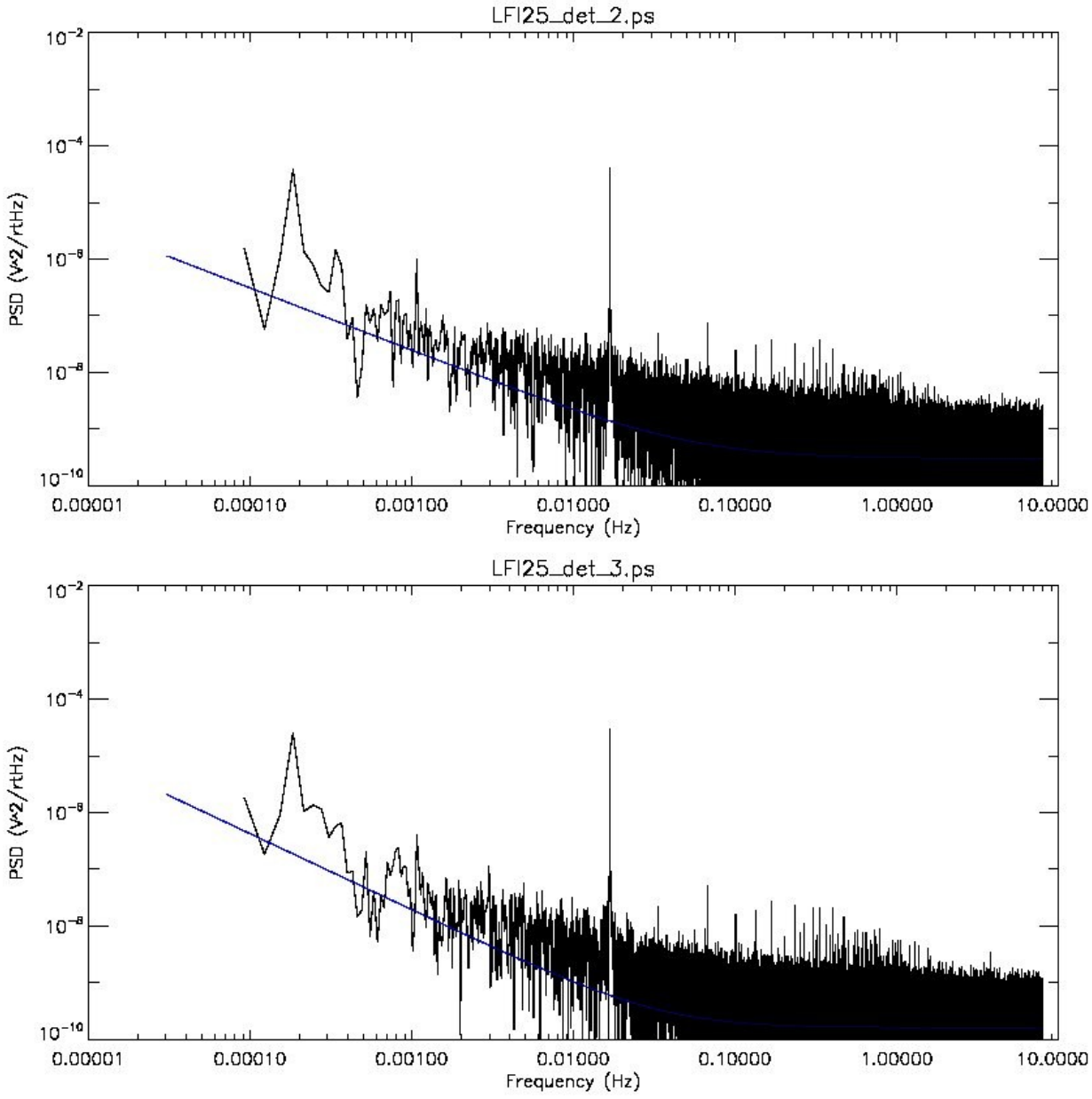
LFI25_det_2.ps
PSD (V^2/rtHz)
Frequency (Hz)
LFI25_det_3.ps
PSD (V^2/rtHz)
Frequency (Hz)

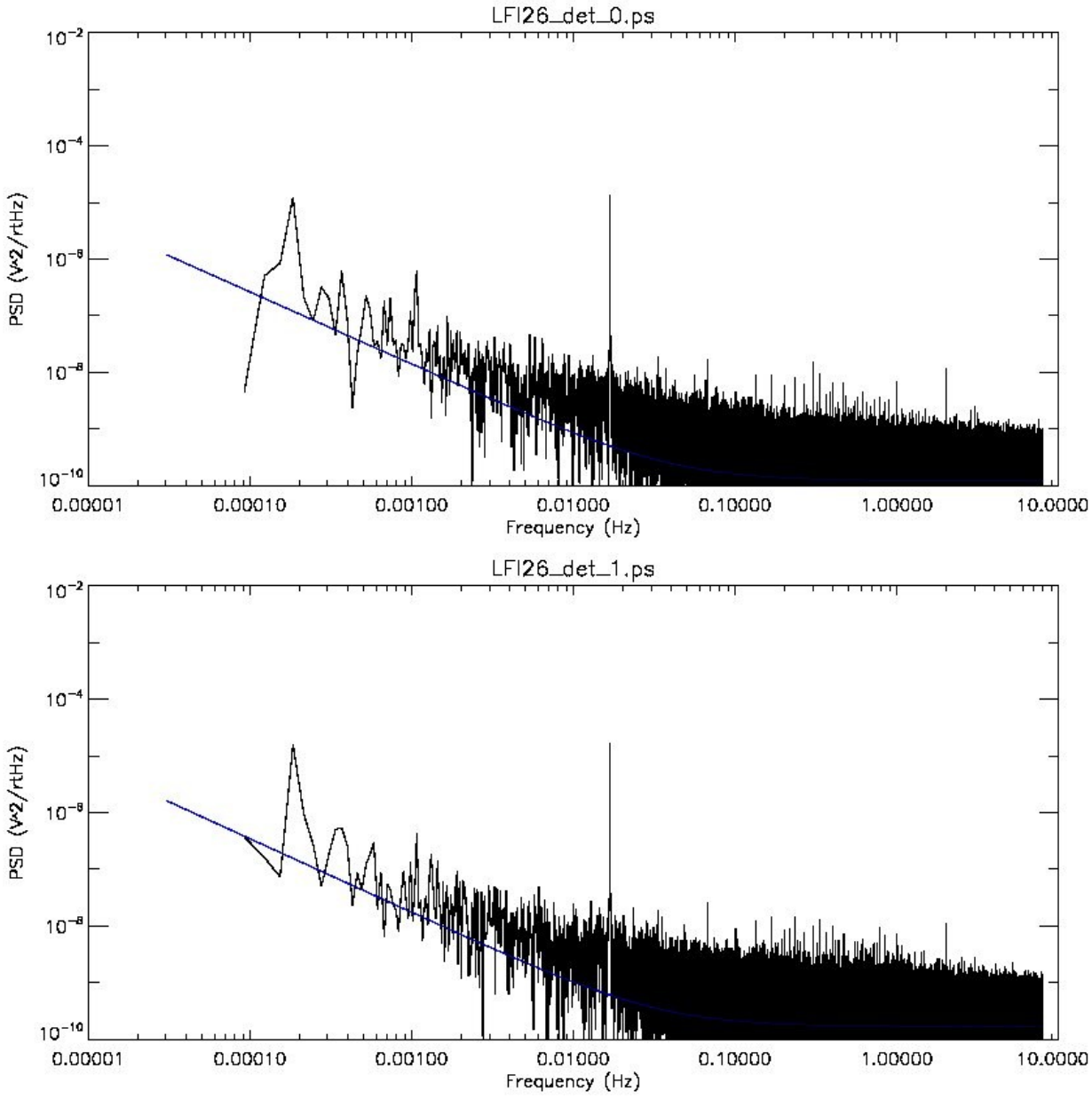
LFI26_det_0.ps
PSD (V^2/rtHz)
Frequency (Hz)
0.00001
0.00010
0.00100
0.01000
0.10000
1.00000
10.0000
LFI26_det_1.ps
PSD (V^2/rtHz)
Frequency (Hz)

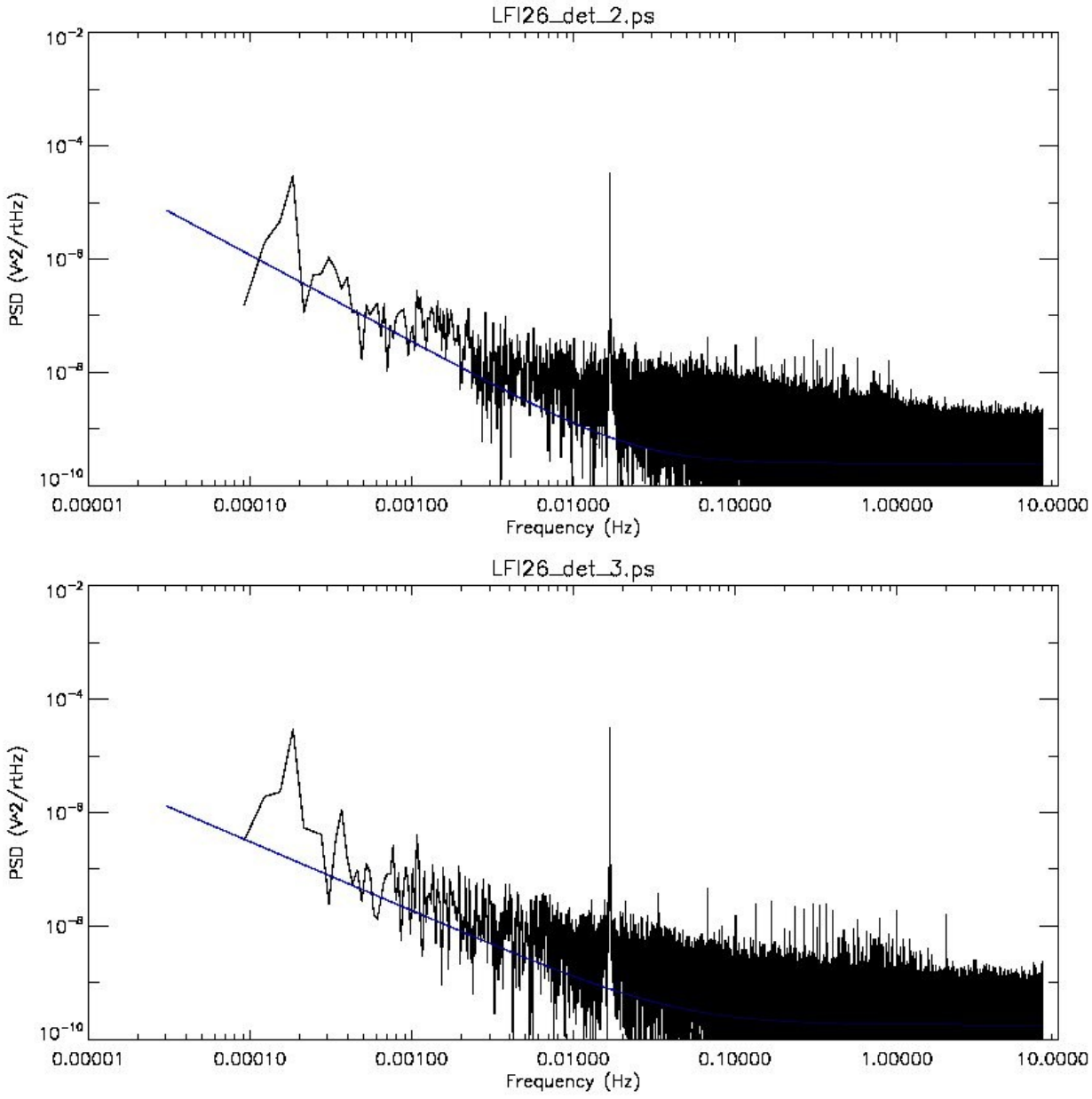
LFI26_det_2.ps
PSD (V^2/rtHz)
Frequency (Hz)
0.00001
0.00010
0.00100
0.01000
0.10000
1.00000
10.0000
LFI26_det_3.ps
PSD (V^2/rtHz)
Frequency (Hz)

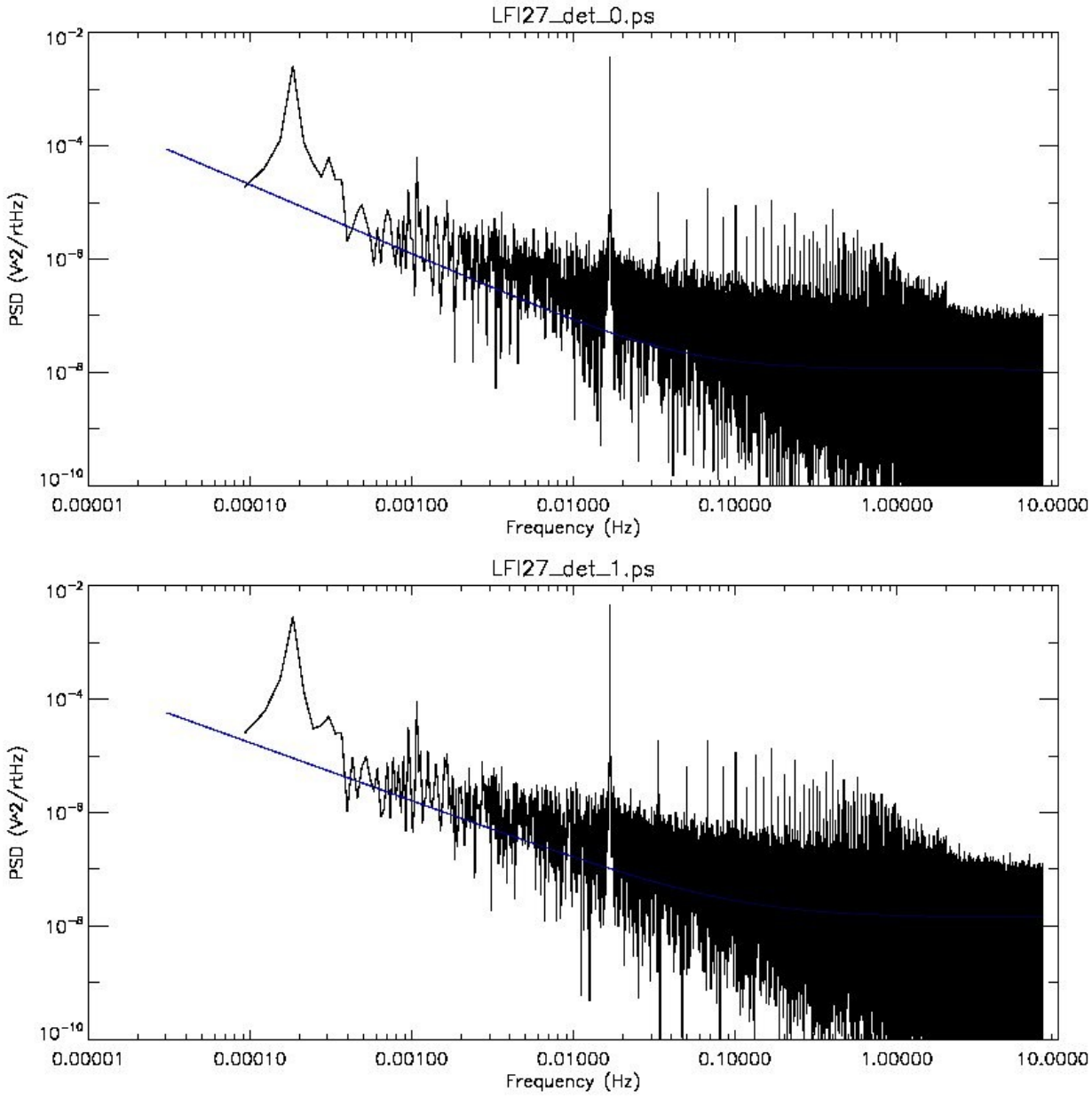
LFI27_det_0.ps
PSD (V^2/rtHz)
Frequency (Hz)
LFI27_det_1.ps
PSD (V^2/rtHz)
Frequency (Hz)

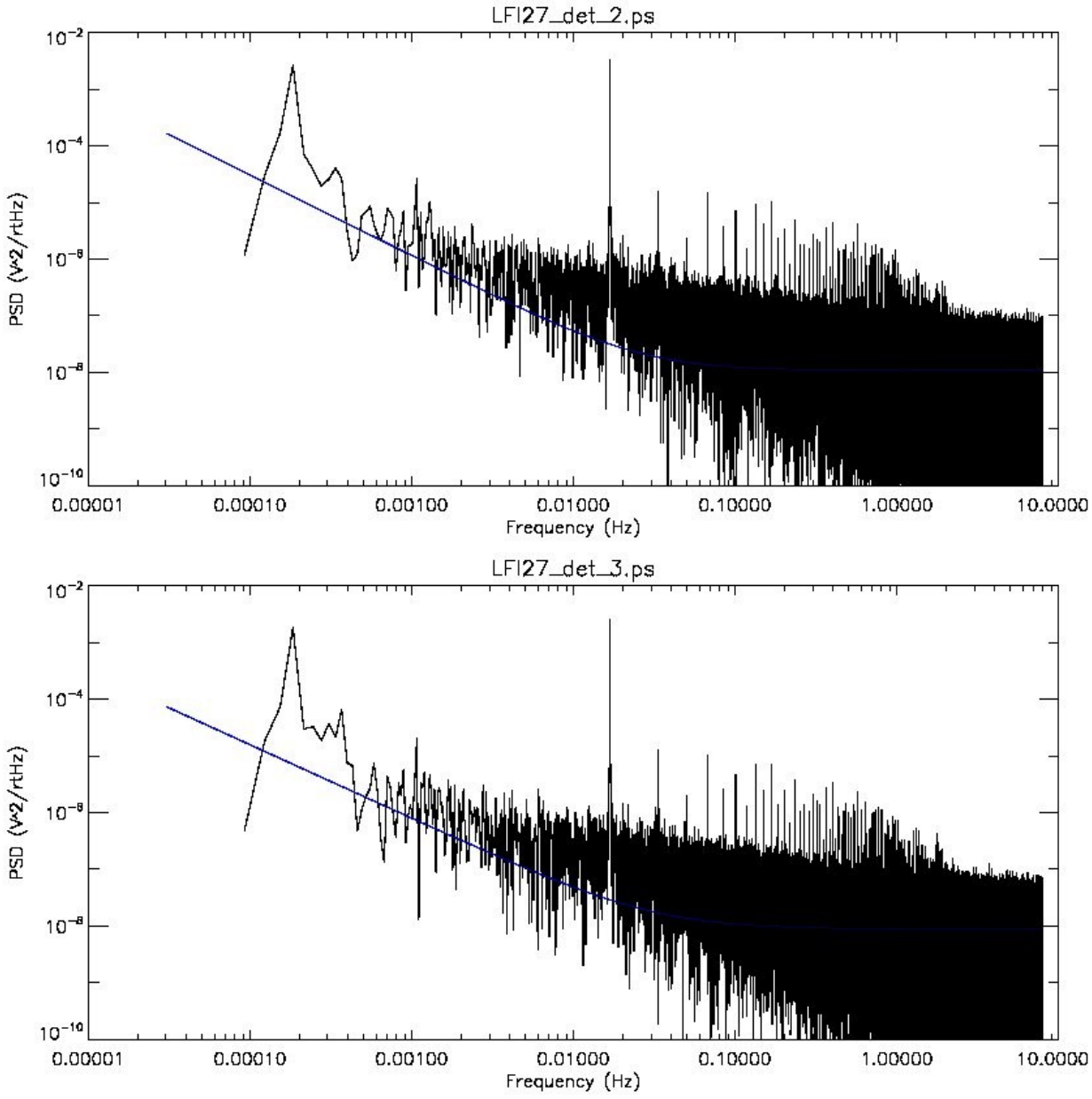
LFI27_det_2.ps
PSD (V^2/rtHz)
Frequency (Hz)
LFI27_det_3.ps
PSD (V^2/rtHz)
Frequency (Hz)

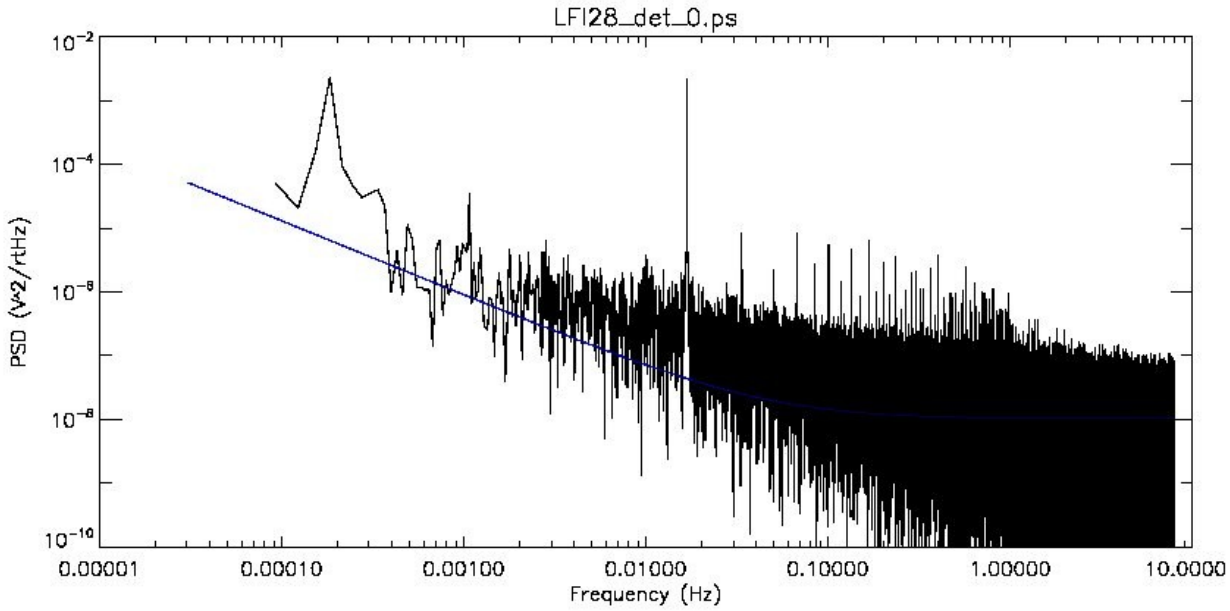
LFI28_det_0.ps
PSD (V^2/rtHz)
Frequency (Hz)
10^-2
10^-4
10^-6
10^-8
10^-10
0.00001
0.00010
0.00100
0.01000
0.10000
1.00000
10.0000

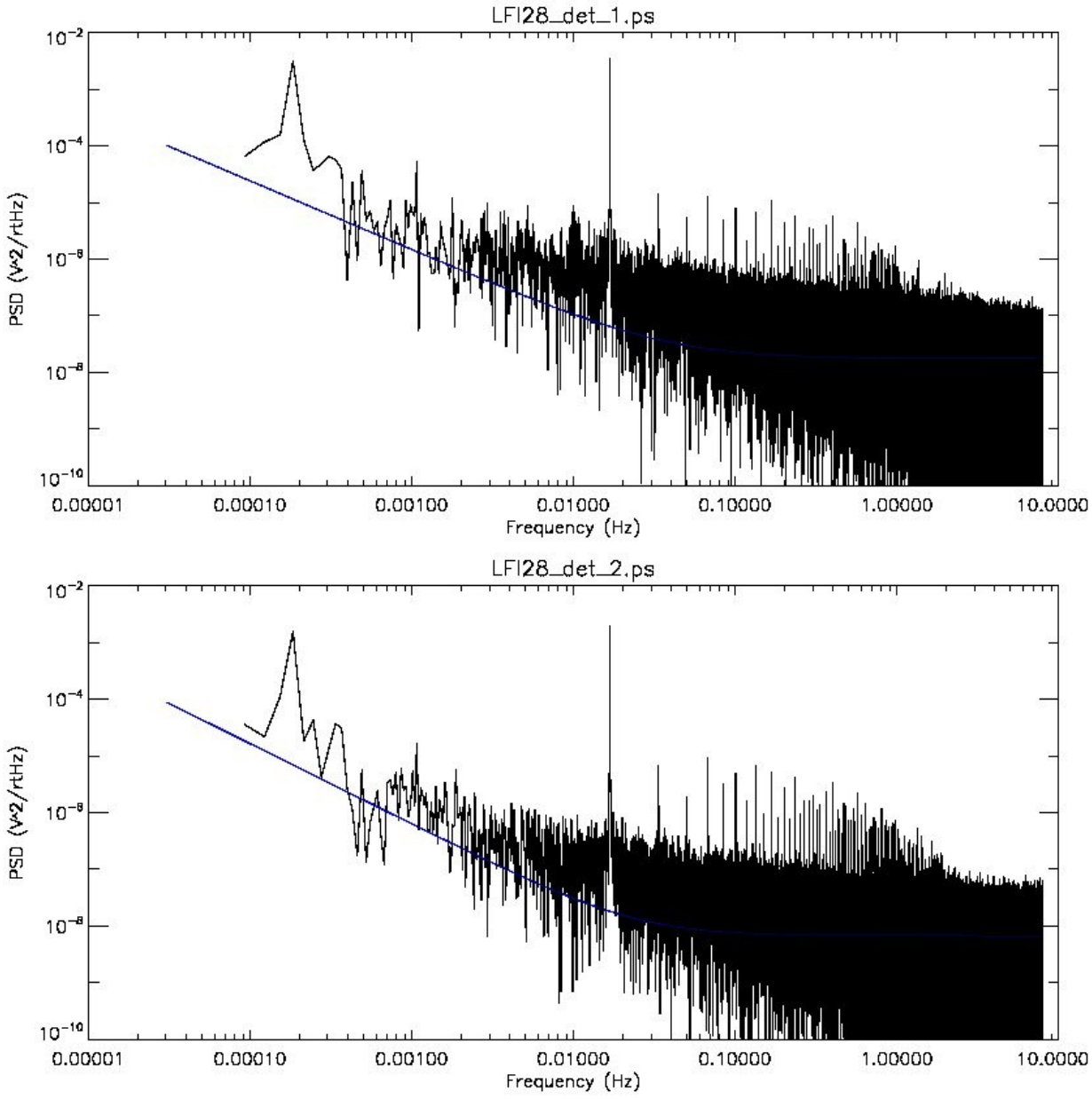
LFI28_det_1.ps
PSD (V^2/rtHz)
Frequency (Hz)
LFI28_det_2.ps
PSD (V^2/rtHz)
Frequency (Hz)

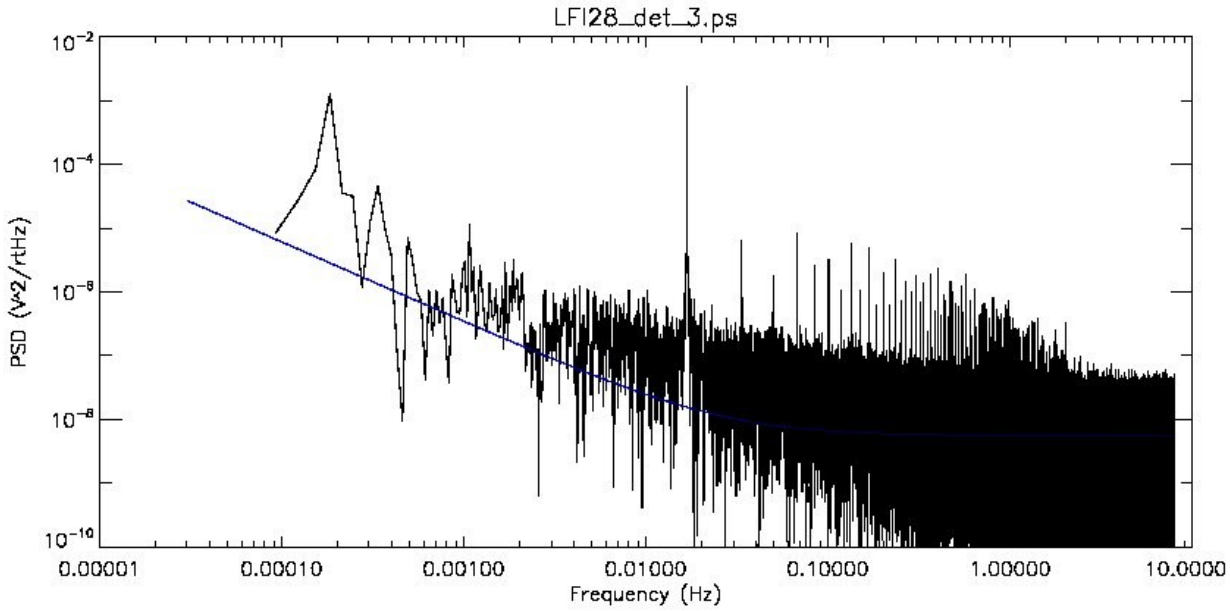
LFI28_det_3.ps
PSD (V^2/rtHz)
Frequency (Hz)
10^-2
10^-4
10^-6
10^-8
10^-10
0.00001
0.00010
0.00100
0.01000
0.10000
1.00000
10.0000